

EFFECTS OF A N₂-FIXING BIOFERTILIZER ON THE RHIZOSPHERE MICROBIOME
AND THE INFLUENCE OF BIOCHAR ON SOIL FERTILITY AND MICROBIAL
COMMUNITIES.

By

SARBJEET NIRLA, M.Sc.

DISSERTATION

Submitted in partial fulfillment of the requirements

for the degree of

DOCTOR OF PHILOSOPHY

at

The University of Texas-Arlington

December 2021

Arlington, Texas

Supervising Committee:

Woo-Suk Chang, Supervising Professor

Michael R. Roner

Matthew Walsh

Matthew Fujita

Sen Xu

ABSTRACT

EFFECTS OF A N₂-FIXING BIOFERTILIZER ON THE RHIZOSPHERE MICROBIOME AND THE INFLUENCE OF BIOCHAR ON SOIL FERTILITY AND MICROBIAL COMMUNITIES.

Sarbjee Niraula, PhD
The University of Texas - Arlington, 2021

Supervising Professor: Woo-Suk Chang

The rhizosphere microbiota and endosymbionts are the major contributors to biogeochemical cycling and significantly impact the associated host plant. Their association with plant roots is inevitable for plant health and development. The application of bio-inoculants that promote plant growth and productivity is a promising alternative to chemical fertilizers in agricultural fields because of their nutrient solubilization activity, and are considered environmentally safe. However, their impact on the soil microbiome has been least studied. The use of bio-inoculants may have favorable or unfavorable impacts on the native microbial community in the rhizosphere. Therefore, we attempt to evaluate the effects of a novel drought-tolerant bioinoculant treatment on the rhizosphere microbial community of the Soybean plant. In addition, constant development and refinement of bio-inoculant are also vital to sustained potential. Traditionally, most studies focused on identifying differentially expressed genes to identify molecular markers to develop a novel bioinoculant. However, underlying molecular mechanisms involve much more complex interactions among genes. We performed a network-based analysis to identify modules and hub genes in *Bradyrhizobium japonicum* under desiccation stress. This study provides further understanding of gene responses to water stress, and helps us develop a novel molecular marker for bio-inoculant selection and development. Along with

developing an efficient bio-inoculant, the persistence of the inoculant in the soil under abiotic stressors is another primary concern. Recently, biochar has been proposed for various agronomic applications, including improved plant growth and soil fertility. We studied the effects of dairy effluent-saturated (SBC) and unsaturated wood-derived biochar (UBC) on Bermudagrass (*Cynodon* spp.) growth, soil fertility, and microbial communities in a greenhouse. Our research will provide a direction to increase the efficiency of bio-inoculant by biochar, thereby helping in sustainable agriculture.

ACKNOWLEDGEMENTS

I would like to express my deepest gratitude and appreciation to my Ph.D. advisor, Dr. Woo-Suk Chang, for his tremendous support and guidance throughout my Ph.D. years. His encouragement and advice have always led me to be a researcher. I am also grateful to my supervising committee Dr. Michael R. Roner, Dr. Matthew Walsh, Dr. Matthew Fujita, and Dr. Sen Xu, for shaping my research with their knowledge and expertise. This work would not have been accomplished without their guidance.

I am sincerely thankful to all the Collaborators, especially Dr. Kunsung Kan, for adding value to my research with their expertise. I would like to thank Phi Sigma Biology for supporting my research. It was a great pleasure to work and share knowledge with the amazing Chang lab team (past and present) and graduate colleagues from the Department. I'm heartily thankful to them for motivating me towards the goal, helping me with my research, and making the journey enjoyable alongside.

I cannot thank the UTA Biology department enough for providing me with great opportunities and platforms for scholarly achievements. I am grateful to all the previous and current staff in the Department for ensuring my academic advancement with the least resistance. It will always be a pride to be a part of UTA.

Above all I would like to thank my wife Nirmala for her unfathomable love and support. Thank you so much for being my lifeline and holding my hands in every situation. I am grateful to my parents, sister, brother, uncle and aunt for their inspirations and help to complete this work. To my lovely little angels, Anjila and Aarika, for bringing brightness into my world. I should not forget to thank my friends (@Kullads), in-laws and relatives who have helped me to achieve my

goal one or the other way. My special thanks to Tulsi Khatri, Kalpana Khatri and Tej Chudali for their direct contribution on my success.

DEDICATION

I would like to dedicate this work to my late grandmother, Gita Devi Niraula, and grandfather, Lakshman Prasad Niraula, who have always been the most loving, caring, and wise personality to all her children. I would also like to dedicate this work to my parents, Shyam Prasad Niraula and Manju Rani Niraula. Their unconditional love and care have made me what I am today.

LIST OF FIGURES

Figure 1-1 An example of a gene co-expression network.	15
Figure 2-1 Physicochemical properties of wood biochar (BC) treated soil. Discriminant analysis (DA) among soil treated with SBC and UBC (A). Principal component analysis (PCA) of soil properties, plant growth parameters and the loading rates of saturated BC (SBC) in soil (B) and unsaturated biochar (UBC) in soil (C).	38
Figure 2-2 Percent increase in the N and P concentration in 10-week samples in comparison to the control.	40
Figure 2-3 Spearman correlation of soil physicochemical variables and plant growth parameters among soil samples treated with saturated and unsaturated biochar (p-value < 0.05 *, p-value < 0.01 **, p-value < 0.001 ***).	41
Figure 2-4 Comparison of stem dry weight (A), root dry weight (B), total plant biomass (C), and the number of leaves (D). Total plant biomass is the combination of stem and root dry weight. Two sample t-test was performed among each group compared (p-value < 0.05*, p-value < 0.01**).	42
Figure 2-5 Microbial community composition. Relative abundance of major taxa at phylum level (A). Principal coordinate analysis of the microbial community at OUT level (B). (Abbreviations: NP; No plant, I; Initial, F; Final).	43
Figure 2-6 Differential abundance of predicted functions between SBC and UBC treated soil. LEFSe analysis of PICRUST2 (A) and FAPROTAX (B) predicted functions in SBC and UBC treated soil among no-plant samples and plant samples, respectively.	44
Figure 3-1 Soybean yield, nodule number and plant dry weight between TXVA and NT treatments. Welch t-test was performed to compare between irrigated and non-irrigated samples. P-value; <0.05 (*), <0.01(**).	75
Figure 3-2 Alpha rarefaction based on Shannon diversity index and the number of observed amplicon sequence variants (ASVs).	76
Figure 3-3 Relative abundances of phyla at initial, 7-week and harvest periods. Each stacked bar plot represents the average of 3 biological replicates.	77
Figure 3-4 Proportions of the genus Bradyrhizobium in the rhizosphere soil between NT and TXVA treatments at 3 time points including initial, 7 weeks, and harvest (A) and during harvest (B). ANOVA was done for each group followed by tukey's hsd to quantify differences in proportions at 3 time points. Welch's t-test was done to compare means of proportions in sub figure B.	78
Figure 3-5 Differences in alpha diversity between bulk and rhizosphere soil among NT and TXVA samples. P-value was calculated by Wilcox's test.	79
Figure 3-6 Principal coordinate analysis based on Weighted UniFrac distance	80
Figure 3-7 Principal coordinate analysis based on Weighted UniFrac distance among NT and TXVA samples in 7-weeks rhizosphere	80
Figure 3-8 Differentially abundant taxa between NT and TXVA treated rhizosphere soil in 7-weeks samples.	82
Figure 3-9 Relative abundances of the most abundant endosymbiont inside the root nodules (A) and the differential abundance of taxa in nodules between NT and TXVA treated samples (B). Relative abundance in NT and TXVA samples represents the average of 6 replicates.	84

Figure 3-10 Scale-free topology of the NT (A) and TXVA (B) rhizosphere networks.	85
Figure 3-11 Cooccurrence network of NT and TXVA treated rhizosphere soils.	85
Figure 3-12 Relative abundances of genus in NT and TXVA rhizosphere network.....	87
Figure 3-13 Differences in PICRUSt2 predicted functions between NT and TXVA during harvest in non-irrigated condition.	88
Figure 3-14 Differences in abundance of Overall Nitrogen fixation in rhizosphere soil between irrigated and non-irrigated conditions during harvest.	88
Figure 4-1: Selection of soft thresholding power to obtain scale independence and mean connectivity pattern (A) and connectivity pattern and scale free topology at selected soft threshold R-square value of 0.9 (B).	107
Figure 4-2: Correlation of connectivity pattern between probes under Desiccation stress (A) and random experimental condition (B).	109
Figure 4-3 : Gene co-expression network construction and module detection in <i>B. japonicum</i> USDA110 under desiccation stress. (A) Gene cluster dendrogram. Three colored horizontal bars represent modules obtained by hierarchical clustering, merging and k-means clustering, respectively, from top to bottom. (B) TOM plot of the network. Yellow region along the diagonal represents modules.	110
Figure 4-4 A relationship among modules. (A) Circos plot showing shared module membership among modules. (B) Cluster dendrogram of module eigengenes along with the desiccation branch node (top panel) and adjacency heatmap (bottom panel).	111
Figure 4-5 : A relationship between module eigengenes and desiccation time. (A) Correlation shows Spearman correlation and values in parentheses shows the number of genes in the respective modules. (B) Gene significance of identified modules.	112
Figure 4-6 Scatterplot of (A) Module membership vs Gene significance for desiccation time in the five significant and (B) Scatterplot of module membership vs intramodular connectivity in the five significant modules in desiccation stress response.	113
Figure 4-7 Module preservation analysis of Desiccation network modules.....	115
Figure 4-8 Network of strongly connected genes in the Darkred module. Connections correspond to the topological overlap greater than 0.165. Purple color represents intramodular hub genes. Size of the nodes corresponds to gene significance, boarder thickness corresponds to module membership and label size corresponds to intramodular connectivity.....	116
Figure 4-9 Network of strongly connected genes in the Darkgreen module. Connections corresponds to the topological overlap greater than 0.13. Purple color represents intramodular hub genes. Size of the nodes corresponds to gene significance; boarder thickness corresponds to module membership and label size corresponds to intramodular connectivity.....	116
Figure S 2-1 Mixture of soil and various ratios of wood-biochar.	58
Figure S 2-2 Plants growth with the different loading ratios of the nutrients saturated biochar.	58
Figure S 2-3 Comparison of stem dry weight (A), root dry weight (B), total plant biomass (C), and the number of leaves (D) among biochar ratios within each biochar saturation condition. Total plant biomass is the combination of stem and root dry weight. Two sample t-test was	

performed among each group compared (p-value < 0.05*, p-value < 0.01**, p-value < 0.001***).....59

Figure S 2-4 Alpha rarefaction curve showing observed OTUs at sampling depth of 74000 reads. [Abbreviations: SBC; Saturated Biochar, USB; Unsaturated Biochar, NP; No plant, I; Initial, F; Final]60

Figure S 2-5 Differentially abundant taxa at class level between SBC and UBC treated soil among plant samples determined by LEfSe analysis.60

Figure S 2-6 Differentially abundant features after 10 weeks period among no-plant samples determined by LEfSe analysis. Comparison was made among no-plant samples with time as class and saturation status subclass.61

Figure S 2-7 LEfSe analysis of (A) FAPROTAX and (B) PICRUSt2 predicted functions showing temporal variation in functional potential of microbial communities in biochar amended soil. Comparison was made among no-plant samples with time as class and saturation status as subclass.61

LIST OF TABLES

Table 1-1 Lists of commonly used biofertilizers in agricultural fields.....	8
Table 1-2 Summary of network topological units.	13
Table 2-1 Characteristics of soil and wood-derived biochar.	39
Table 3-1 Soil chemical properties from 7-week samples.....	74
Table 3-2 Network topological properties of NT and TXVA network	86
Table 4-1 GenePix Microarray datasets downloaded from NCBI GEO database.	105
Table 4-2 Functional enrichment analysis of modules that are positively correlated with the time of desiccation. The enrichment analysis was performed using a DAVID functional enrichment tool.....	114

TABLE OF CONTENTS

ABSTRACT.....	ii
ACKNOWLEDGEMENTS	iv
DEDICATION	vi
LIST OF FIGURES.....	vii
LIST OF TABLES	x
Chapter 1.....	1
Introduction.....	1
Soybean rhizosphere microbiomes:.....	2
Biological nitrogen fixation:.....	5
Biofertilizers in the agricultural fields:	6
Biochar as a soil conditioner:	9
Effects of biochar on soil physicochemical properties:	11
Effects of biochar on microbial community:	11
Network analysis in microbial diversity and gene expression:.....	12
Microbial co-occurrence network:	14
Gene co-expression network:	15
References:.....	17
Chapter 2.....	28
Dairy Effluent-Saturated Biochar Alters Microbial Communities and Enhances Bermudagrass Growth and Soil Fertility	28
Introduction:	29
Materials and Methods:.....	33
Results:	38
Discussion:.....	45
Conclusions:	48
References:.....	50
Chapter 3.....	65
Effects of a Drought-Tolerant Bioinoculant on the Microbial Community in the Soybean Rhizosphere	65
Abstract:.....	65
Introduction:	66
Materials and Methods:.....	69
Results:	74
Discussion:.....	89
References:.....	94
Chapter 4.....	102
Construction and Analysis of Weighted Gene Co-expression Network of <i>Bradyrhizobium japonicum</i> Under Desiccation Stress.....	102
Abstract:	102
Introduction:	103
Materials & Methods:	105

Results:	109
Discussion:	117
References:	122
Chapter 5.....	127
Conclusion	127
References:	132

Chapter 1

Introduction

Microbial communities in soil play a significant role in maintaining the dynamics of biogeochemical cycles, and their association with plant roots is inevitable for plant health and development. More specifically, the rhizosphere microbiota and endosymbionts have direct impacts on the nutrition of the associated host plant. These interactions are more prominent in leguminous plants, such as soybeans, which have largely been studied as a model plant of high economic and nutritional value. To meet the growing demand for agricultural crops and decrease the use of synthetic fertilizers, development of biofertilizers has been gaining more attention in recent years. However, it is necessary to evaluate the impact of biofertilizers (e.g., bio-inoculants) in the soil microbiome, in addition to the plant growth and crop yield. Use of bio-inoculants in the rhizosphere may impose a positive or negative impact on the native microbial community in the rhizosphere. Most studies have made conclusions about the use of biofertilizers solely based on the observation of aboveground biomass. This may not truly reflect the complete picture of the effects of biofertilizers unless the overall impact on the soil microbiome is assessed. The aboveground qualities are mostly dependent upon the belowground biotic and abiotic properties. Therefore, in our study, we attempted to evaluate the effects of biofertilizer treatment on the belowground microbial community. Similarly, to develop such an inoculant we strove to decipher underlying molecular mechanisms in response to environmental stresses such as desiccation. We performed a network-based analysis to identify modules and hub genes in *Bradyrhizobium japonicum* under desiccation stress. This study provides us with a further understanding of gene

responses to the water stress and helps us develop a novel molecular marker for bio-inoculant selection and development. In addition to development of an efficient bio-inoculant, the persistence of the inoculant in the soil under abiotic stresses is another major concern. Biochar, a charcoal, has been acknowledged to alleviate the limitations of sustainable agriculture. We studied the effects of biochar amendment with dairy wastewater on plant growth, soil physicochemical properties, and microbial communities. This study will pave the way to increase the efficiency of biochar, thereby improving plant health and soil fertility.

Soybean rhizosphere microbiomes:

Rhizosphere is a narrow zone immediately surrounding the root surface of the plant. Plant species play a major role in shaping the structure of microbial communities in the rhizosphere. Soybean is one of the most valuable crops all over the world, accounting for 68% of legume crop production and 77% of the nitrogen fixed by them globally (Herridge et al., 2008). Its growth, vigor, and yield are greatly influenced by symbiotic association with the endosymbiont *B. japonicum*. Through the symbiotic relationship, the endosymbiont fix atmospheric nitrogen to ammonia and act as a personalized source of nitrogen to the host. Therefore, soybean requires minimum or no nitrogen fertilizers to be added in the soil as compared to 34 to 120 kg ha⁻¹ required for corn cultivation (Jankowski et al., 2018). In general, focusing on improvement of efficiency of symbiotic nitrogen fixation would cause estimated annual benefit of about \$1.07 billion in the U.S. alone (Tauer, 1989). Soybean is widely cultivated in many states of the U.S. for food, biodiesel, and oil, which accounts for 90% of the oil seed production (Herridge et al., 2008). In 2017, crop value production of soybean was estimated to be \$41 billion, second largest figure after corn in the U.S. (USDA, 2009).

Rhizosphere is a very complex and important microenvironment. The interactions of plants and microorganisms within the rhizosphere greatly affect the biogeochemical cycling of carbon, nitrogen, and phosphorus in the ecosystem (Xu et al., 2008). Exudates from plant roots, including carbohydrates, amino acids, organic acids, and flavonoids, are the major driving forces in the regulation of microbial diversity and activity in the rhizosphere (Philippot et al., 2013). The composition of rhizosphere microbial communities represents a subset of the populations present in bulk soil. Selection based on plant exudates causes differences in relative abundance of various microbial populations ranging from positively to negatively affecting plant growth. Key microbial communities exerting beneficial effects on plants include plant growth-promoting rhizobacteria (PGPR), symbiotic nitrogen-fixing bacteria, and arbuscular mycorrhizal (AM) fungi. PGPR can affect beneficial plant root-microbe interactions by modulating the availability of nutrients, inhibiting phytopathogens, and/or producing and releasing secondary metabolites. The most commonly found bacterial phyla in the soybean rhizosphere are Proteobacteria, Actinobacteria, Bacteroidetes, Nitrospirae, Frimicutes, Verrucomicrobia and Acidobacteria (Xu et al., 2008). Among them, proteobacteria are the most abundant, especially alpha-proteobacteria, which include rhizobia. Rhizobia belong to family Rhizobiaceae including several genera such as *Rhizobium*, *Azorhizobium*, *Allorhizobium*, *Sinorhizobium*, *Mesorhizobium*, and *Bradyrhizobium* (Castro-Sowinski et al., 2007). These bacteria establish a symbiotic association with their specific leguminous host plant, where *Bradyrhizobium* is the endosymbiont of soybean.

Over the past few decades, the advancement in next generation sequencing (NGS) technologies along with the ever-optimizing computational analysis tools has greatly enhanced the ability to articulate an enormous amount of microbial diversity as well as their functional potential. This has enabled us to study the vast majority of unculturable microbes in the environment. Several

molecular markers (J. Liang et al., 2014) including 16S rRNA genes have been used to study the phylogeny and diversity of microbial community from the environment which provides a low-cost alternative to the whole metagenome sequencing. The 16S rRNA gene contains highly conserved regions alternating with the hypervariable regions that have more than 1,000 times substitution rates than the former to identify heterogeneity (Peer et al., 1996). These conserved regions facilitate efficient priming sites for primer design, whereas hypervariable regions act as a molecular clock (Woese, 1987a). Additionally, conserved regions separate bacteria into different clades, while hypervariable regions provide a trustworthy estimation of evolutionary relationships and taxonomic information. These properties allow us to consider the 16S rRNA gene as an ideal molecular marker to study bacterial communities from different environments, including soil (Philippot et al., 2013), water, air, human gut, volcanic vents, deep ocean, and glaciers.

Although a few studies attempted to use full length of 16S rRNA gene sequences (Rosselli et al., 2016), it is still not widespread in use. Due to limitations in sequencing read length, partial sequences of rRNA genes have been largely used to decipher bacterial community up to the taxonomic depth of the species level. Nine hypervariable regions, independently or in combination, show their own strength and weaknesses. Some hypervariable regions (e.g., V2 and V8) possess low phylogenetic resolution at the phylum level in comparison to others (Yang et al., 2016). Therefore, the selection of partial sequence is contingent upon the community environment, host type, and research questions. In this study, we used the V3-V4 region, which allows for amplification of a broad spectrum of bacterial taxa with sufficient variability (García-López et al., 2020) along with reduced amplification of specific mitochondrial and chloroplast genes from host plants.

Biological nitrogen fixation:

Biological nitrogen fixation (BNF) contributes around half of annual nitrogen inputs into the biosphere. It is an important source of nitrogen in agriculture as well as natural ecosystems. BNF is carried out by a specialized group of prokaryotes, either in a free-living state or as an endosymbiont. Particularly, the latter case is called symbiotic nitrogen fixation (SNF).

SNF is a mutualistic relationship in which plants provide a niche and carbon source to bacteria in exchange for fixed atmospheric nitrogen such as ammonia. It involves a series of host-microbe interactions triggered by complex chemical compounds and structural modification. Root exudates such as flavonoids and iso-flavonoids from legume plants are recognized by a host specific endosymbiont, initiating the secretion of lipochitooligosaccharide known as nodulation (Nod) factors (Long, 1996). Nod factors induce the tight curling of root hairs, and thereby the colonized bacterial cells are entrapped within the curl (Fisher & Long, 1992). These bacteria invade the root hairs and migrate through an infection thread, a cellulosic tube formed by the extension of cellulosic plant cell wall, towards the root cortex. These cortical cells proliferate to form a swollen structure on roots, called a root nodule. Within the nodule, rhizobia divide rapidly and differentiate into swollen, misshapen, and branched cells, called bacteroids, which convert atmospheric di-nitrogen into ammonia. Bacteroids get surrounded by portion of the plant cell membrane, forming a sac-like structure known as symbiosomes (Fischer, 1994).

After formation of bacteroids, nitrogen fixation is triggered by *nif* and *fix* genes inside the oxygen depleted environment. These organisms reduce atmospheric nitrogen into ammonia with the help of nitrogenase, a complex enzyme that has two components, a heterotetrameric core (Mo-Fe protein) encoded by *nifD* and *nifK*, and a dinitrogenase reductase subunit (Fe protein) encoded

by *nifH* (Fischer, 1994; Rong Li et al., 2020). Regulation of *nifHDK* genes is governed by the transcriptional activator NifA (Fischer, 1994), which in turn controlled by the RegS/RegR two-component system and NifA self (H. Li et al., 2010). In addition to the nitrogenase complex, *fix* genes are also required for microaerobic respiration and heme biosynthesis within the nodule (Mesa et al., 2008). Finally, large proportion of fixed ammonia is absorbed in the plant cytosol and assimilated via glutamine synthetase/glutamate synthase to glutamic acids and other nitrogenous compounds, while small portion is assimilated by bacteroids via glutamate dehydrogenase (Ohyama & Kumazawa, 1980).

Biofertilizers in the agricultural fields:

Nitrogen, phosphorus, and potassium are the three main fertilizers used in agriculture and their demand in the world is constantly increasing over the past decades (FAO, 2019). Excess use of these chemical fertilizers can pollute air, ground water, and surface water by volatilization, leaching, and runoff, respectively. Growing public health issues involved in environmental hazards due to the increasing use and production of synthetic chemical fertilizers (USEPA, 1999; Von Blottnitz et al., 2006) necessitates the implementation of alternative fertilization in agriculture. Biofertilizers are a promising low-cost, environmentally friendly alternative to chemical fertilizers. These can benefit plant growth and crop yield via nitrogen fixation, phosphorus and potassium solubilization, inhibition of plant pathogens, and abiotic stress tolerance.

Specifically, in leguminous crops N-fixing biofertilizers have shown a great potential to lessen the increasing demand of chemical nitrogen fertilizers, thereby making nitrogen available to plants naturally. In 2015, nitrogen alone accounted for about 59% to the total fertilizer use in the U.S. (<https://www.epa.gov/report-environment>). *B. japonicum* is a known endosymbiont of

soybean plant that provides personalized source of nitrogen. Similarly, there are many other endosymbionts that fix atmospheric nitrogen for their specific host plants such as *Rhizobium*, *Sinorhizobium*, *Mesorhizobium*, and *Azorhizobium* (Bhattacharyya & Jha, 2012). Apart from these, diazotrophic bacteria such as *Azospirillum*, *Burkholderia*, *Clostridium*, and *Azotobacter* fix atmospheric nitrogen in the free-living state (Dal Cortivo et al., 2020; Trabelsi & Mhamdi, 2013). *Azospirillum* has been most successfully used in many parts of the world for several years now (Okon & Labandera-Gonzalez, 1994).

Several PGPRs are known to perform phosphate and potassium solubilization. Bacterial genera, such as *Achromobacter*, *Aerobacter*, *Agrobacterium*, *Bacillus*, *Burkholderia*, *Erwinia*, *Flavobacterium*, *Micrococcus*, *Pseudomonas* and *Rhizobium*, are capable of solubilizing insoluble inorganic phosphate compounds (Rodríguez & Fraga, 1999).

Transgenic plants have been developed to withstand abiotic and biotic stresses. However, development cost and regulations on genetically modified organism (GMO) make it an expensive choice in comparison to the bio-inoculant treatment. *Rhizobial* inoculants have been successfully used to increase the soybean yield in many parts of the world (Halwani et al., 2021) and protect plants from environmental stresses (Table 1-1). In a study of Egamberdieva and colleagues, *B. japonicum* as an inoculant has shown a synergistic effect with *Stenotrophomonas rhizophila* in nodulation and growth of soybean under salt stress (Egamberdieva, Jabborova, et al., 2016). In addition to legume plants, *Achromobacter piechaudii* ARV8 has been found to induce transient water stress tolerance in both tomato and pepper plants (Mayak et al., 2004). Rhizobacteria have also been found to alleviate plant drought stress. For example, *Paenibacillus polymyxa* B2 induced drought tolerance of *Arabidopsis thaliana* (Timmusk & Wagner, 1999). Similarly, maize plants

under drought stress performed well after inoculation with *Pseudomonas spp.* (Sandhya et al., 2010). Review of Trabelsi and Mhamdi has also summarized the impact of inoculants on soil microbial community, providing an overview of the importance and complexity of the interaction (Trabelsi and Mhamdi, 2013).

Table 1-1 Lists of commonly used biofertilizers in agricultural fields

Biofertilizer	Application method	Attributes	References
<i>Achromobacter piechaudii</i> ARV8	Seedling treated with bacterial suspension	Reduced transient water stress in tomato & pepper	(Mayak et al., 2004)
<i>Bacillus megaterium</i>	Seed inoculation	Increased yield in Wheat	(Dal Cortivo et al., 2020)
<i>Bradyrhizobium japonicum</i> <i>BDYD1</i> + <i>Stenotrophomonas rhizophila ep-17</i>	Seedling inoculation in mixture	Increased Soybean growth & nutrient uptake under salt stress	(Egamberdieva, Jabborova, et al., 2016)
<i>Paenibacillus polymyxa B2</i>	Soil inoculation	Enhanced drought tolerance of <i>Arabidopsis thaliana</i>	(Timmusk & Wagner, 1999)
<i>Bradyrhizobium japonicum</i> 532 C, USDA 30, USDA 31	Seed inoculation	Cold tolerant inoculant used in soybean field	(H. Zhang et al., 2003)
<i>Azospirillum brasilense</i> <i>Azospirillum lipoferum</i>	Field inoculation	Enhance overall plant growth, yield.	(Okon & Labandera-Gonzalez, 1994)
<i>Pseudomonas spp.</i>	Seed Inoculation	Enhance tomato growth & yield Increased growth, osmoregulation and antioxidant status of maize under drought	(Hernández-Montiel et al., 2017) (Sandhya et al., 2010)

Apart from nutrient enrichment activities, biofertilizers selectively enhance population of other PGPR and reduce the proportions of plant pathogens (Bhattacharyya & Jha, 2012). In fact, the initial composition of soil microbiomes (especially the presence of pathogen-suppressing *Pseudomonas* and *Bacillus*) could determine the fate of plant pathogenic disease (Wei et al., 2019). Some studies report shifts in overall microbial population, whereas in most of the studies bio-inoculant did not show differences in rhizosphere microbiomes (Dal Cortivo et al., 2020; Lottmann et al., 2000). In a study of Schwieger and Tebbe, inoculation of alfalfa plants with *Sinorhizobium meliloti* L33 strain selectively decreased the abundance of γ -proteobacteria and increased the abundance of α -proteobacteria in the rhizosphere soil (Schwieger & Tebbe, 2000). Similarly, actinomycetes strains such as *Streptomyces* spp., *Micromonospora* spp., *Thermobifida* spp. are known to confer protection against root pathogenic fungi (Bhattacharyya & Jha, 2012). *Streptomyces* spp. showed antagonism against *Pectobacterium carotovorum* that causes a soft rot disease in tomato (Dias et al., 2017). Some of the mechanisms by which PGPR fight phytopathogens include production of iron-chelating siderophores, antibiotics, and hydrogen cyanides (Bhattacharyya & Jha, 2012). Despite the beneficial potential of biofertilizers, their efficiency and persistence in the field is challenging due to differences in regional agricultural practices and environmental stress. Thus, an alternative strategy for sustainability could be the use of biochar as soil amendment in agricultural fields.

Biochar as a soil conditioner:

Biochar, also known as black carbon, is a charcoal used for soil conditioning. It is an organic material produced by the pyrolysis of biomass under limited oxygen concentrations or in the absence of oxygen (Lehmann, 2007). During the pyrolysis, biochar sequesters atmospheric

CO₂ into aromatic organic carbon that remains stable for prolonged time (Glaser, 2007). Although biochar basically contains crystalline sheet of graphene and amorphous aromatic compounds, its structural and functional properties vary largely due to feedstock materials used, and pyrolysis temperature and duration (Buss et al., 2018; Lehmann, 2007; Semida et al., 2019). Pyrolysis temperature generally ranges from 200-800°C. Feedstock materials include plant soft tissues (e.g., straw, leaves), wood, and organic wastes (e.g., sludge or manure).

The use of biochar to increase soil fertility in agriculture is dated back to 2,000 years ago from terra preta soil in the Amazon basin a.k.a. ‘Amazonian dark earth’ (N. J. H. Smith, 1980). Terra preta soil is extremely rich in soil organic matter and the nutrient properties have been preserved for centuries, thereby adding value to its agricultural use (Glaser, 2007). Currently, biochar is gaining enormous attention as a means for enhancing soil fertility, aiding sustainable agricultural production, alleviating adverse abiotic stresses, and improving soil biotic components. Positive impacts on plant productivity and nutrient cycling in multiple ecosystems (Biederman & Stanley Harpole, 2013) show its potential to keep the balance between food demand with increasing global population and sufficient food supply with enhancing crop yield. In addition to its synergistic effect with other agricultural practices, biochar gives added benefits by modifying bulk density in barren sandy soil (Głąb et al., 2016). Based on a number of studies, biochar has shown a great potential to be an environmentally friendly organic substitute in the field for long term benefit of agricultural productivity (Ding et al., 2017; A. Zhang et al., 2012). Adsorption of nutrient and minerals and relatively slower surface oxidation of biochar particles (B. Liang et al., 2006) ensure long term availability of nutrients and labile carbon to the plants (Hagemann et al., 2017). Biochar application could serve as an effective alternative to increase soybean yield by alleviating drought and salinity stresses (Y. Zhang et al., 2020).

Effects of biochar on soil physicochemical properties:

Changes in soil physicochemical properties due to a soil amendment with biochar have been widely studied. Biochar application has shown to increase porosity (Batista et al., 2018), bulk density (Głąb et al., 2016), pH (Buss et al., 2018), electrical conductivity (EC), cation exchange capacity (CEC) (B. Liang et al., 2006), and other micro/macro nutrients (Lehmann et al., 2003). Carbon and nitrogen can be accumulated by CO₂ sequestration or photosynthesis and BNF, respectively (Glaser, 2007). Niraula and colleagues found an increase in the ratio of nitrogen and phosphorus in the wood biochar amended soil in comparison to the control soil in a greenhouse experiment (Niraula et al., 2021). Retained nutrients in biochar have shown slow leaching rates in the Ferralsol, an upland soil of the Amazon basin (Lehmann et al., 2003). Such changes in soil properties have been largely found to enhance soil fertility and increase crop productivity. In addition, biochar sequesters nutrients, and thereby decreases their leaching rate. Biochar also increases aeration and soil water holding capacity due to high total porosity. It could retain more water in small pores to make it available for plants and microorganisms. Biochar has shown to increase bioavailable water capacity by more than 22% (Głąb et al., 2016; Peake et al., 2014).

Effects of biochar on microbial community:

In addition to the soil physicochemical properties, biochar influences soil biological properties to a greater extent. However, the effect of biochar on microbial community has received less attention. Several studies suggest that biochar application changes microbial abundance and alters the microbial composition (Jenkins et al., 2017; Palansooriya et al., 2019). Effects associated with changes in physical properties are less prominent than those triggered by chemical changes.

There are several mechanisms by which biochar can affect the microbial population. Included are porous structure and high surface area that provides a better habitat for the microbiota (Batista et al., 2018), a wide range of niches, increased pH, enhanced nutrient availability (Liao et al., 2019), increased water retention rate, adsorption of harmful chemicals, and surface areas for biofilm formation (Hill et al., 2019). Kim et al. observed a 25% increase in bacterial species richness in terra preta Anthrosols compared to pristine forest soil (Kim et al., 2007). An increase in abundance of N-fixing bacteria was observed in wood biochar amended bulk soil (Niraula et al., 2021). Biochar amendment also increased the abundance of N-fixing bacteria in the rhizosphere soil as well as abundance of other bacteria (e.g., Firmicutes and Bacteroidetes) that assimilate plant-derived carbon (Liao et al., 2019). In addition, there was a change in the rhizosphere bacterial community and diversity in response to biochar treatment. Similarly, biofilm formation by *Escherichia coli* on biochar surface and higher final cell densities suggest that biochar can potentially enhance the metabolic potential of microbes and protect them from stressful environmental conditions (Hill et al., 2019). Although biochar has significant impacts on microbial communities, the spatial and temporal variations because of natural phenomena remain prominent (Jenkins et al., 2017).

Network analysis in microbial diversity and gene expression:

Network analysis has been used in many fields including social sciences, psychology, microbial ecology (De Menezes et al., 2015), and gene interactions (Hu et al., 2018). Here, I have used the network-based analysis to explore the link between taxon in the soybean rhizosphere and the gene transcripts of its endosymbiont. The network properties are highly reproducible in various fields and can be used to extract subject-related information. Topological features of many

networks can be used to describe and compare a network to answer ecological questions that can merely be possible by general alpha and beta diversity analyses. Complex networks can be divided or clustered into densely connected sub-networks, called modules, which have strong connections among the nodes. Several topological measures can be used to describe the role of network members and their interactions such as degree, network betweenness, betweenness centrality, and clustering coefficient. Likewise, density, modularity, and global clustering coefficient are other parameters to define the whole network. These network topologies have been summarized in Table 1-2.

Table 1-2 Summary of network topological units.

Network Topology	Descriptions
Degree	Number of connections (edges) of a node (vertex)
Modularity	Measure of separability of densely connected sub networks.
Density	Complexity of a network
Clustering coefficient	Clustering coefficient of a node is a ratio of observed number of links between node's neighbors to number of all possible links between node's neighbors.
Betweenness centrality	The number of times a node (i.e., an item in the network) acts as a connector along the shortest path between two other nodes
Average path length	Average of the shortest paths between each pair of vertices.
Hub nodes	Nodes with large number of connections within a network or a module

Microbial co-occurrence network:

Alpha/beta diversity estimation and taxonomic abundances is a great way to access the response of microbial communities to the environmental factors. These methods, however, may not provide the information about their direct interaction and their role in ecological processes. Microbial co-occurrence network can lead us one step further to deciphering their interactions in intricate details. In addition, the next generation sequencing technology helps to directly identify microbial species in a greater detail. Thus, obtained presence-absence or abundance data can be used to construct networks to predict ecological relationships between microorganisms, change in their interaction pattern in response to environmental perturbation and their contributions in ecosystem processes. There are several dedicated tools to perform microbial co-occurrence network analysis such as MINAP, igraph, SparCC, CoNet, and SPIEC-EASI (Röttjers & Faust, 2018). The most used similarity-based network inference method uses correlation-based measures where the positive correlation indicates co-presence and negative correlation indicates mutual exclusion pattern of two species. In the network, a vertex represents an ASV/OTU/taxa, and the edge represents the strength of connection between two vertices. Although empirically the association is straightforward, the interpretation can be challenging since a single association may represent multiple ecological relationships. For example, co-presence can represent niche overlap, cross-feeding, co-aggregation in biofilms or co-colonization, whereas negative association can be due to amensalism, prey-predator relationship or competition (Faust & Raes, 2012).

Network topological features can be used to make meaningful biological interpretation of microbial interaction. For example, module clusters within a network may represent groups of

microbial species sharing same ecological niches (De Menezes et al., 2015). A node with high degree within a module represents an intramodular hub species that plays a central role in ecological functioning (Mendes et al., 2014).

Gene co-expression network:

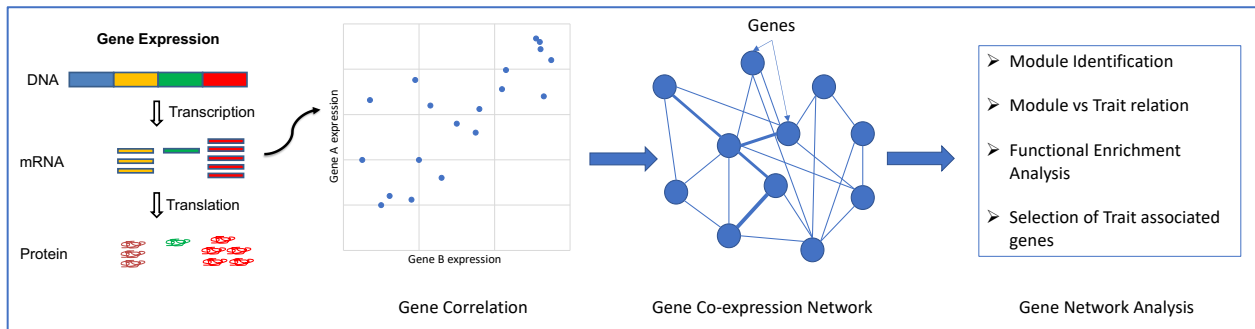


Figure 1-1 An example of a gene co-expression network.

Like the microbial co-occurrence network, gene co-expression network is constructed using the expression value of individual genes obtained from microarray or RNA-seq experiments (Figure 1-1). Here, I refer to nodes as genes or transcripts and connections between them as their expression pattern under certain condition. Based on the type of connection, these networks can be broadly classified as weighted and un-weighted network. In a weighted network, a connection represents the strength of correlation or adjacency, whereas in an un-weighted network connections solely represent presence or absence of co-expression at a given correlation threshold. Gene co-expression networks have been used in disease prediction (van Dam et al., 2018), functional gene annotation, pathway identification, marker gene identification (Hu et al., 2018), and functional association of modules with disease (Bakhtiarizadeh et al., 2018). Highly co-

expressed genes, identified by correlations/topological overlap, are clustered into modules that may represent certain biological functions or regulatory pathways (van Dam et al., 2018).

References:

- Bakhtiarizadeh, M. R., Hosseinpour, B., Shahhoseini, M., Korte, A., & Gifani, P. (2018). Weighted gene co-expression network analysis of endometriosis and identification of functional modules associated with its main hallmarks. *Frontiers in Genetics, 9*(OCT), 1–15. <https://doi.org/10.3389/fgene.2018.00453>
- Batista, E. M. C. C., Shultz, J., Matos, T. T. S., Fornari, M. R., Ferreira, T. M., Szpoganicz, B., De Freitas, R. A., & Mangrich, A. S. (2018). Effect of surface and porosity of biochar on water holding capacity aiming indirectly at preservation of the Amazon biome. *Scientific Reports, 8*(1), 1–9. <https://doi.org/10.1038/s41598-018-28794-z>
- Bhattacharyya, P. N., & Jha, D. K. (2012). Plant growth-promoting rhizobacteria (PGPR): Emergence in agriculture. *World Journal of Microbiology and Biotechnology, 28*(4), 1327–1350. <https://doi.org/10.1007/s11274-011-0979-9>
- Biederman, L. A., & Stanley Harpole, W. (2013). Biochar and its effects on plant productivity and nutrient cycling: A meta-analysis. *GCB Bioenergy, 5*(2), 202–214. <https://doi.org/10.1111/gcbb.12037>
- Buss, W., Shepherd, J. G., Heal, K. V., & Mašek, O. (2018). Spatial and temporal microscale pH change at the soil-biochar interface. *Geoderma, 331*(April), 50–52. <https://doi.org/10.1016/j.geoderma.2018.06.016>
- Castro-Sowinski, S., Herschkovitz, Y., Okon, Y., & Jurkevitch, E. (2007). Effects of inoculation with plant growth-promoting rhizobacteria on resident rhizosphere microorganisms. *FEMS*

Microbiology Letters, 276(1), 1–11. <https://doi.org/10.1111/j.1574-6968.2007.00878.x>

Dal Cortivo, C., Ferrari, M., Visioli, G., Lauro, M., Fornasier, F., Barion, G., Panozzo, A., & Vamerali, T. (2020). Effects of Seed-Applied Biofertilizers on Rhizosphere Biodiversity and Growth of Common Wheat (*Triticum aestivum* L.) in the Field. *Frontiers in Plant Science*, 11(February), 1–14. <https://doi.org/10.3389/fpls.2020.00072>

De Menezes, A. B., Prendergast-Miller, M. T., Richardson, A. E., Toscas, P., Farrell, M., Macdonald, L. M., Baker, G., Wark, T., & Thrall, P. H. (2015). Network analysis reveals that bacteria and fungi form modules that correlate independently with soil parameters. *Environmental Microbiology*, 17(8), 2677–2689. <https://doi.org/10.1111/1462-2920.12559>

Dias, M. P., Bastos, M. S., Xavier, V. B., Cassel, E., Astarita, L. V., & Santarém, E. R. (2017). Plant growth and resistance promoted by *Streptomyces* spp. in tomato. *Plant Physiology and Biochemistry*, 118, 479–493. <https://doi.org/10.1016/j.plaphy.2017.07.017>

Ding, Y., Liu, Y., Liu, S., Huang, X., Li, Z., Tan, X., Zeng, G., & Zhou, L. (2017). Potential Benefits of Biochar in Agricultural Soils: A Review. *Pedosphere*, 27(4), 645–661. [https://doi.org/10.1016/S1002-0160\(17\)60375-8](https://doi.org/10.1016/S1002-0160(17)60375-8)

Egamberdieva, D., Jabborova, D., & Berg, G. (2016). Synergistic interactions between *Bradyrhizobium japonicum* and the endophyte *Stenotrophomonas rhizophila* and their effects on growth, and nodulation of soybean under salt stress. *Plant and Soil*, 405(1–2), 35–45. <https://doi.org/10.1007/s11104-015-2661-8>

FAO. (2019). *World fertilizer trends and outlook to 2022*.

- Faust, K., & Raes, J. (2012). Microbial interactions: From networks to models. *Nature Reviews Microbiology*, 10(8), 538–550. <https://doi.org/10.1038/nrmicro2832>
- Fischer, H.-M. (1994). Genetic regulation of nitrogen fixation in Rhizobia. *Microbiological Reviews*, 58(3), 352–386.
- Fisher, R. F., & Long, S. R. (1992). Rhizobium-plant signal exchange. *Nature*, 357(6380), 655–660. <https://doi.org/10.1038/357655a0>
- García-López, R., Cornejo-Granados, F., Lopez-Zavala, A. A., Sánchez-López, F., Cota-Huizar, A., Sotelo-Mundo, R. R., Guerrero, A., Mendoza-Vargas, A., Gómez-Gil, B., & Ochoa-Leyva, A. (2020). Doing more with less: A comparison of 16S hypervariable regions in search of defining the shrimp microbiota. *Microorganisms*, 8(1). <https://doi.org/10.3390/microorganisms8010134>
- Głąb, T., Palmowska, J., Zaleski, T., & Gondek, K. (2016). Effect of biochar application on soil hydrological properties and physical quality of sandy soil. *Geoderma*, 281, 11–20. <https://doi.org/10.1016/j.geoderma.2016.06.028>
- Glaser, B. (2007). Prehistorically modified soils of central Amazonia: A model for sustainable agriculture in the twenty-first century. *Philosophical Transactions of the Royal Society B: Biological Sciences*, 362(1478), 187–196. <https://doi.org/10.1098/rstb.2006.1978>
- Hagemann, N., Joseph, S., Schmidt, H. P., Kammann, C. I., Harter, J., Borch, T., Young, R. B., Varga, K., Taherymoosavi, S., Elliott, K. W., McKenna, A., Albu, M., Mayrhofer, C., Obst, M., Conte, P., Dieguez-Alonso, A., Orsetti, S., Subdiaga, E., Behrens, S., & Kappler, A.

- (2017). Organic coating on biochar explains its nutrient retention and stimulation of soil fertility. *Nature Communications*, 8(1), 1–11. <https://doi.org/10.1038/s41467-017-01123-0>
- Halwani, M., Reckling, M., Egamberdieva, D., Omari, R. A., Bellingrath-Kimura, S. D., Bachinger, J., & Bloch, R. (2021). Soybean Nodulation Response to Cropping Interval and Inoculation in European Cropping Systems. *Frontiers in Plant Science*, 12(June). <https://doi.org/10.3389/fpls.2021.638452>
- Hernández-Montiel, L. G., Chiquito-Contreras, C. J., Murillo-Amador, B., Vidal-Hernández, L., Quiñones-Aguilar, E. E., & Chiquito-Contreras, R. G. (2017). Efficiency of two inoculation methods of *Pseudomonas putida* on growth and yield of tomato plants. *Journal of Soil Science and Plant Nutrition*, 17(4), 1003–1012. <https://doi.org/10.4067/S0718-95162017000400012>
- Herridge, D. F., Peoples, M. B., & Boddey, R. M. (2008). Global inputs of biological nitrogen fixation in agricultural systems. In *Plant and Soil*. <https://doi.org/10.1007/s11104-008-9668-3>
- Hill, R. A., Hunt, J., Sanders, E., Tran, M., Burk, G. A., & Mlsna, T. E. (2019). Effect of Biochar on Microbial Growth: A Metabolomics and Bacteriological Investigation in *E. coli*. *Environmental Science and Technology*, 53(5), 2635–2646. <https://doi.org/10.1021/acs.est.8b05024>.Effect
- Hu, Y., Pan, J., Xin, Y., Mi, X., Wang, J., Gao, Q., & Luo, H. (2018). Gene expression analysis reveals novel gene signatures between young and old adults in human prefrontal cortex. *Frontiers in Aging Neuroscience*, 10(AUG), 1–15. <https://doi.org/10.3389/fnagi.2018.00259>

- Jankowski, K. J., Neill, C., Davidson, E. A., Macedo, M. N., Costa, C., Galford, G. L., Maracahipes Santos, L., Lefebvre, P., Nunes, D., Cerri, C. E. P., McHorney, R., O'Connell, C., & Coe, M. T. (2018). Deep soils modify environmental consequences of increased nitrogen fertilizer use in intensifying Amazon agriculture. *Scientific Reports*, 8(1), 1–11. <https://doi.org/10.1038/s41598-018-31175-1>
- Jenkins, J. R., Viger, M., Arnold, E. C., Harris, Z. M., Ventura, M., Miglietta, F., Girardin, C., Edwards, R. J., Rumpel, C., Fornasier, F., Zavalloni, C., Tonon, G., Alberti, G., & Taylor, G. (2017). Biochar alters the soil microbiome and soil function: results of next-generation amplicon sequencing across Europe. *GCB Bioenergy*, 9(3), 591–612. <https://doi.org/10.1111/gcbb.12371>
- Kim, J. S., Sparovek, G., Longo, R. M., De Melo, W. J., & Crowley, D. (2007). Bacterial diversity of terra preta and pristine forest soil from the Western Amazon. *Soil Biology and Biochemistry*, 39(2), 684–690. <https://doi.org/10.1016/j.soilbio.2006.08.010>
- Lehmann, J. (2007). Bio-energy in the black. *Frontiers in Ecology and the Environment*, 5(7), 381–387. <https://doi.org/10.4324/9780203007020-14>
- Lehmann, J., Pereira da Silva Jr, J., Steiner, C., Nehls, T., Zech, W., & Glaser, B. (2003). Nutrient availability and leaching in an archaeological Anthrosol and a Ferralsol of the Central Amazon basin: fertilizer, manure and charcoal amendments. *Plant And*, 249, 343–357.
- Li, H., Xu, F., Ren, X., & Chen, S. (2010). Functional analysis of the fixL/fixJ and fixK genes in *Azospirillum brasilense* Sp7. *Annals of Microbiology*, 60(3), 469–480. <https://doi.org/10.1007/s13213-010-0065-9>

- Liang, B., Lehmann, J., Solomon, D., Kinyangi, J., Grossman, J., O'Neill, B., Skjemstad, J. O., Thies, J., Luizão, F. J., Petersen, J., & Neves, E. G. (2006). Black Carbon Increases Cation Exchange Capacity in Soils. *Soil Science Society of America Journal*, 70(5), 1719–1730. <https://doi.org/10.2136/sssaj2005.0383>
- Liang, J., Sun, S., Ji, J., Wu, H., Meng, F., Zhang, M., Zheng, X., Wu, C., & Zhang, Z. (2014). Comparison of the rhizosphere bacterial communities of zigongdongdou soybean and a high-methionine transgenic line of this cultivar. *PLoS ONE*, 9(7), 1–10. <https://doi.org/10.1371/journal.pone.0103343>
- Liao, H., Li, Y., & Yao, H. (2019). Biochar Amendment Stimulates Utilization of Plant-Derived Carbon by Soil Bacteria in an Intercropping System. *Frontiers in Microbiology*, 10(June), 1–13. <https://doi.org/10.3389/fmicb.2019.01361>
- Long, S. R. (1996). Rhizobium symbiosis: Nod factors in perspective. *Plant Cell*, 8(10), 1885–1898. <https://doi.org/10.1105/tpc.8.10.1885>
- Lottmann, J., Heuer, H., Vries, J. D., Mahn, A., During, K., Wackernagel, W., Smalla, K., & Berg, G. (2000). Establishment of introduced antagonistic bacteria in the rhizosphere of transgenic potatoes and their effect on the bacterial community. *FEMS Microbiology Ecology*, 33(1), 41–49. [https://doi.org/10.1016/S0168-6496\(00\)00042-8](https://doi.org/10.1016/S0168-6496(00)00042-8)
- Mayak, S., Tirosh, T., & Glick, B. R. (2004). Plant growth-promoting bacteria that confer resistance to water stress in tomatoes and peppers. *Plant Science*, 166(2), 525–530. <https://doi.org/10.1016/j.plantsci.2003.10.025>

- Mendes, L. W., Kuramae, E. E., Navarrete, A. A., Van Veen, J. A., & Tsai, S. M. (2014). Taxonomical and functional microbial community selection in soybean rhizosphere. *ISME Journal*, 8(8), 1577–1587. <https://doi.org/10.1038/ismej.2014.17>
- Mesa, S., Hauser, F., Friberg, M., Malaguti, E., Fischer, H. M., & Hennecke, H. (2008). Comprehensive assessment of the regulons controlled by the FixLJ-FixK 2-FixK1 cascade in *Bradyrhizobium japonicum*. *Journal of Bacteriology*, 190(20), 6568–6579. <https://doi.org/10.1128/JB.00748-08>
- Niraula, S., Choi, Y. K., Payne, K., Muir, J. P., Kan, E., & Chang, W. S. (2021). Dairy effluent-saturated biochar alters microbial communities and enhances bermudagrass growth and soil fertility. *Agronomy*, 11(9). <https://doi.org/10.3390/agronomy11091794>
- Ohyama, T., & Kumazawa, K. (1980). Nitrogen assimilation in soybean nodules ii 15n2assimilation in bacteroid and cytosol fractions of soybean nodules. *Soil Science and Plant Nutrition*, 26(2), 205–213. <https://doi.org/10.1080/00380768.1980.10431204>
- Okon, Y., & Labandera-Gonzalez, C. A. (1994). Agronomic applications of azospirillum: An evaluation of 20 years worldwide field inoculation. *Soil Biology and Biochemistry*, 26(12), 1591–1601. [https://doi.org/10.1016/0038-0717\(94\)90311-5](https://doi.org/10.1016/0038-0717(94)90311-5)
- Palansooriya, K. N., Wong, J. T. F., Hashimoto, Y., Huang, L., Rinklebe, J., Chang, S. X., Bolan, N., Wang, H., & Ok, Y. S. (2019). Response of microbial communities to biochar-amended soils: a critical review. *Biochar*, 1(1), 3–22. <https://doi.org/10.1007/s42773-019-00009-2>

- Peake, L. R., Reid, B. J., & Tang, X. (2014). Quantifying the influence of biochar on the physical and hydrological properties of dissimilar soils. *Geoderma*, 235–236, 182–190. <https://doi.org/10.1016/j.geoderma.2014.07.002>
- Peer, Y. Van De, Chapelle, S., Wachter, R. De, Biochemie, D., Uia, U. A., & Antwerpen, B.-. (1996). *A quantitative map of nucleotide substitution rates in bacterial rRNA*. 24(17), 3381–3391.
- Philippot, L., Raaijmakers, J. M., Lemanceau, P., & Van Der Putten, W. H. (2013). Going back to the roots: The microbial ecology of the rhizosphere. *Nature Reviews Microbiology*, 11(11), 789–799. <https://doi.org/10.1038/nrmicro3109>
- Rodríguez, H., & Fraga, R. (1999). Phosphate solubilizing bacteria and their role in plant growth promotion. *Biotechnology Advances*, 17(4–5), 319–339. [https://doi.org/10.1016/S0734-9750\(99\)00014-2](https://doi.org/10.1016/S0734-9750(99)00014-2)
- Rong Li, Chen, H., Yang, Z., Yuan, S., & Zhou, X. (2020). Research status of soybean symbiosis nitrogen fixation. *Oil Crop Science*, 5(1), 6–10. <https://doi.org/10.1016/j.ocsci.2020.03.005>
- Rosselli, R., Romoli, O., Vitulo, N., Vezzi, A., Campanaro, S., De Pascale, F., Schiavon, R., Tiarca, M., Poletto, F., Concheri, G., Valle, G., & Squartini, A. (2016). Direct 16S rRNA-seq from bacterial communities: A PCR-independent approach to simultaneously assess microbial diversity and functional activity potential of each taxon. *Scientific Reports*, 6(August), 1–12. <https://doi.org/10.1038/srep32165>
- Röttgers, L., & Faust, K. (2018). From hairballs to hypotheses—biological insights from microbial

networks. *FEMS Microbiology Reviews*, 42(6), 761–780.
<https://doi.org/10.1093/femsre/fuy030>

Sandhya, V., Ali, S. Z., Grover, M., Reddy, G., & Venkateswarlu, B. (2010). Effect of plant growth promoting *Pseudomonas* spp. on compatible solutes, antioxidant status and plant growth of maize under drought stress. *Plant Growth Regulation*, 62(1), 21–30.
<https://doi.org/10.1007/s10725-010-9479-4>

Schwieger, F., & Tebbe, C. C. (2000). Effect of field inoculation with *Sinorhizobium meliloti* L33 on the composition of bacterial communities in rhizospheres of a target plant (*Medicago sativa*) and a non-target plant (*Chenopodium, album*) - Linking of 16S rRNA gene-based single-strand conforma. *Applied and Environmental Microbiology*, 66(8), 3556–3565.
<https://doi.org/10.1128/AEM.66.8.3556-3565.2000>

Semida, W. M., Beheiry, H. R., Sétamou, M., Simpson, C. R., Abd El-Mageed, T. A., Rady, M. M., & Nelson, S. D. (2019). Biochar implications for sustainable agriculture and environment: A review. *South African Journal of Botany*, 127, 333–347.
<https://doi.org/10.1016/j.sajb.2019.11.015>

Smith, N. J. H. (1980). Anthrosols and Human Carrying Capacity in Amazonia. *Annals of the Association of American Geographers*, 70(4), 553–566.

Tauer, L. W. (1989). Economic impact of future biological nitrogen fixation technologies on United States agriculture. *Plant and Soil*. <https://doi.org/10.1007/BF02370418>

Timmusk, S., & Wagner, E. G. H. (1999). The plant-growth-promoting rhizobacterium

- Paenibacillus polymyxa induces changes in Arabidopsis thaliana gene expression: A possible connection between biotic and abiotic stress responses. *Molecular Plant-Microbe Interactions*, 12(11), 951–959. <https://doi.org/10.1094/MPMI.1999.12.11.951>
- Trabelsi, D., & Mhamdi, R. (2013). Microbial inoculants and their impact on soil microbial communities: A review. *BioMed Research International*, 2013. <https://doi.org/10.1155/2013/863240>
- USDA. (2009). World agricultural supply and demand estimates (WASDE). In *Usda*. <http://www.usda.gov/oce/commodity/wasde/>
- USEPA. (1999). *Estimating Risk from Contaminants Contained in Agricultural Fertilizers Draft Report*. August, 1–160.
- van Dam, S., Vösa, U., van der Graaf, A., Franke, L., & de Magalhães, J. P. (2018). Gene co-expression analysis for functional classification and gene-disease predictions. *Briefings in Bioinformatics*, 19(4), 575–592. <https://doi.org/10.1093/bib/bbw139>
- Von Blottnitz, H., Rabl, A., Boiadjev, D., Taylor, T., & Arnold, S. (2006). Damage costs of nitrogen fertilizer in Europe and their internalization. *Journal of Environmental Planning and Management*, 49(3), 413–433. <https://doi.org/10.1080/09640560600601587>
- Wei, Z., Gu, Y., Friman, V. P., Kowalchuk, G. A., Xu, Y., Shen, Q., & Jousset, A. (2019). Initial soil microbiome composition and functioning predetermine future plant health. *Science Advances*, 5(9), 1–12. <https://doi.org/10.1126/sciadv.aaw0759>
- Woese, C. R. (1987). Bacterial Evolution Background

Microbiology. <https://doi.org/10.1139/m88-093>

- Yang, B., Wang, Y., & Qian, P.-Y. (2016). Sensitivity and correlation of hypervariable regions in 16S rRNA genes in phylogenetic analysis. *BMC Bioinformatics*, *17*(1), 135. <https://doi.org/10.1186/s12859-016-0992-y>
- Zhang, A., Bian, R., Pan, G., Cui, L., Hussain, Q., Li, L., Zheng, J., Zheng, X., Han, X., & Yu, X. (2012). Effects of biochar amendment on soil quality, crop yield and greenhouse gas emission in a Chinese rice paddy: A field study of 2 consecutive rice growing cycles. *Field Crops Research*, *127*, 153–160.
- Zhang, H., Prithiviraj, B., Charles, T. C., Driscoll, B. T., & Smith, D. L. (2003). Low temperature tolerant *Bradyrhizobium japonicum* strains allowing improved nodulation and nitrogen fixation of soybean in a short season (cool spring) area. *European Journal of Agronomy*, *19*(2), 205–213. [https://doi.org/10.1016/S1161-0301\(02\)00038-2](https://doi.org/10.1016/S1161-0301(02)00038-2)
- Zhang, Y., Ding, J., Wang, H., Su, L., & Zhao, C. (2020). Biochar addition alleviate the negative effects of drought and salinity stress on soybean productivity and water use efficiency. *BMC Plant Biology*, *20*(1), 1–11. <https://doi.org/10.1186/s12870-020-02493-2>

Chapter 2

Dairy Effluent-Saturated Biochar Alters Microbial Communities and Enhances Bermudagrass Growth and Soil Fertility

Sarbjee Niraula ¹, Yong-Keun Choi ², Kristen Payne ³, James P. Muir ^{4,5}, Eunsung Kan ^{4,5,*} and Woo-Suk Chang ¹

Recently, biochar has been proposed for various agronomic applications including improved plant growth and soil fertility. In this study, the effects of dairy effluent-saturated (SBC) and unsaturated wood-derived biochar (UBC) on Bermudagrass (*Cynodon* spp.) growth, soil fertility and microbial communities were investigated in a greenhouse pot study. SBC and UBC were mixed with sandy loam soil at various loading rates (0, 1, 2, 4, and 8%) to grow Bermudagrass for 10 weeks. Soil physicochemical properties and plant growth measurements were taken, followed by 16S rRNA (V3-V4) amplicon sequencing of soil bacterial communities. Amendment of SBC to soil altered the soil physicochemical properties and increased the concentrations of N and P in the soil at 2 to 8% loading rates compared to UBC treated soil. The addition of SBC to soil also increased the overall plant biomass compared to UBC with more effects on aboveground biomass. Differential abundance analysis of taxa showed enrichment of Proteobacteria in UBC-amended soil, whereas *Firmicutes* and *Nitrospirae* were abundant in SBC-amended soil. Interestingly, enrichment of photosynthetic and N-fixing bacteria was observed in both SBC and UBC-amended soils after 10 weeks of treatments. However, oxidative phosphorylation and biotin metabolisms were found to be more abundant in SBC-amended soil compared to UBC-amended soil. Overall, our study suggested that amendment of SBC to soil resulted in enhanced soil

nutrients, microbial capacity and Bermudagrass growth than that of UBC. Therefore, application of SBC to soil in field trials would be merited to identify sustainable and effective practices for enhancing plant growth, soil fertility and soil bacterial community.

Introduction:

Biochar (BC) is a porous carbon material produced by thermal conversion (i.e., pyrolysis) of organic matter under limited oxygen concentration (Lehmann, 2007). It exhibits a wide range of physicochemical properties based on feedstock (Batista et al., 2018), pyrolysis conditions (Steinbeiss et al., 2009), and nutrient saturation onto BC (Kizito et al., 2019). It also shows high potential in sustainable agriculture for mitigating greenhouse gas (GHG) emission (Lehmann, 2007; A. Zhang et al., 2012). However, outcomes of BC application in agricultural fields are greatly influenced by soil types, BC-soil mixture ratios, and climatic conditions (Jeffery et al., 2011; Kizito et al., 2019). Thus, a substantial knowledge gap exists for optimizing the use of BC in agriculture.

Use of charred biomass in agriculture dates back several thousand years as evidenced by the studies of “Terra Preta” soil in the Amazon basin (Glaser, 2007). Observation of the fertile nature of such soil vis-à-vis surrounding soils led to production and use of biochar in modern agriculture. BC, as a soil amendment, increases fertility of soil (Ding et al., 2016) thereby enhancing crop yield and plant biomass (Jeffery et al., 2011). It increases cation exchange capacity (CEC) (B. Liang et al., 2006) and availability of organic carbon, and microbial activity (Domene et al., 2014) while providing buffering capacity to maintain appropriate pH (Buss et al., 2018; Pandit et al., 2018). As much as a 10-fold increase in crop productivity has been observed in biochar-amended fields (Jeffery et al., 2011). Sequestered C in BC remains in the soil for prolonged periods, acting as a C

sink (Glaser, 2007). BC produced by slow pyrolysis under medium temperature (300 to 600 °C) sequesters more C than that under relative higher temperature (600 to 900 °C) (Ding et al., 2017). In addition to CO₂, it also reduces emission of other harmful GHG including CH₄, and N₂O as opposed to traditional manure application (A. Zhang et al., 2012). The environmentally friendly nature of BC gives added benefits to its widespread use in agriculture.

With increased porosity and water retention capacity, BC exhibit heterogenous ionic properties that determine its ability to retain nutrients from soil, added manure or fertilizer by adsorption (Mukherjee et al., 2011). Organic coating on the manure-amended biochar or soil aged biochar provides labile nutrients rather than biochar surface oxidation (Hagemann et al., 2017). Therefore, amendment of biochar with nutrient compounds before application in the field could achieve optimum short-term benefits from low application rates. Most studies suggest that biochar application rates of more than 10 Mg ha⁻¹ enhance crop yields under field condition (Kizito et al., 2019; Pandit et al., 2018), which might not be economically feasible from a farm perspective. Biochar increases crop yield performance only in the second and third year after application, suggesting soil delayed acclimatization under field conditions (Pandit et al., 2018; A. Zhang et al., 2012).

BC can adsorb N, P, K, and organic matter from anaerobic digestates, livestock wastewater and landfill leachates (Hale et al., 2013; Kizito et al., 2019; Y. Yao et al., 2012) and prevents leaching of nutrients through soil profiles (Y. Yao et al., 2012). Yao and co-workers (Y. Yao et al., 2012) observed that peanut hull BC pyrolyzed at 600 °C reduced the total amount of NO₃⁻, NH₄⁺, and PO₄³⁻ in leachates by 34, 34.7, and 20.6%, respectively, from sandy soil. BC is more stable than most soil organic matter, therefore, nutrients from dairy effluents become available to plants over

longer periods. Meta-analysis shows greater crop yield potential of BC, especially in low nutrient, acidic soils in high-rainfall tropical regions (Jeffery et al., 2017). Dairies in Texas are mostly concentrated in regions with sandy loam soil, low in organic matter and prone to drought. Several BC types, including those derived from hardwood, increase water holding capacity of sandy loam soil with low organic matter (Basso et al., 2013; Batista et al., 2018). Therefore, in our study, we saturated BC with dairy effluents that could be a promising alternative to improving sandy soil nutrient and water holding efficiency in terms of application rate, availability of nutrients, and waste management.

Soil microbiomes play a crucial role in agricultural fields by regulating dynamics of biogeochemical cycle. The complexity of microbial communities in soil is largely governed by soil physicochemical properties. pH fluctuations (Domene et al., 2014), water retention capacity (Batista et al., 2018), C-N ratio, and surface area for biological activities are key factors governing changes in the biological properties of the soil (Lehmann et al., 2011). Labile organic carbon and other nutrients leaching from BC serve as substrates for soil organic matter degradation to support microbial growth for an extended period (J. L. Smith et al., 2010). Therefore, BC has been used as a soil conditioner in soil with low organic matter and nutrients (Kizito et al., 2019). However, the availability of those substrates is dependent upon BC mineralization degree and rate by abiotic and biotic means (Lehmann et al., 2011). On the other hand, BC-mediated changes in soil microbiota can also be dependent upon the amount of BC applied. Yao and co-workers (Q. Yao et al., 2017) observed a change in the type of microbes in soil in response to the BC-soil mixture ratio. Therefore, further study of biotic factors is imperative to better understand the mode of action by which BC improves overall soil health.

BC-induced changes in soil biological properties can be assessed by evaluating soil microbial community structure and their functional potentials. Increased soil fertility following BC application is attributed to an increase in microbial biomass and diversity in addition to the availability of nutrients (Domene et al., 2014; Sun et al., 2013). BC amendment has a synergistic effect in the rhizosphere by enhancing colonization of rhizobia that assimilate plant-derived carbon (Liao et al., 2019). Variations in the type of microorganisms being colonized are greatly influenced by the BC property associated with the type of organic matter being pyrolyzed (Steinbeiss et al., 2009). Such properties leave the mechanisms by which BC affects microbiome composition and abundance relatively underexplored.

Although studies have determined effects of BC on plant growth, soil fertility, and microbial communities, few examined the effects of dairy effluent nutrient-saturated BC on plant growth, soil fertility, and microbial communities compared with pristine BC (without any nutrient loading). In our study, our objective was to compare the effect of unsaturated (raw) wood-derived BC (UBC) and dairy effluent nutrient-saturated wood-derived BC (SBC) on the growth of Bermudagrass (*Cynodon* spp.), soil fertility, and microbial communities in the rhizosphere and bulk soil. We used Bermudagrass (*Cynodon* spp.) to evaluate the effects of BC on plant growth because it is a widely cultivated pantropical grass used around dairies in north Texas as a forage. The 16S rRNA amplicon sequencing was performed to assess the taxonomy, alpha-beta diversity and functional potential of soil bacterial community. The statistical correlations among plant growth, soil fertility and microbial community for the application of BC on Bermudagrass were investigated.

Materials and Methods:

Soil and BC Preparation:

Sandy loam soil collected from the top 20 cm of Windthorst fine sandy loams, (fine, mixed, thermic, Udic Paleustaf) was used in our pot experiment (Muir et al., 2017; United States Department of Agriculture Soil Conservation Service, 1973). Sandy loam soils are prevalent in North Texas where dairy concentrated animal feeding operations exist; however, it possesses low nutrients, and low water holding capacity vis-à-vis what forage crops grown for those dairies require. We used BC (produced from pine chip) purchased from Confluence Energy (Kremmling, CO, USA). This was ground and sieved ($< 100 \mu\text{m}$) for greater effective soil properties. We saturated BC with the nutrients in dairy effluent taken from the 2nd lagoon of Southwest Regional Dairy Center at Tarleton State University (Stephenville, TX, USA). To saturate the nutrients (mostly N and P) onto BC, 1 L of the dairy effluent was stirred at 150 rpm with 100 g of BC for 3 days. The dairy effluent nutrient-saturated BC (SBC) was centrifuged at 3500 rpm for 10 min and dried at 60°C for 12 h prior to incorporating into pot soil. The pristine BC (UBC), without any nutrient loading from dairy effluent, was incorporated directly after sieving.

Greenhouse procedures:

In a greenhouse located at Texas A&M AgriLife Research Center, Texas A&M University (Stephenville, TX, USA), SBC or UBC was added to sandy loam soil at 0, 1, 2, 4, and 8% of soil on a dry weight basis and mixed in 1.2-L pots by hand. A total of 1193 g of soil mixture in each pot contained 11.93, 23.86, 47.72, and 95.44 g of BC to make 1, 2, 4, and 8% BC, respectively

(Figure S 2-1). Soil in pots with SBC and UBC at 2% and 4% BC rates were compared to no-plant samples and measurements were taken at initial and final time points.

Because Bermudagrass propagates vegetatively, it was pre-cultured before the experiment, and a 15 cm sprig was transplanted into each pot. Pots were watered using 100 mL of reverse osmosis water every 3 days. The pot experiment was conducted in the greenhouse for 70 days with controlled temperature (28 °C) and relative humidity (<40% RH). All treatment combinations were applied in triplicate pots constituting three blocks which consisted of tables within the greenhouse.

Bermudagrass growth measurement:

The number of leaves per plant was recorded at 1-week intervals during the pot experiments (70 days to observe the effects of BC on the plant growth). Plant growth was measured in the afternoon (1600 to 1800 h).

Soil and Bermudagrass analyses:

On Days 0 and 70, the soil in each pot was sampled for element composition analyses. The elemental composition of the soils with various ratios of BC addition (0–8%) was determined by an inductively coupled plasma emission spectroscopy (Spectro Radial Modula ICP, Spectro analytical Instruments). On Day 70, Bermudagrass was cut at the base and separated from washed roots. After harvesting the plants, stems and roots were dried at 55 °C in a forced-air oven until weight loss ceased, weighed, and then ground through a 1-mm screen using a shear mill. Carbon and N contents (percentage and yield on a dry matter basis) in stem and root were determined by combustion using an Elementar vario Macro C and N analyzer (Elementar Americas, Inc., Mt. Laurel, NJ, USA).

Microbial community analysis in bulk and rhizosphere soil:

Library preparation and sequencing:

Rhizosphere soils were collected from each pot and genomic DNA was extracted in triplets using DNeasy PowerSoil Kit, Qiagen, Hilden, Germany as recommended by the manufacturer. 16SrRNA V3-V4 hypervariable region was PCR amplified using Illumina adaptor ligated universal primers 341F (5'-tcgtcggcagcgtcagatgtgtataagagacagCCTACGGGNGGCWGCAG-3') and 806R (5'-gtctcgtgggctcggagatgtgtataagagacagGACTACNVGGGTWTCTAAT-3') from each triplet. The thermocycler condition was maintained at 94 °C for 3 min, followed by 25 cycles of 94 °C for 30 sec, 55 °C for 30 sec, 72 °C for 30 sec and a final extension of 72 °C for 3 min. PCR products were gel extracted visually in 1% agarose gel and purified by using QIAquick Gel Extraction Kit, Qiagen, Hilden, Germany. Purified PCR products in triplets were mixed in equal concentration for each sample and sent to Genomics and Bioinformatics Service, College Station, TX, USA, for further library preparation and sequencing in Illumina MiSeq V3 sequencer to produce 300 bp paired end reads. The raw sequencing data were deposited in the NCBI Sequence Read Archive (SRA) database with the BioProject accession ID PRJNA758431 (SRR15671103-SRR15671121).

Bioinformatics for read processing:

Sequences were analyzed using QIIME 2-2019.7 (Bolyen et al., 2018). Briefly, demultiplexed paired end sequences were denoised, dereplicated, and chimera filtered using DADA2 (Callahan et al., 2016) plugin with the following input parameters; —p-trim-left-f 17, —p-trunc-len-f 280, —p-trim-left-r 20, —p-trunc-len-r 200. Thus, produced amplicon sequence variants (ASVs), considered as 100% Operational taxonomic units (OTUs), were clustered to 97% OTUs (named

as OTUs from here onwards) by using open reference-based clustering algorithm in vsearch plugin against trained GreenGenes 13_8 database. To train the database, V3-V4 region of reference reads were extracted using our primer set followed by assigning taxonomy using naïve-bayes classifier in feature-classifier plugin. Singleton ASVs were filtered out prior to clustering to reduce possible sequencing artifacts. Clustered OTUs were further aligned using mafft (Kato et al., 2002) (via q2-alignment) to construct a phylogenetic tree with fasttree2 (Price et al., 2010) (via q2-phylogeny). Taxonomies were assigned from trained GreenGenes 13_8 97% OTUs (McDonald et al., 2012) using naïve Bayes classifier in q2-feature-classify plugin (Bokulich et al., 2018).

Predicted functional profiling of microbial communities:

Functional potential of microbial communities was evaluated using phylogenetic investigation of Communities by Reconstruction of Unobserved States (PICRUSt) version 2.2.0_b (Douglas et al., 2019) and Functional Annotation of Prokaryotic Taxa (FAPROTAX) version 1.2.1 (Louca et al., 2016). PICRUSt2 (Douglas et al., 2019) is the updated most recent version of the most widely used previous version PICRUSt (Langille et al., 2013). OTUs were placed into reference tree of 20000 full 16S sequences from prokaryotic genomes from IMG database using ‘place_seqs.py,’ which gives tree in Newick format by using GAPP (Czech & Stamatakis, 2019) after utilizing HMMER (<http://hmmer.org/>) to place OTUs in the reference tree, followed by rearrangement of OTUs to their best position by EPA-NG (Barbera et al., 2019). Hidden-state prediction of genomic content of sequences is done by ‘hsp.py’, that wraps castor R package (Louca & Doebeli, 2018) to normalize OTUs by 16S copy number and multiply by their functional predictions to produce a predicted metagenome. Prediction was done with default nearest sequenced taxon index (NSTI) cutoff value 2. Low NSTI value indicates closer placement of OTU from nearest sequenced

neighbors, giving more accurate prediction (Langille et al., 2013). Finally, KEGG pathway abundances were inferred using 'pathway_pipeline.py' that performs structural pathway mapping using MinPath (Ye & Doak, 2009).

Additionally, we performed functional annotation using FAPROTAX version 1.2.1, which is the most updated version. The database contains 90 functional groups with 8236 members, which was curated from experimental literatures (Louca et al., 2016).

Statistical analysis:

All results were present as average values. Spearman correlation, discriminant analysis (DA), and principal component analysis (PCA) were performed to evaluate the relationships between the physicochemical properties of soil and BC mixtures (i.e., pH, growth, conductivity, element compositions) and the loaded ratios of SBC and UBC using Minitab 16 Statistical Software (Minitab Inc., State College, PA, USA) and XLSTAT software (Addinsoft, New York, NY, USA). Statistical significance was set as $p \leq 0.05$, 0.01, and 0.001.

Permutational multivariate analysis of variance (PERMANOVA) test was performed to identify differences in beta diversities among SBC and UBC, as well as between initial and final sampling times. Linear discriminant analysis effect size (LEfSe) (Segata et al., 2012) was performed to identify differentially abundant features at taxonomic as well as function levels between two different treatment groups using Galaxy Version 1.0 at <http://huttenhower.sph.harvard.edu/galaxy/>. LEfSe performs Kruskal–Wallis sum-rank test between classes (groups) to identify differential abundance followed by additional pairwise Wilcoxon rank-sum test to check consistency of differences among subclasses. Finally, effect size

of each differentially abundant features were estimated using linear discriminant analysis (LDA) (Segata et al., 2012).

Results:

Soil physicochemical properties:

Discriminant analysis (DA) of physicochemical properties of soil treated with SBC and UBC showed distinct clusters suggesting differences in soil chemical properties after 10 weeks in response to SBC (Figure 2-1 A).

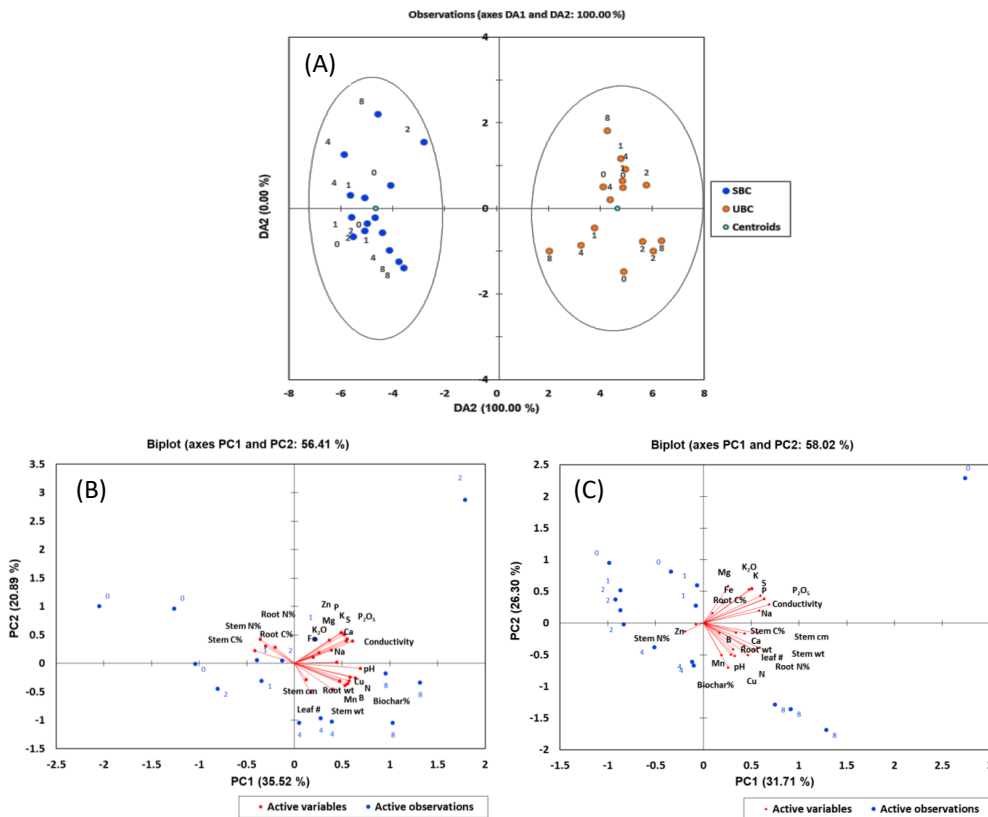


Figure 2-1 Physicochemical properties of wood biochar (BC) treated soil. Discriminant analysis (DA) among soil treated with SBC and UBC (A). Principal component analysis (PCA) of soil properties, plant growth parameters and the loading rates of saturated BC (SBC) in soil (B) and unsaturated biochar (UBC) in soil (C).

Table 2-1 shows the physicochemical properties of the soil (sandy loam soil) and UBC used for this study. Overall, the soil possessed low element contents except for Fe and high levels of electrical conductivity (EC) and low water holding capacity (Table 2-1). In contrast, N, P, Ca, and Mg contents and water holding capacity (56.60 mL water/100 g dry soil) in the BC pots were much higher than those in the sandy loam soil (Table 2-1). In addition, the saturation of BC with the dairy effluent increased as follows: 0.19 mg/g of N, 0.09 mg/g of P, and 3.12 mg/g of COD which were adsorbed onto the surface of SBC.

Table 2-1 Characteristics of soil and wood-derived biochar.

Parameters	Soil	Wood Biochar
pH	6.06	8.80
Electrical conductivity (mmhos/cm)	131.90	0.11
Water holding capacity (mL water/100 g dry material)	26.90	56.60
N (mg/g)	0.55	4.06
P (mg/g)	0.09	0.20
K (mg/g)	1.20	1.34
Ca (mg/g)	0.98	4.62
Mg (mg/g)	0.59	1.12
Na (mg/g)	0.13	0.44
Fe (mg/g)	7.74	0.66
Zn (mg/g)	0.02	0.06
Cu (mg/g)	0.01	0.11
Mn (mg/g)	0.11	0.43
S (mg/g)	0.07	0.08
B (mg/g)	0.00	0.01
Organic carbon (%)	0.30	0.64

Principal component analysis of SBC- and UBC-treated soil showed that all physicochemical properties were positively correlated with the high BC rates and variation observed among SBC loading rates were less prominent than those observed in UBC (Table 2-1 B,C). We measured the N and P concentration at 10 weeks in each pot receiving BC. The percent increase in N and P concentrations at 2, 4 and 8% BC rates compared to the control pots were relatively higher in SBC than UBC (Figure 2-2).

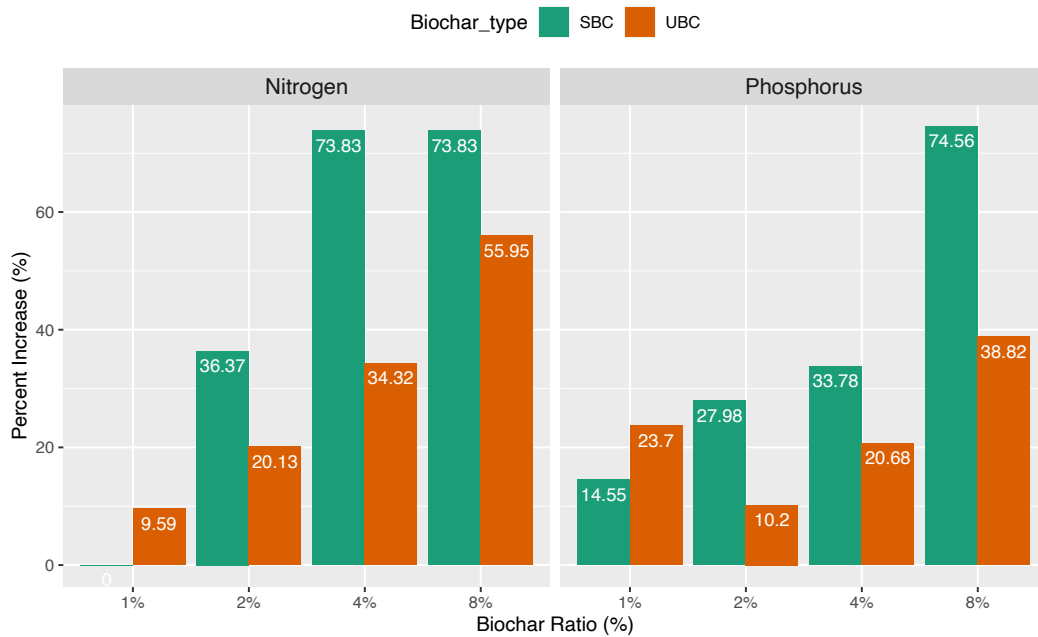


Figure 2-2 Percent increase in the N and P concentration in 10-week samples in comparison to the control.

Nitrogen concentration increased from 0 to 73.83% in SBC and 9.59 to 55.95% in UBC relative to the control soils. Similarly, P concentration increased from 14.55 to 74.56% in SBC and 23.7 to 38.82% in UBC. Spearman correlation of BC ratio with soil physicochemical variable showed positive correlation of N with BC ratio in both SBC and UBC treated soil whereas P was only positively correlated in SBC treated soil (Figure 2-3).

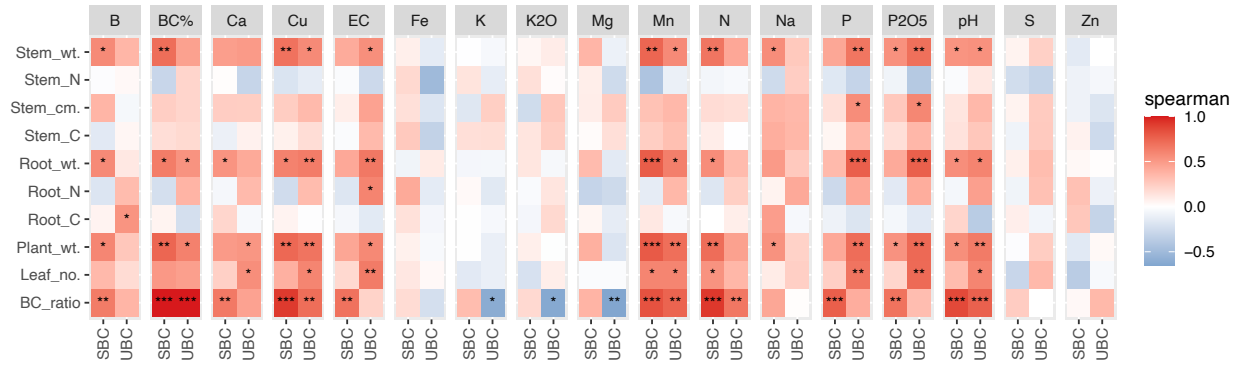


Figure 2-3 Spearman correlation of soil physicochemical variables and plant growth parameters among soil samples treated with saturated and unsaturated biochar (p-value < 0.05 *, p-value < 0.01 **, p-value < 0.001 ***).

Effects on plant biomass:

Soil amendments with SBC and UBC led to overall increase in the growth of the Bermuda grass (Figure S 2-2). The addition of SBC to soil at 1 to 4% resulted in enhanced stem dry weight (Figure 2-4 A): SBC at 1% ($p < 0.01$), 2% ($p < 0.05$) and 4% ($p < 0.01$). Compared with the SBC-amended soil, the plant in the UBC-amended soil had lower stem dry weight. On the other hand, the root dry weight in the SBC and UBC-amended soil increased along with the loading rates (Figure 2-4 B). However, only the BC loading rate of 2% ($p < 0.05$) had clear differences in root dry weight from those in the SBC and UBC-amended soil. Overall plant biomass (stem and herbage dry weight combined) increased ($p < 0.05$) in SBC-treated soil compared to UBC-treated soil at all BC rates (Figure 2-4 C). However, comparison of plant biomass between BC rates showed greater biomass only at 8% rates in UBC, whereas both 4 and 8% showed increases in pots receiving SBC (Figure S 2-3 C). On the other hand, adding 8% BC increased ($p < 0.05$) number of leaves (Figure S 2-3 D; Figure 2-4 D). No differences were observed in number of leaves among SBC-treated soil at all BC rates ($p > 0.05$). Therefore, the application of SBC at 1 to 8% to soil enhanced plant growth, while only application of UBC at 8% led to a clear positive effect on the

plant growth. These results implied that the loading rates of UBC and SBC also influenced the growth of Bermudagrass during the pot experiment.

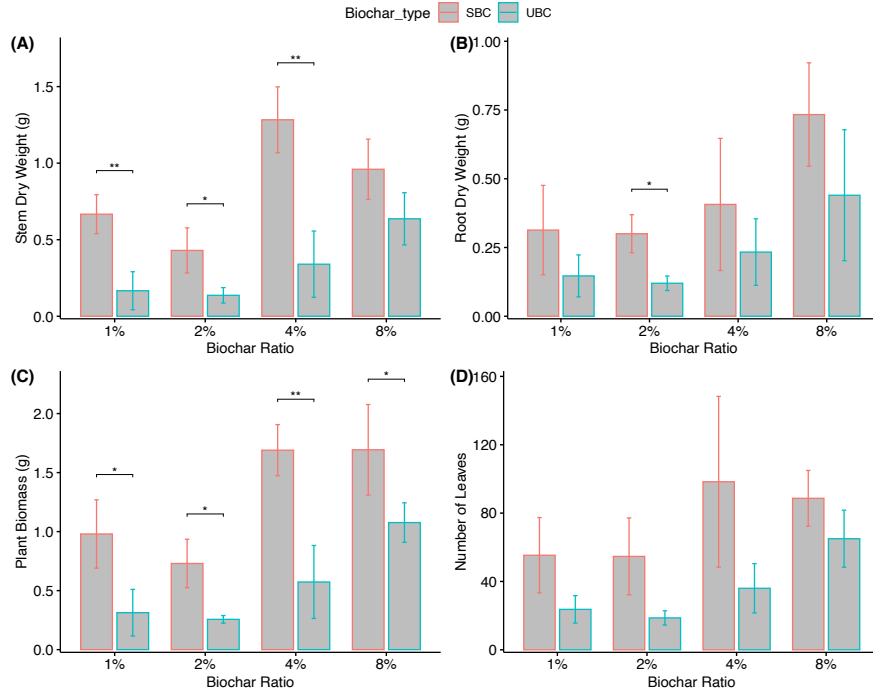


Figure 2-4 Comparison of stem dry weight (A), root dry weight (B), total plant biomass (C), and the number of leaves (D). Total plant biomass is the combination of stem and root dry weight. Two sample t-test was performed among each group compared (p-value < 0.05*, p-value < 0.01**).

Microbial community composition:

A total of 4,547,668 paired end reads (300 bp) were obtained with an average of 239,350 reads per sample. After denoising, dereplication, and chimera filtering, a total of 3,143,571 high-quality reads were obtained with an average read length of 413 bp. To reduce possible noise and sequencing errors, singleton ASVs were filtered out resulting in remaining 3,143,038 reads. Following filtering, sequences were clustered into 9702 OTUs at 97% similarity threshold where the number of reads per sample ranged from a minimum of 74,515 to a maximum of 243,196 reads.

We rarefied OTUs at the depth of 74,000 reads/sample for alpha and beta-diversity analysis, which was nearly enough to cover most of the bacterial community in our samples as shown in the rarefaction curve approaching asymptote in (Figure S 2-4).

There were 12 phyla with more than 1% cumulative relative abundance shared among all samples. Proteobacteria was the most abundant phylum in all samples except for initial and 0% UBC, followed by *Acidobacteria*, *Actinobacteria*, *Chloroflexi* and *Bacteroidetes* (Figure 2-5 A). However, in initial soil, *Firmicutes*, *Actinobacteria*, *Chloroflexi* and *Proteobacteria* were the most abundant phyla in the given orders. LEfSe analysis showed 15 differentially abundant features (LDA > 2) between SBC and UBC in plant samples. Alpha-proteobacteria (LDA = 3.3, $p = 0.02$) were more abundant in UBC, whereas *Nitrospirae* (LDA = 2.48, $p = 0.02$) and *Firmicutes* (LDA = 2.98, $p = 0.02$) were more abundant in soil receiving SBC (Figure S 2-5). Similarly, after 10 weeks, no-plant soils with BC, showed an increased abundance of many photosynthetic genera such as *Rhodopila*, *Rhodobacter*, *Oscillatoria*, *Planktothrix*, *Pseudanabaena*, *Nodosilinea*, *Phormidium*, and N-fixing genera such as *Mesorhizobium*, *Devosia* genera were abundant in BC amended soil (Figure S 2-6).

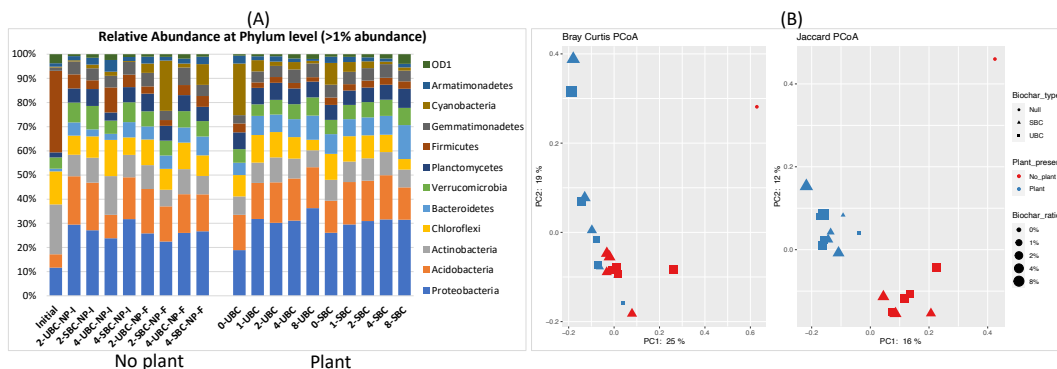


Figure 2-5 Microbial community composition. Relative abundance of major taxa at phylum level (A). Principal coordinate analysis of the microbial community at OTU level (B). (Abbreviations: NP; No plant, I; Initial, F; Final).

We compared the beta diversity of the overall samples based on Bray–Curtis and Jaccard distance matrices to determine how communities varied based on abundance and presence-absence. We performed a PERMANOVA test to compare the differences in beta-diversity among groups. Most differences were observed in the type of OTU present based on rhizosphere and non-rhizosphere soil ($p = 0.001$) (Figure 2-5 B). Furthermore, BC ratio caused a quantitative variation ($p < 0.05$) in the community composition (Figure 2-5 B).

We predicted functional potential of microbial communities using PICRUSt2 and FAPROTAX. OTUs with NSTI > 2 were not included for PICRUSt2 prediction, which increases the accuracy of predicted function (Langille et al., 2013). After 10 weeks, KEGG pathway showed increases in photosynthesis and related functions in soil amended with BC (Figure S 2-7 B). The result is further confirmed by abundance of FAPROTAX-predicted phototrophy and photoautotrophy in the final sample (Figure S 2-7 A). Similarly, oxidative phosphorylation and biotin metabolism were greater in SBC than UBC-treat soils (Figure 2-6 A). FAPROTAX identified more abundant nitrification and aerobic nitrite oxidation in soils receiving SBC (Figure 2-6 B).

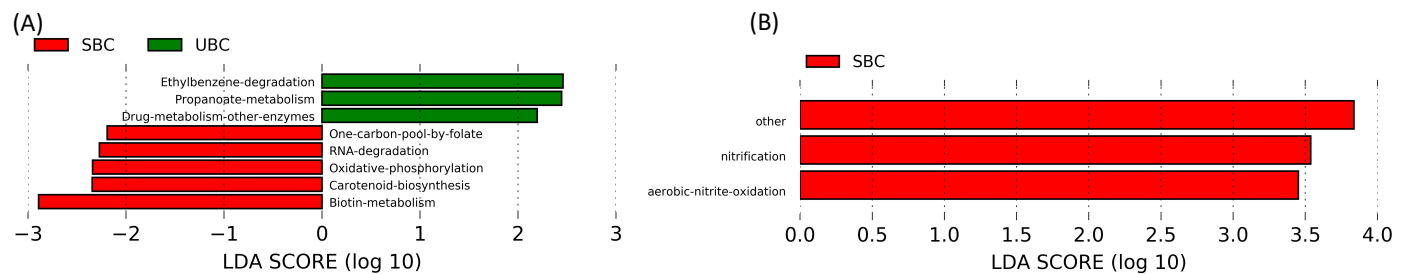


Figure 2-6 Differential abundance of predicted functions between SBC and UBC treated soil. LEfSe analysis of PICRUSt2 (A) and FAPROTAX (B) predicted functions in SBC and UBC treated soil among no-plant samples and plant samples, respectively.

Discussion:

Alteration of soil chemical properties in response to biochar saturation:

Saturating UBC with dairy effluent resulted in distinct soil chemical properties compared to soil receiving UBC, as observed by discriminant analysis. These mainly correlated with higher biochar rates within each condition. However, SBC resulted in very similar nutrient content at all loading rates in contrast to the UBC (Figure 2-1 B,C). In general, BC treatment increases total soil N content in the soil (Biederman & Stanley Harpole, 2013). Biochar can absorb N and P on its surface, both nutrients abundant in dairy wastewater (Demirel et al., 2005), thereby making it available for a long period of time (Hagemann et al., 2017). Biochar mainly contains Ca-bound P (Xu et al., 2014), which is also suggested by the high amount of Ca in the wood biochar in Table 2-1. This effect can be seen in our experiment where the percent increase in N and P concentration are relatively higher in SBC- than UBC-treated soil (Figure 2-2). Both UBC and SBC increased the concentration of N and P in the soils. In addition, these macronutrients along with B, Ca, Cu, Mn, and P₂O₅ increased with greater BC rates (Figure 2-3). UBC and SBC treated soil increased the pH of soil while decreasing the EC in soil mainly due to high pH and low EC of BCs as found in Table 2-1. This suggests that the greater BC rates in soil favor increases in soil chemical reactivity thereby absorbing more nutrients from the dairy effluent. However, accurate economic assessment for agronomic applications of SBC and UBC will be made after large scale use on farms. Nonetheless, since SBC contained greater concentration of nutrients than UBC, possible price of SBC would be higher than that of UBC (USD 300–600/ton of biochar, average price of USD 400/ton of biochar).

Enhanced plant growth due to biochar saturation:

Amendment of soil with SBC led to the overall increase in Bermudagrass growth. Our study corroborates other studies that observed increased plant growth and productivity (Pandit et al., 2018; Yue et al., 2017). The effect was seen more on the aboveground shoot compared to belowground root development, a favorable trait for forage grass. Some studies have observed increased productivity only a few years after BC application (Pandit et al., 2018), which is partly due to slow breakdown of the nutrients from raw biochar and acclimatization time (J. L. Smith et al., 2010). In our study, we observed a pronounced immediate effect of BC saturation on plant growth within 10 weeks of growth. This emphasizes the significance of BC saturation prior to its application in the agricultural field. Additionally, pronounced effects at as low as 1% SBC rate suggests the efficacy of low BC application rates on farmland as a commercial biological alternative.

Plant biomass, including number of leaves, was consistently lower in pots receiving 1 and 2% UBC than that of control (Figure S 2-3 C,D). Biochar application has not always shown increases in plant growth parameters as exemplified by Yue et al. (Yue et al., 2017). In contrast, all our saturated W-BC rates consistently showed an increase in aboveground plant biomass compared to control pots, with greatest increase at 4% (Figure S 2-3 A). An increase in biomass with UBC treated soil was only observed in pots receiving 8%, suggesting greater short-term efficacy of BC only after saturation with dairy effluent. Dairy effluents contain more nutrients in their bioavailable form facilitating assimilation of nutrient compounds by plants (Demirel et al., 2005). As seen in Figure 2-3, we observed a positive correlation of plant biomass with N and BC ratio associated with SBC-treated soil, suggesting efficient utilization of N by the plant in addition to increased N

content in soil. This may be attributed to the active nitrification of ammonium to nitrates in bioavailable form as indicated by differentially abundant phylum *Nitrospira* in SBC-treated soil (Daims et al., 2015) (Figure S 2-5). Our results suggest greater N-cycling following saturation rather than greater N accumulation in soil. In contrast, soil P did not correlate with plant biomass in pots receiving SBC although there is a positive correlation with BC rates (Figure 2-3). This could indicate slower P release in SBC-treated soil due to increased Ca-bound P in dairy effluent and increased pH associated with soil nitrate, which is found to inhibit P uptake by the plant (Xu et al., 2014).

SBC and UBC mediated changes in microbial community and their functional potential:

We observed differences in microbial community abundance mainly between plant and no-plant samples as well as presence-absence of OTUs. These suggest that BC favors the stratification of specific bacterial community, especially plant growth-promoting bacteria, selectively favored by plant root exudates which provide substrate and/or surface area to increase their abundance. Other studies have found that BC not only provides soil labile-C for degradation (J. L. Smith et al., 2010) but also alters the growth of rhizosphere bacterial community that assimilate plant root exudates (Liao et al., 2019). We observed an increased abundance of N-fixing bacteria in the control soil after 10 weeks (Figure S 2-6) in response to overall BC treatment, which indicates enhanced biological N-fixation. Additionally, increased abundance of genera such as *Devosia*, which is well known to perform bioremediation (Talwar et al., 2020), further emphasizes the significance of BC in remediating toxic chemical fertilizers in agricultural fields. This is an added benefit to the sequestration of greenhouse gases.

Few studies have evaluated the metabolic potential of microorganisms in BC-amended soil (Sun et al., 2016). Increases in oxidative phosphorylation in SBC compared to UBC-treated soil indicate better aeration in the former thereby providing energy efficient conditions for microbes (Figure 2-6A). In photoelectron spectroscopy, co-composted BC increases O/C ratio on the surface (Hagemann et al., 2017). In addition, biotin metabolism is abundant in SBC, an essential cofactor for enzymes involved in key metabolic pathways such as fatty acid metabolism, amino acid metabolism and Krebs cycle. Notably, biotin is stable at higher temperature and pH (Streit & Entcheva, 2003), thereby making it a key candidate for metabolic homeostasis in heat stress conditions. On the other hand, increased *Nitrospira* in soil containing SBC (Figure S 2-5) suggests active anaerobic ammonia oxidation that plays an important role in N-cycling. Saturation of biochar with dairy effluent showed potential to increase soil nutrient content, thereby stabilizing excess nitrogenous compounds that might otherwise leach out to contaminate the environment.

Conclusions:

This study investigated the effects of dairy effluent-nutrient loading and application rates on the growth of Bermudagrass, soil properties and microbial communities. SBC, produced from saturation of UBC with dairy effluent, possessed increased nutrients in soil, particularly N and P, resulting in enhanced plant growth and promoting bacteria in the soil. Thus, the application of SBC for enhanced soil fertility and plant growth could be more effective and economical route than UBC (pristine BC) for enhancing agricultural productivity and dairy waste management, thereby mitigating eutrophication and environmental pollution. The BC-mediated changes of soil microbiome showed that photosynthetic and N-fixing genera were predominant after 10 weeks. Similarly, the increased abundance of *Nitrospira* in SBC-treated soil indicates efficient utilization

of ammonia which is available in higher concentration in dairy effluent. The PCA analysis also suggested that SBC could result in uniformity in soil physicochemical properties among different BC loading rates. In our study, both SBC and UBC showed more impact on aboveground biomass than the root biomass of Bermudagrass. Overall, both UBC and SBC at various loading rates should positively influence herbage production in a field setting. Further work will include largescale field studies to validate the outcomes from our greenhouse study so that farmers can apply SBC in crop fields to improve agricultural practices by integrating environmental health and economic profitability. For more economical applications, increased efficacy of SBC at lower rates might be a key to minimize the need of large-scale use of BCs in agricultural fields.

Funding: This research was funded by the Texas A&M University Chancellor Research Initiative Fund, grant number 435680, and U.S. Department of Agriculture, grant number TEX09764.

References:

- Barbera, P., Kozlov, A. M., Czech, L., Morel, B., Darriba, D., Flouri, T., & Stamatakis, A. (2019). EPA-ng: Massively Parallel Evolutionary Placement of Genetic Sequences. *Systematic Biology*, 68(2), 365–369. <https://doi.org/10.1093/sysbio/syy054>
- Basso, A. S., Miguez, F. E., Laird, D. A., Horton, R., & Westgate, M. (2013). Assessing potential of biochar for increasing water-holding capacity of sandy soils. *GCB Bioenergy*, 5(2), 132–143. <https://doi.org/10.1111/gcbb.12026>
- Batista, E. M. C. C., Shultz, J., Matos, T. T. S., Fornari, M. R., Ferreira, T. M., Szpoganicz, B., De Freitas, R. A., & Mangrich, A. S. (2018). Effect of surface and porosity of biochar on water holding capacity aiming indirectly at preservation of the Amazon biome. *Scientific Reports*, 8(1), 1–9. <https://doi.org/10.1038/s41598-018-28794-z>
- Biederman, L. A., & Stanley Harpole, W. (2013). Biochar and its effects on plant productivity and nutrient cycling: A meta-analysis. *GCB Bioenergy*, 5(2), 202–214. <https://doi.org/10.1111/gcbb.12037>
- Bokulich, N. A., Kaehler, B. D., Rideout, J. R., Dillon, M., Bolyen, E., Knight, R., Huttley, G. A., & Caporaso, J. G. (2018). Optimizing taxonomic classification of marker-gene amplicon sequences with QIIME 2 's q2-feature-classifier plugin. *Microbiome*, 6(90), 1–17.
- Bolyen, E., Rideout, J. R., Dillon, M. R., Bokulich, N. A., Abnet, C. C., Gabriel, A., Ghalith, A., Alexander, H., Alm, E. J., Arumugam, M., Asnicar, F., Bai, Y., Bisanz, J. E., Bittinger, K., Brejnrod, A., Brislawn, C. J., Brown, C. T., Benjamin, J., Mauricio, A., ... Willis, A. D. (2018). QIIME 2 : Reproducible , interactive , scalable , and extensible microbiome data science. *PeerJ Preprints*, 6:e27295v2.

- Buss, W., Shepherd, J. G., Heal, K. V., & Mašek, O. (2018). Spatial and temporal microscale pH change at the soil-biochar interface. *Geoderma*, 331(April), 50–52.
<https://doi.org/10.1016/j.geoderma.2018.06.016>
- Callahan, B. J., Mcmurdie, P. J., Rosen, M. J., Han, A. W., Johnson, A. J. A., & Holmes, S. P. (2016). DADA2 : High-resolution sample inference from Illumina amplicon data. *Nature Methods*, 13(7). <https://doi.org/10.1038/nmeth.3869>
- Czech, L., & Stamatakis, A. (2019). Scalable methods for analyzing and visualizing phylogenetic placement of metagenomic samples. In *PLoS ONE* (Vol. 14, Issue 5).
<https://doi.org/10.1371/journal.pone.0217050>
- Daims, H., Lebedeva, E. V., Pjevac, P., Han, P., Herbold, C., Albertsen, M., Jehmlich, N., Palatinszky, M., Vierheilig, J., Bulaev, A., Kirkegaard, R. H., Von Bergen, M., Rattei, T., Bendinger, B., Nielsen, P. H., & Wagner, M. (2015). Complete nitrification by *Nitrospira* bacteria. *Nature*, 528(7583), 504–509. <https://doi.org/10.1038/nature16461>
- Demirel, B., Yenigun, O., & Onay, T. T. (2005). Anaerobic treatment of dairy wastewaters: A review. *Process Biochemistry*, 40(8), 2583–2595.
<https://doi.org/10.1016/j.procbio.2004.12.015>
- Ding, Y., Liu, Y., Liu, S., Huang, X., Li, Z., Tan, X., Zeng, G., & Zhou, L. (2017). Potential Benefits of Biochar in Agricultural Soils: A Review. *Pedosphere*, 27(4), 645–661.
[https://doi.org/10.1016/S1002-0160\(17\)60375-8](https://doi.org/10.1016/S1002-0160(17)60375-8)
- Ding, Y., Liu, Y., Liu, S., Li, Z., Tan, X., Huang, X., Zeng, G., Zhou, L., & Zheng, B. (2016). Biochar to improve soil fertility. A review. *Agronomy for Sustainable Development*, 36(2).
<https://doi.org/10.1007/s13593-016-0372-z>

- Domene, X., Mattana, S., Hanley, K., Enders, A., & Lehmann, J. (2014). Medium-term effects of corn biochar addition on soil biota activities and functions in a temperate soil cropped to corn. *Soil Biology and Biochemistry*, *72*, 152–162.
<https://doi.org/10.1016/j.soilbio.2014.01.035>
- Douglas, G. M., Maffei, V. J., Zaneveld, J., Yurgel, S. N., Brown, J. R., Taylor, C. M., Huttenhower, C., & Langille, M. G. I. (2019). PICRUSt2: an improved and extensible approach for metagenome inference. *BioRxiv*.
- Glaser, B. (2007). Prehistorically modified soils of central Amazonia: A model for sustainable agriculture in the twenty-first century. *Philosophical Transactions of the Royal Society B: Biological Sciences*, *362*(1478), 187–196. <https://doi.org/10.1098/rstb.2006.1978>
- Hagemann, N., Joseph, S., Schmidt, H. P., Kammann, C. I., Harter, J., Borch, T., Young, R. B., Varga, K., Taherymoosavi, S., Elliott, K. W., McKenna, A., Albu, M., Mayrhofer, C., Obst, M., Conte, P., Dieguez-Alonso, A., Orsetti, S., Subdiaga, E., Behrens, S., & Kappler, A. (2017). Organic coating on biochar explains its nutrient retention and stimulation of soil fertility. *Nature Communications*, *8*(1), 1–11. <https://doi.org/10.1038/s41467-017-01123-0>
- Hale, S. E., Alling, V., Martinsen, V., Mulder, J., Breedveld, G. D., & Cornelissen, G. (2013). The sorption and desorption of phosphate-P, ammonium-N and nitrate-N in cacao shell and corn cob biochars. *Chemosphere*, *91*(11), 1612–1619.
<https://doi.org/10.1016/j.chemosphere.2012.12.057>
- Jeffery, S., Abalos, D., Prodana, M., Bastos, A. C., Van Groenigen, J. W., Hungate, B. A., & Verheijen, F. (2017). Biochar boosts tropical but not temperate crop yields. *Environmental Research Letters*, *12*(5). <https://doi.org/10.1088/1748-9326/aa67bd>

- Jeffery, S., Verheijen, F. G. A., van der Velde, M., & Bastos, A. C. (2011). A quantitative review of the effects of biochar application to soils on crop productivity using meta-analysis. *Agriculture, Ecosystems and Environment*, *144*(1), 175–187.
<https://doi.org/10.1016/j.agee.2011.08.015>
- Katoh, K., Misawa, K., Kuma, K., & Miyata, T. (2002). MAFFT : a novel method for rapid multiple sequence alignment based on fast Fourier transform. *Nucleic Acids Research*, *30*(14), 3059–3066.
- Kizito, S., Luo, H., Lu, J., Bah, H., Dong, R., & Wu, S. (2019). Role of nutrient-enriched biochar as a soil amendment during maize growth: Exploring practical alternatives to recycle agricultural residuals and to reduce chemical fertilizer demand. *Sustainability (Switzerland)*, *11*(11). <https://doi.org/10.3390/su11113211>
- Langille, M. G. I., Zaneveld, J., Caporaso, J. G., McDonald, D., Knights, D., Reyes, J. A., Clemente, J. C., Burkepile, D. E., Vega Thurber, R. L., Knight, R., Beiko, R. G., & Huttenhower, C. (2013). Predictive functional profiling of microbial communities using 16S rRNA marker gene sequences. *Nature Biotechnology*, *31*(9), 814–821.
<https://doi.org/10.1038/nbt.2676>
- Lehmann, J. (2007). Bio-energy in the black. *Frontiers in Ecology and the Environment*, *5*(7), 381–387. <https://doi.org/10.4324/9780203007020-14>
- Lehmann, J., Rillig, M. C., Thies, J., Masiello, C. A., Hockaday, W. C., & Crowley, D. (2011). Biochar effects on soil biota - A review. *Soil Biology and Biochemistry*, *43*(9), 1812–1836.
<https://doi.org/10.1016/j.soilbio.2011.04.022>
- Liang, B., Lehmann, J., Solomon, D., Kinyangi, J., Grossman, J., O'Neill, B., Skjemstad, J. O.,

- Thies, J., Luizão, F. J., Petersen, J., & Neves, E. G. (2006). Black Carbon Increases Cation Exchange Capacity in Soils. *Soil Science Society of America Journal*, 70(5), 1719–1730.
<https://doi.org/10.2136/sssaj2005.0383>
- Liao, H., Li, Y., & Yao, H. (2019). Biochar Amendment Stimulates Utilization of Plant-Derived Carbon by Soil Bacteria in an Intercropping System. *Frontiers in Microbiology*, 10(June), 1–13. <https://doi.org/10.3389/fmicb.2019.01361>
- Louca, S., & Doebeli, M. (2018). Efficient comparative phylogenetics on large trees. *Bioinformatics*, 34(6), 1053–1055. <https://doi.org/10.1093/bioinformatics/btx701>
- Louca, S., Parfrey, L. W., & Doebeli, M. (2016). Decoupling function and taxonomy in the global ocean microbiome. *Science (New York, N.Y.)*, 353(6305), 1272–1277.
<https://doi.org/10.1126/science.aaf4507>
- McDonald, D., Price, M. N., Goodrich, J., Nawrocki, E. P., Desantis, T. Z., Probst, A., Andersen, G. L., Knight, R., & Hugenholtz, P. (2012). An improved Greengenes taxonomy with explicit ranks for ecological and evolutionary analyses of bacteria and archaea. *The ISME Journal*, 6(3), 610–618. <https://doi.org/10.1038/ismej.2011.139>
- Muir, J. P., Terrill, T. H., Mosjidis, J. A., Luginbuhl, J. M., Miller, J. E., Burke, J. M., & Coleman, S. W. (2017). Season progression, ontogenesis, and environment affect *Lespedeza cuneata* herbage condensed tannin, fiber, and crude protein concentrations. *Crop Science*, 57(1), 515–524. <https://doi.org/10.2135/cropsci2016.07.0605>
- Mukherjee, A., Zimmerman, A. R., & Harris, W. (2011). Surface chemistry variations among a series of laboratory-produced biochars. *Geoderma*, 163(3–4), 247–255.
<https://doi.org/10.1016/j.geoderma.2011.04.021>

- Pandit, N. R., Mulder, J., Hale, S. E., Zimmerman, A. R., Pandit, B. H., & Cornelissen, G. (2018). Multi-year double cropping biochar field trials in Nepal: Finding the optimal biochar dose through agronomic trials and cost-benefit analysis. *Science of the Total Environment*, 637–638, 1333–1341. <https://doi.org/10.1016/j.scitotenv.2018.05.107>
- Price, M. N., Dehal, P. S., & Arkin, A. P. (2010). FastTree 2 – Approximately Maximum-Likelihood Trees for Large Alignments. *PLoS ONE*, 5(3). <https://doi.org/10.1371/journal.pone.0009490>
- Segata, N., Waldron, L., Ballarini, A., Narasimhan, V., Jousson, O., & Huttenhower, C. (2012). Metagenomic microbial community profiling using unique clade-specific marker genes. *Nature Methods*, 9, 811. <https://doi.org/10.1038/nmeth.2066>
- Smith, J. L., Collins, H. P., & Bailey, V. L. (2010). The effect of young biochar on soil respiration. *Soil Biology and Biochemistry*, 42(12), 2345–2347. <https://doi.org/10.1016/j.soilbio.2010.09.013>
- Steinbeiss, S., Gleixner, G., & Antonietti, M. (2009). Effect of biochar amendment on soil carbon balance and soil microbial activity. *Soil Biology and Biochemistry*, 41(6), 1301–1310. <https://doi.org/10.1016/j.soilbio.2009.03.016>
- Streit, W. R., & Entcheva, P. (2003). Biotin in microbes, the genes involved in its biosynthesis, its biochemical role and perspectives for biotechnological production. *Applied Microbiology and Biotechnology*, 61(1), 21–31. <https://doi.org/10.1007/s00253-002-1186-2>
- Sun, D., Meng, J., & Chen, W. (2013). Effects of abiotic components induced by biochar on microbial communities. *Acta Agriculturae Scandinavica Section B: Soil and Plant Science*, 63(7), 633–641. <https://doi.org/10.1080/09064710.2013.838991>

- Sun, D., Meng, J., Xu, E. G., & Chen, W. (2016). Microbial community structure and predicted bacterial metabolic functions in biochar pellets aged in soil after 34 months. *Applied Soil Ecology*, *100*, 135–143. <https://doi.org/10.1016/j.apsoil.2015.12.012>
- Talwar, C., Nagar, S., Kumar, R., Scaria, J., Lal, R., & Negi, R. K. (2020). Defining the Environmental Adaptations of Genus *Devosia*: Insights into its Expansive Short Peptide Transport System and Positively Selected Genes. *Scientific Reports*, *10*(1), 1–18. <https://doi.org/10.1038/s41598-020-58163-8>
- United States Department of Agriculture Soil Conservation Service. (1973). *Soil Survey of Erath County, Texas*. https://www.nrcs.usda.gov/Internet/FSE_MANUSCRIPTS/texas/erathTX1973/erathTX1973.pdf
- Xu, G., Sun, J. N., Shao, H. B., & Chang, S. X. (2014). Biochar had effects on phosphorus sorption and desorption in three soils with differing acidity. *Ecological Engineering*, *62*, 54–60. <https://doi.org/10.1016/j.ecoleng.2013.10.027>
- Yao, Q., Liu, J., Yu, Z., Li, Y., Jin, J., Liu, X., & Wang, G. (2017). Changes of bacterial community compositions after three years of biochar application in a black soil of northeast China. *Applied Soil Ecology*, *113*, 11–21. <https://doi.org/10.1016/j.apsoil.2017.01.007>
- Yao, Y., Gao, B., Zhang, M., Inyang, M., & Zimmerman, A. R. (2012). Effect of biochar amendment on sorption and leaching of nitrate, ammonium, and phosphate in a sandy soil. *Chemosphere*, *89*(11), 1467–1471. <https://doi.org/10.1016/j.chemosphere.2012.06.002>
- Ye, Y., & Doak, T. G. (2009). A parsimony approach to biological pathway reconstruction/inference for genomes and metagenomes. *PLoS Computational Biology*,

5(8), 1–8. <https://doi.org/10.1371/journal.pcbi.1000465>

Yue, Y., Cui, L., Lin, Q., Li, G., & Zhao, X. (2017). Efficiency of sewage sludge biochar in improving urban soil properties and promoting grass growth. *Chemosphere*, *173*, 551–556. <https://doi.org/10.1016/j.chemosphere.2017.01.096>

Zhang, A., Bian, R., Pan, G., Cui, L., Hussain, Q., Li, L., Zheng, J., Zheng, X., Han, X., & Yu, X. (2012). Effects of biochar amendment on soil quality, crop yield and greenhouse gas emission in a Chinese rice paddy: A field study of 2 consecutive rice growing cycles. *Field Crops Research*, *127*, 153–160.

Supplements:

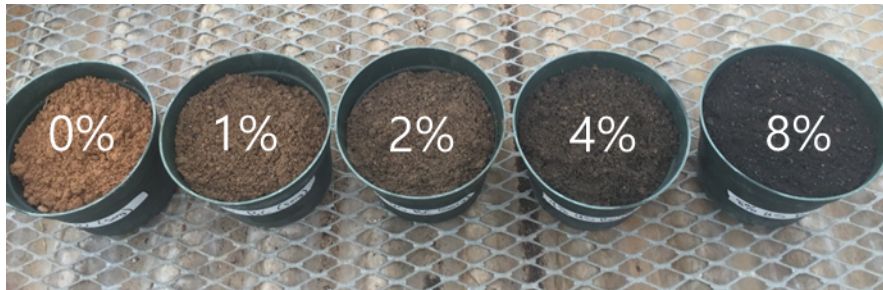


Figure S 2-1 Mixture of soil and various ratios of wood-biochar.



Figure S 2-2 Plants growth with the different loading ratios of the nutrients saturated biochar.

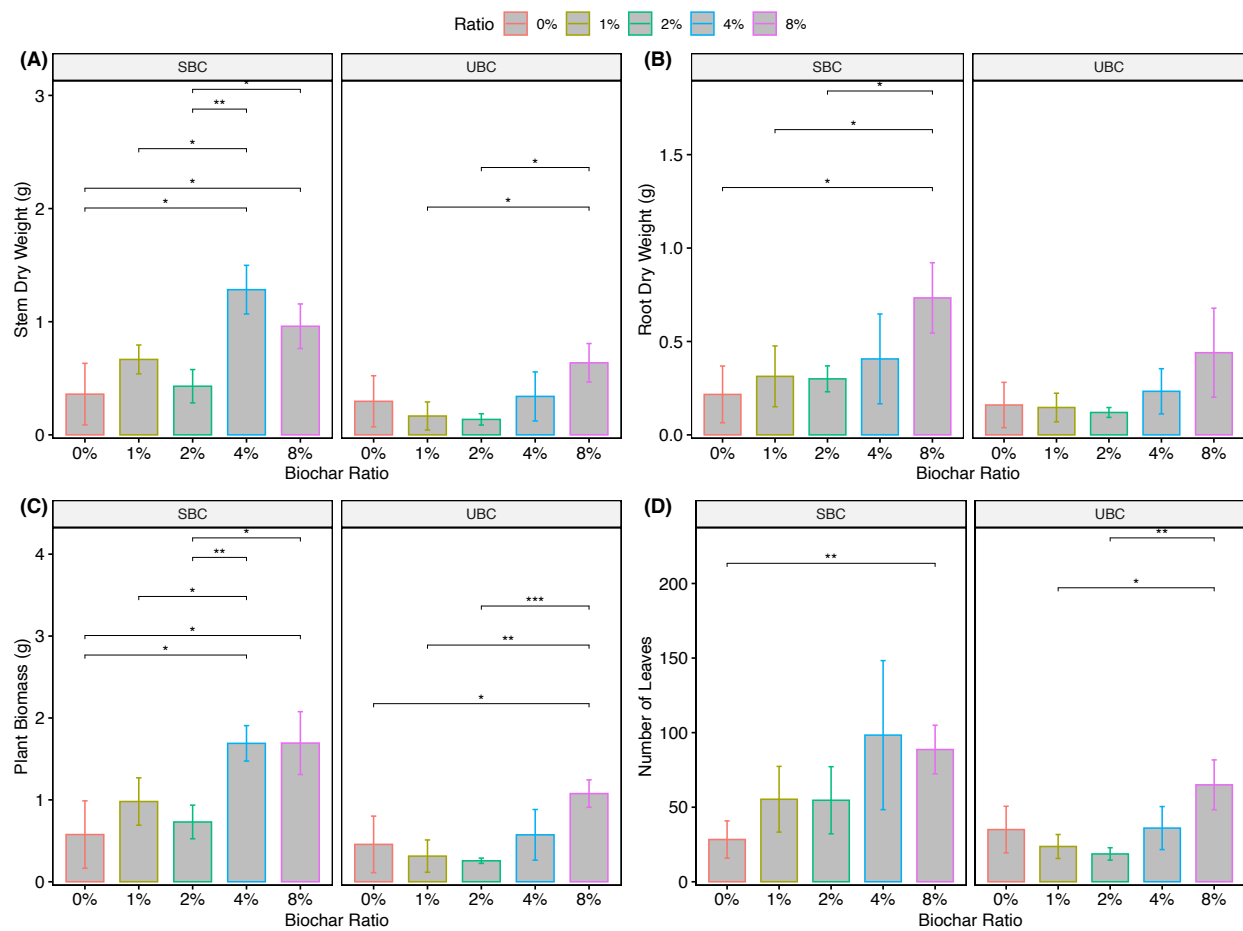


Figure S 2-3 Comparison of stem dry weight (A), root dry weight (B), total plant biomass (C), and the number of leaves (D) among biochar ratios within each biochar saturation condition. Total plant biomass is the combination of stem and root dry weight. Two sample t-test was performed among each group compared (p-value < 0.05*, p-value < 0.01**, p-value < 0.001***).

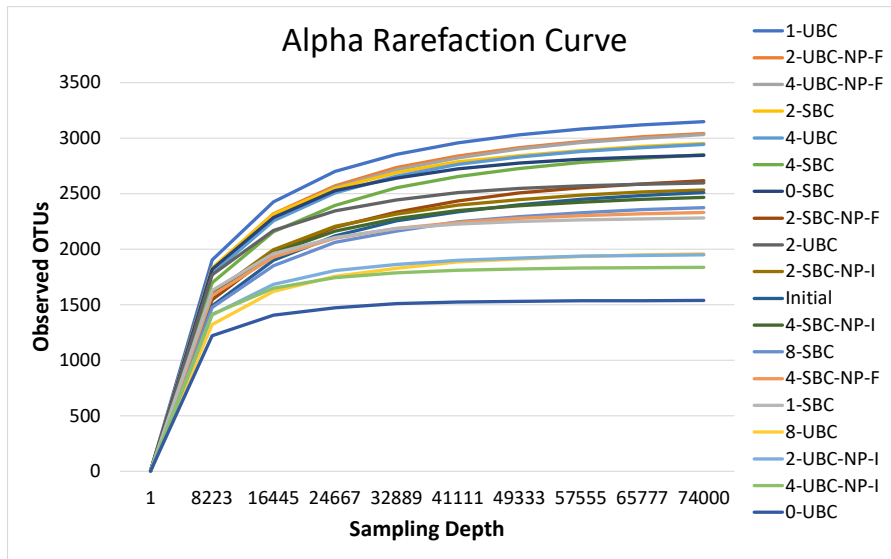


Figure S 2-4 Alpha rarefaction curve showing observed OTUs at sampling depth of 74000 reads. [Abbreviations: SBC; Saturated Biochar, USB; Unsaturated Biochar, NP; No plant, I; Initial, F; Final]

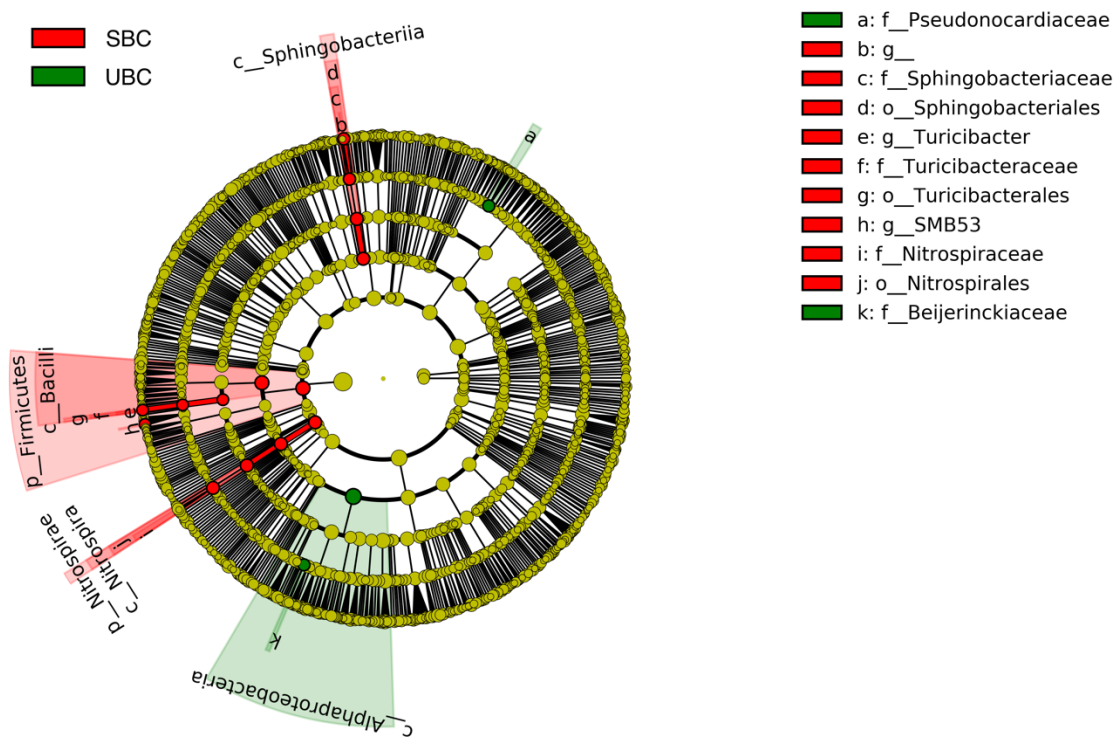


Figure S 2-5 Differentially abundant taxa at class level between SBC and UBC treated soil among plant samples determined by LEFSe analysis.

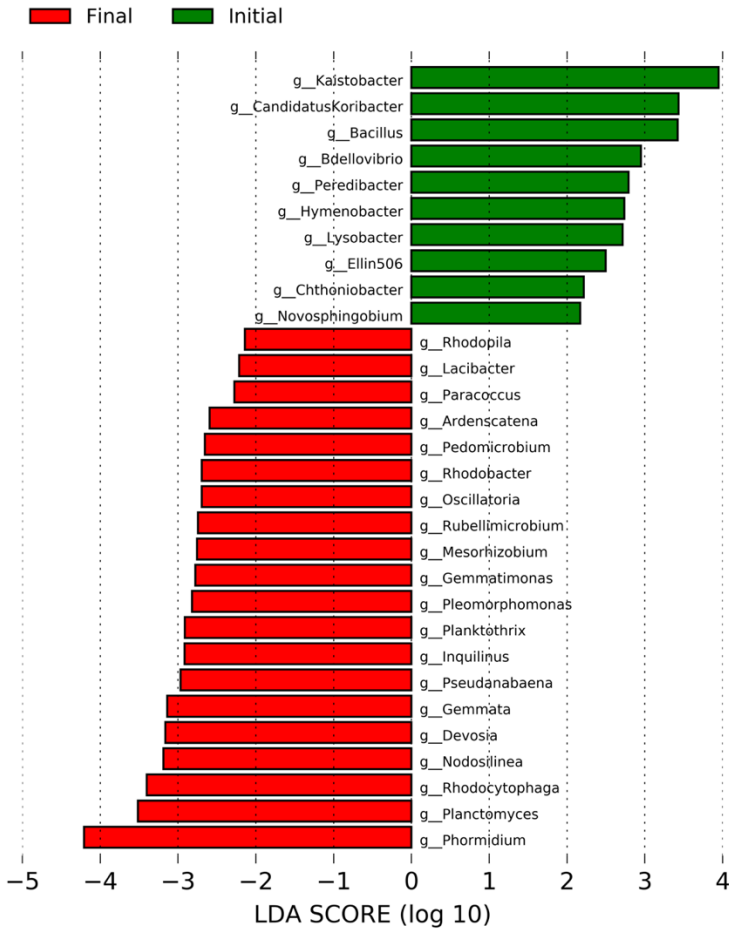
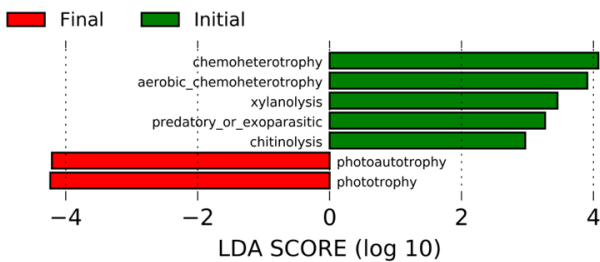


Figure S 2-6 Differentially abundant features after 10 weeks period among no-plant samples determined by LEfSe analysis. Comparison was made among no-plant samples with time as class and saturation status subclass.

(A)



(B)

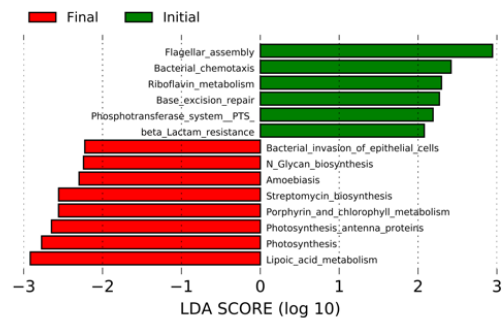


Figure S 2-7 LEfSe analysis of (A) FAPROTAX and (B) PICRUST2 predicted functions showing temporal variation in functional potential of microbial communities in biochar amended soil. Comparison was made among no-plant samples with time as class and saturation status as subclass.

Multiple Author Release for Master’s Thesis or Doctoral Dissertation

Thesis / Dissertation Writer Name: Sarbjeet Niraula _____

Co-Author Name: Eunsun Kan _____

Title(s) of Co-Authored Work(s):

- Dairy Effluent Saturated Biochar Alters

- Microbial Communities and Enhances

- Bermudagrass and Soil Fertility

- _____
- _____

Co-Author Statement of Consent:

As the co-author of the above named work(s), I acknowledge the above-named thesis / dissertation writer as the primary author of the work(s) listed above. I authorize the thesis / dissertation writer named above to use the listed work(s) in their thesis / dissertation. I further agree that the thesis / dissertation writer may use this work to comply with requirements for graduation.

Co-Author Signature: Eunsung Kan Digitally signed by Eunsung Kan
Date: 2021.12.03 09:38:08
-06'00' _____

Date: 12/03/2021 _____

Please maintain a copy of this completed form for your records.

You may be entitled to know what information The University of Texas at Arlington (UT Arlington) collects concerning you. You may review and have UT Arlington correct this information according to procedures set forth in UTS 139. The law is found in sections 552.021, 552.023 and 559.004 of the Texas Government Code.

Multiple Author Release for Master’s Thesis or Doctoral Dissertation

Thesis / Dissertation Writer Name: Sarbjeeet Niraula

Co-Author Name: James P. Muir

Title(s) of Co-Authored Work(s):

- Dairy Effluent Saturated Biochar Alters
- Microbial Communities and Enhances
- Bermudagrass and Soil Fertility
-
-

Co-Author Statement of Consent:

As the co-author of the above named work(s), I acknowledge the above-named thesis / dissertation writer as the primary author of the work(s) listed above. I authorize the thesis / dissertation writer named above to use the listed work(s) in their thesis / dissertation. I further agree that the thesis / dissertation writer may use this work to comply with requirements for graduation.

Co-Author Signature: James P. Muir Digital Signer: James P. Muir
DN: E=jpmuir@ag.tamu.edu, CN=James P. Muir
Date: 2021.12.06
11:36:03 -06:00

Date: December 6, 2021

Please maintain a copy of this completed form for your records.

You may be entitled to know what information The University of Texas at Arlington (UT Arlington) collects concerning you. You may review and have UT Arlington correct this information according to procedures set forth in UTS 139. The law is found in sections 552.021, 552.023 and 559.004 of the Texas Government Code.

Multiple Author Release for Master's Thesis or Doctoral Dissertation

Thesis / Dissertation Writer Name: Sarbjeeet Niraula

Co-Author Name: Yong-Keun Choi

Title(s) of Co-Authored Work(s):

Dairy Effluent Saturated Biochar Alters

Microbial Communities and Enhances

Bermudagrass and Soil Fertility

Co-Author Statement of Consent:

As the co-author of the above named work(s), I acknowledge the above-named thesis / dissertation writer as the primary author of the work(s) listed above. I authorize the thesis / dissertation writer named above to use the listed work(s) in their thesis / dissertation. I further agree that the thesis / dissertation writer may use this work to comply with requirements for graduation.

Co-Author Signature: 

Date: 12-03-2021

Please maintain a copy of this completed form for your records.

You may be entitled to know what information The University of Texas at Arlington (UT Arlington) collects concerning you. You may review and have UT Arlington correct this information according to procedures set forth in UTS 139. The law is found in sections 552.021, 552.023 and 559.004 of the Texas Government Code.

Chapter 3

Effects of a Drought-Tolerant Bioinoculant on the Microbial Community in the Soybean Rhizosphere

Abstract:

Application of bioinoculants that promote plant growth and productivity is a promising alternative to the use of chemical fertilizers in agricultural fields. Their use is rapidly increasing because of the nutrient solubilization activity and environment-friendly nature. However, their impact on native soil microbiomes have been least studied. In this research, we evaluated the effects of a seed-inoculated novel drought-tolerant bioinoculant on the microbial community of bulk soil, rhizospheres, and root nodules of the soybean plant in the field. The field experiment was performed at a drought-prone site in Yoakum, TX. Soil samples were collected at 7 weeks after planting as well as at harvest for evaluation of soil physicochemical properties and the microbiome analysis based on 16S rRNA (V3-V4 regions) sequences. We observed reduced evenness and the transient shift (only at 7 weeks) in the rhizosphere bacterial community because of the inoculant treatment. The bio-inoculant increased the proportions of nitrogen fixing and phosphate solubilizing plant growth promoting rhizobacteria (PGPR) in the rhizosphere, including the soybean endosymbiont *Bradyrhizobium japonicum*. Similarly, it showed beneficial effects on the co-occurrence pattern of the bacterial community where the proportion of mutually exclusive interactions and clustering coefficient was decreased. However, the modularity and density of the network were increased. Since there was no difference in the soil physicochemical properties, such as pH, nitrogen, phosphorus, potassium, and organic matter between the control and bioinoculant

treated samples, we considered that effects of the confounding environmental variables on the outcome were minimal. Our results suggest that the novel drought-tolerant bio-inoculant not only improves the crop yield, but also enhances the quality of bacterial communities in the rhizosphere. This study also provides evidence of the mechanism by which the bio-inoculant interacts with the local bacterial community to enhance plant growth.

Introduction:

Biofertilizers are a group of bacterial or fungal strains that are used in agricultural fields to enhance plant growth and crop production. Application of biofertilizers is gaining more attention in recent years as a potential alternative to the chemical fertilizers and pesticides in the agricultural system, as they are environmentally friendly, low cost, and easy to use. There are several well-known bacterial genera that have been used as a biofertilizer, such as *Pseudomonas*, *Bradyrhizobium*, *Bacillus*, *Rhizobium*, *Azotobacter*, *Burkholderia*, *Achromobacter*, *Agrobacterium*, *Aereobacter*, *Micrococcus*, *Flavobacterium*, and *Erwinia* (Hernández-Montiel et al., 2017; Okon & Labandera-Gonzalez, 1994; Rodríguez & Fraga, 1999). Bio-inoculants have been found to enhance plant growth by fixing atmospheric nitrogen, solubilizing insoluble phosphorus (P), protecting plants against pathogens, altering nutrient composition, and increasing the abundance of plant growth promoting rhizobacteria (PGPR) (Dias et al., 2017; Rodríguez & Fraga, 1999; Trabelsi & Mhamdi, 2013).

Especially for leguminous plants such as soybean, the availability of an efficient and compatible endosymbiont in soil is very important as it provides a personalized source of nitrogen (N) supplying about 50 - 60% of the N requirement of the host (Salvagiotti et al., 2008). These values could even reach up to 70 - 85% of the N requirement in well-managed fields (Alves et al.,

2003). Soybean accounts for 68% of legume crop production and 77% of the N fixed by legume crops globally (Herridge et al., 2008). It is widely cultivated in the U.S. for food, biodiesel, and oil that made an estimated \$46 billion value production in 2020 (USDA, 2021). In the past, *Bradyrhizobium* strains were introduced to agricultural fields from different parts of the world to increase soybean yield (Alves et al., 2003; Halwani et al., 2021). Also, Halwani and colleagues suggest that the symbiotic performance of the soybean nodulating bacteria remaining in the soil may not be sufficient (Halwani et al., 2021). Availability of these strains can give large economic and ecological benefits as they help to reduce the use of synthetic N fertilizers. It has long been estimated that focusing on improvement of the efficiency of symbiotic nitrogen fixation (SNF) alone would cause estimated annual benefit of \$1.067 billion in the U.S. alone (Tauer, 1989). Therefore, continuous efforts should be made for the selection and development of *Bradyrhizobium* strains to achieve sustainable yield and improved economy (Alves et al., 2003). For example, soybean plants inoculated with cold tolerant *Bradyrhizobium japonicum* strains USDA 30 and 31, where were isolated from North America, resulted in increased nodule numbers, nodule weight, shoot N content, and N-fixation compared to the widely used inoculant in Canadian fields (H. Zhang et al., 2003).

Host-symbiont interactions in soybean plants are greatly affected by abiotic stresses. Drought is a major abiotic factor that causes adverse effects on the symbiotic relationship (Kunert et al., 2016), rhizosphere microbiomes (Naylor & Coleman-Derr, 2018), and ultimately agricultural productivity. Owing to global climate changes, Naumann and colleagues estimated that the magnitude and frequency of drought is likely to be doubled in 30% of the global landmass under stringent mitigation policies including central America and parts of Southern America (Naumann et al., 2018). It also has a direct impact on soil microbial communities responsible for

the biogeochemical cycle. Drought causes a decrease largely in Gram-negative phyla Proteobacteria, Verrucomicrobia, and Bacteroidetes (Acosta-Martínez et al., 2014). Proteobacteria have been linked to play a key role in the N cycle including *B. japonicum* responsible for N fixation in soybean root nodules. Although drought-tolerant soybean varieties have been introduced, their growth, vigor, and yield are greatly influenced by the symbiotic association with their endosymbiont *B. japonicum* as well as its survivability under drought.

High-throughput sequencing technologies have facilitated rapid and efficient microbial community analysis by direct sequencing of 16S ribosomal RNA (rRNA) genes, a small subunit of rRNA gene in prokaryotes. Properties of 16S rRNA genes in prokaryotes such as ubiquity, functional constancy, larger size with many domains, and different mutation rates, make them the ultimate molecular chronometer (Mizrahi-Man et al., 2013; Woese, 1987b). Most of the previous studies have been performed in controlled environments with low depth reads (Rascovan et al., 2016), quantitative PCR (qPCR), or denaturing gradient gel electrophoresis (DGGE) (JIN et al., 2009). In this study, we have used 16S rRNA V3-V4 sequences to study microbial diversity and co-occurrence networks. Microbial network analyses have been increasingly used to investigate microbial community structures in a broad range of habitats including ocean, soil, and human. Several studies have shown that soil microbial communities are modular with non-random co-occurrence patterns in nature (Barberán et al., 2012). These modules are densely inter-connected nodes that can be interpreted as groups of taxa with overlapping niches (Faust & Raes, 2012; Newman & Girvan, 2004). Although interpretations of these networks are not straightforward, the microbial network analysis allows us to predict hub species as well as their interactions. It also helps us identify alternative community states and niches.

In this study, we evaluated the effects of a novel drought-tolerant *Bradyrhizobium* inoculant on the soybean rhizosphere microbiome in the field. The bio-inoculant was previously isolated from a drought prone region in South Texas.

Materials and Methods:

Seed inoculation and planting:

A drought prone region at Yoakum, TX (29°16'N 97°07'W) was selected for performing the field experiment. The TXVA strain was grown in Arabinose-gluconate (AG) media (Sadowsky et al., 1987) at 30°C incubator with vigorous shaking at 200rpm until the O.D._{600nm} reached approximately 1.5. Dyna Grow S52RS86 (maturity group 5E) soybean cultivar (Reiter et al., 2018) was selected for the experiment. Plantation was done using a 2-row vacuum planter (Monosem ATI, Inc., Lenoxa, KS, USA) set at a seeding rate of 33 seed m⁻¹, corresponding to 55,847 seeds ha⁻¹. For seed inoculation, 1 lb of soybean seeds were mixed with 10ml of TXVA culture before sowing. The application rate was determined by ensuring complete coverage with inoculum, such that every seed was glistening but allowed absorption into the seedcoat within 5 minutes. All other agricultural practices were followed as normal.

To avoid cross-contamination, control seeds or no treatment (NT) seeds were planted first followed by inoculant treated seeds. Five plots for each control and inoculant treatment were assigned as random plot design. Each plot had five 20' long rows and 5' space between two plots. For the irrigation treatment, the same random plot design was replicated on the other side of the field with a 50' spacer between them. The drought condition was maintained in one side of the field with no irrigation after 7-weeks post planting. Planting was done on April 2, 2019.

Plant and soil collection and physicochemical property evaluation:

Plant samples and soil samples were collected from the field at 7-weeks (R1 stage) post planting (May 22, 2019) and harvest time on Sep 6, 2019. For soil collection, 3 different samples from different locations were combined to make one sample. Plant height was measured in the field from crown region to the top flowering node. Plants were cut from the crown region for weight and yield measurements. Roots were dug up with the shovel and placed in Ziplock bags along with bulk soil. Soil and root samples were transported to lab within 12 h and kept in -80°C until processed. Plants were dried at room temperature for several days for plant dry weight measurement. Loosely attached soil to the root surface were removed by gentle shaking and remaining attached rhizosphere soils were collected using a sterile brush. In addition, nodules were removed from the root and stored in 30% glycerol at -80°C until processed. Soil samples were sent to Soil, Water and Forage Testing Laboratory at Texas A&M for physicochemical property evaluation. We also measured the field capacity (FC) of the soil collected from the field. Briefly, we collected soil in 3x3 gal pots and saturated with water. Water was left for percolation for 2-3 days by covering the mouth of the pot until no further runoff observed. Volumetric water content (VWC) was measured using VWC meter (ML3 ThetaProbe, Delta-T Devices Ltd, Cambridge, UK) and FC was measured by oven drying (115°C) 100 g of soil taken from 10-15 cm deep from the top.

Library preparation and 16S rRNA gene sequencing:

DNA was isolated from each triplicate by using PowerSoil DNA isolation kit (Qiagen, Germany), following manufacturer's instruction. Nodules were surface-sterilized and crushed aseptically

prior to DNA extraction. Surface sterilization was done by washing 3 times with 0.9% NaCl, followed by washing twice with 3% sodium hypochlorite and finally washing 3 times with sterile water. Surface sterility was ensured by rolling the surface sterilized nodules on YEM agar and incubating at 30°C for 48 h. After DNA extraction, the concentration and purity of DNA was accessed using nanodrop spectrophotometer. Amplification and sequencing of 16S rRNA process was followed as previously described in Niraula et al., 2021. PCR amplification of 16S rRNA v3-v4 hypervariable region was carried out in triplets of 25µl reaction volume containing; KAPA HiFi master mix and Illumina adaptor ligated universal primers 341F (5'-tcgtcggcagcgtcagatgtgtataagagacagCCTACGGGNGGCWGCAG-3') and 806R (5'-gtctcgtgggctcggagatgtgtataagagacagGACTACNVGGGTWTCTAAT-3'). The thermocycler condition was maintained as follows: i) initial denaturation at 94°C for 3 min, followed by ii) 25 cycles of 94°C for 30 sec, 55°C for 30 sec, and 72°C for 30 sec, and iii) a final extension of 72°C for 3 min. PCR products were confirmed visually on 1% agarose gel and purified by using QIAquick PCR purification Kit (Qiagen, Germany). Purified PCR products were sent to Genome Sequencing and Analysis Facility (GSAF), Austin, Texas for barcoding and sequencing in Illumina MiSeq sequencer to produce 300 bp paired end reads.

Sequence preprocessing and taxonomic assignments:

Primer sequences were trimmed from raw sequences using cutadapt 2.4. QIIME2-2019.7 (Bolyen et al., 2018). Sequences were further denoised, dereplicated, and chimera filtered (consensus based) using DADA2 (Callahan et al., 2016) plugin with the following input parameters; --p-trunc-len-f 280, --p-trunc-len-r 200, --p-trim-left-f 17, --p-trim-left-r 21. Representative sequences were then aligned using mafft (Kato et al., 2002) (via q2-alignment) to construct a phylogenetic tree

with fasttree2 (Price et al., 2010) (via q2-phylogeny). To assign the taxonomy, SILVA-139-99 reference reads were first extracted using 341F/806R primers with minimum read length 100 bp followed by taxonomic assignments using classify-consensus-vsearch plugin with default setting. Sequences classified as mitochondria and chloroplast were removed from further analysis. Thus, obtained amplicon sequence variants (ASVs) with frequency 1 were filtered out to minimize possible sequencing artifacts.

Functional prediction:

The functional potential of the microbial community was determined by using the Phylogenetic Investigation of Communities by Reconstruction of Unobserved States (PICRUSt2) version 2.4.1 (Langille et al., 2013) and Functional Annotation of Prokaryotic Taxa (FAPROTAX) version 1.2.4 (Louca et al., 2016). PICRUSt was used to predict the functional potential of the community based on marker genes. Before function prediction, we ensured the nearest-sequenced taxon index (NSTI) value for each of our ASVs to be less than 2 using hsp.py function in PICRUSt2.

Network construction:

Two co-occurrence networks were constructed for TXVA and NT rhizosphere samples separately using Fastspar SparCC correlation (Friedman & Alm, 2012), which has shown robustness for handling compositional data (Berry & Widder, 2014; Friedman & Alm, 2012). For each network construction, we combined all TXVA rhizosphere and NT rhizosphere samples, respectively. To reduce the possible bias caused by different sampling space and time, ASVs present in at least 3 samples were considered for each inoculant treatment (TXVA=1186 ASVs and NT=1404 ASVs). Additionally, we compared the specialist ASVs from different sample

groups to ensure that the number of those specialist ASVs do not exceed the maximum threshold (30% habitat specialist) as recommended by Berry and Widder (2014). Network specificity was found to decline sharply above that threshold. In our case, those were in the range of 9.95-24.44% for TXVA samples and 11.08-23.79% for NT samples. P-values were determined by performing Fastpar correlations on 1000 times permuted of the ASV table using parallel threads. Highly correlated OTUs (≤ -0.8 or ≥ 0.8) with P -value ≤ 0.01 were only retained. In the constructed networks, the nodes and edges represent ASVs and significant pairwise association between nodes, respectively.

Networks were analyzed using igraph 1.2.4 package in R. Correlation networks were clustered into modules using Girvan Newman algorithm (Newman & Girvan, 2004) (`cluster_edge_betweenness`), in which communities were clustered into modules based on the edge betweenness of each edge in the network. Topological properties of the network such as modularity, clustering coefficient, edge density, diameter, average path length, betweenness centrality, and hub scores were calculated. Furthermore, A scale-free network topology was ensured using `fit.power.law ()` function in igraph. Alongside, 1000 Erdős-Rényi random networks (Erdős & Rényi, 2011) of equal size (same number of nodes and edges as that of TXVA and NT each) were generated followed by calculation of modularity, global clustering coefficient, network diameter, and average path length. Finally, network visualization and graphic modifications were performed using Cytoscape 3.7.1 (Shannon et al., 2003) and Gephi 0.9.2 (Bastian et al., 2009).

Statistical analysis:

QIIME2, R, and STAMP were used for all statistical analysis. PERMANOVA was performed to identify differences in bacterial communities. Wilcoxon test was performed to compare alpha

diversities. Welch *t*-test and ANOVA analyses were done in R. Likewise, LEFSe was carried out to determine differentially abundant taxa using Galaxy version 1.0.0 at <https://huttenhower.sph.harvard.edu/galaxy/>.

Results:

Physical and chemical properties of soil:

Soil in Yoakum, Texas is a sandy loam soil. The field capacity was calculated as $20.4 \pm 0.87\%$. Soil pH is the most important abiotic factor in determining soil health. The soil pH ranged from 5.7 to 6.7 and from 5.9 to 6.3 in the TXVA and NT-treated soil, respectively. Nitrogen (NO_3N), P, and potassium (K) were in the range of 5-13 ppm, 16-28 ppm and 73-145 ppm, respectively, in the TXVA-treated bulk soil. For the NT-treated soil, NPK were in the range of 4-12 ppm, 14-28 ppm, and 71-162 ppm, respectively. We did not observe any significant differences among TXVA and NT treatments. Summary of the soil chemical properties is shown in Table 3-1.

Table 3-1 Soil chemical properties from 7-week samples.

Sample	TXVA	NT
pH	6.28 ± 0.14	6.18 ± 0.10
EC (umhos/cm)	61 ± 8.46	88.33 ± 6.96
NO₃N (ppm)	6.83 ± 1.28	8.83 ± 1.12
P (ppm)	23.17 ± 2.02	19.83 ± 1.92
K (ppm)	108.17 ± 11.23	105.5 ± 12.99
Ca (ppm)	811.67 ± 62.93	744 ± 88.25
Mg (ppm)	185.67 ± 6.26	176.17 ± 12.14
S (ppm)	2.83 ± 0.17	2.67 ± 0.21

Na (ppm)	40 ± 5.21	27.83 ± 6.87
Fe (ppm)	12.35 ± 1.32	11.78 ± 1.12
Zn (ppm)	0.47 ± 0.05	0.53 ± 0.06
Mn (ppm)	17.01 ± 0.99	15.71 ± 0.95
Cu (ppm)	0.47 ± 0.03	0.41 ± 0.02
OC (%)	0.47 ± 0.02	0.49 ± 0.04
OM (%)	0.82 ± 0.03	0.85 ± 0.08

Plant growth measurements:

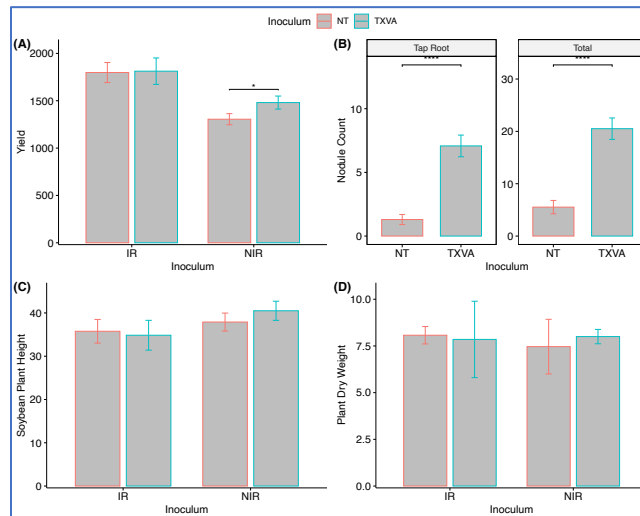


Figure 3-1 Soybean yield, nodule number and plant dry weight between TXVA and NT treatments. Welch t-test was performed to compare between irrigated and non-irrigated samples. P-value; <0.05 (*), <0.01(**).

We observed a statistically significant yield increase of the TXVA-inoculated soybean in the non-irrigated plot (Figure 3-1 A). However, we did not observe differences in soybean yields between the TXVA and NT-inoculated soybean in the irrigated plot (Figure 3-1 A). Additionally, TXVA inoculated samples produced the higher number of nodules on the tap root as well as on the total root system (Figure 3-1 B). These nodule samples were collected during 7 weeks of growth, which

is considered the active nodulation phase. The plant height and dry weight of the soybean plant were similar between TXVA and NT-inoculated samples for both irrigated and non-irrigated conditions (Figure 3-1 C/D).

Sequence preprocessing and quality control:

After quality filtering, denoising, chimera filtration, and removing host-associated rRNA, a total of 1,369,993 high quality reads were obtained with an average of 37,154 reads per sample (maximum=68,914 and minimum=5,394). A total of 15,719 ASVs were retained in 63 samples. Most of the bacterial diversity and the number of ASVs present in the samples were captured by the sequenced read depth for respective samples as observed by the alpha rarefaction curves (Figure 3-2 A/B).

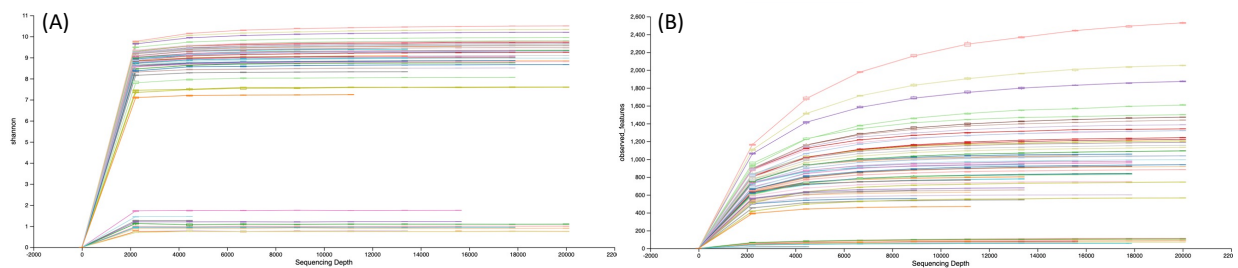


Figure 3-2 Alpha rarefaction based on Shannon diversity index and the number of observed amplicon sequence variants (ASVs).

Taxonomic summary of bulk soil, rhizosphere soil and nodules:

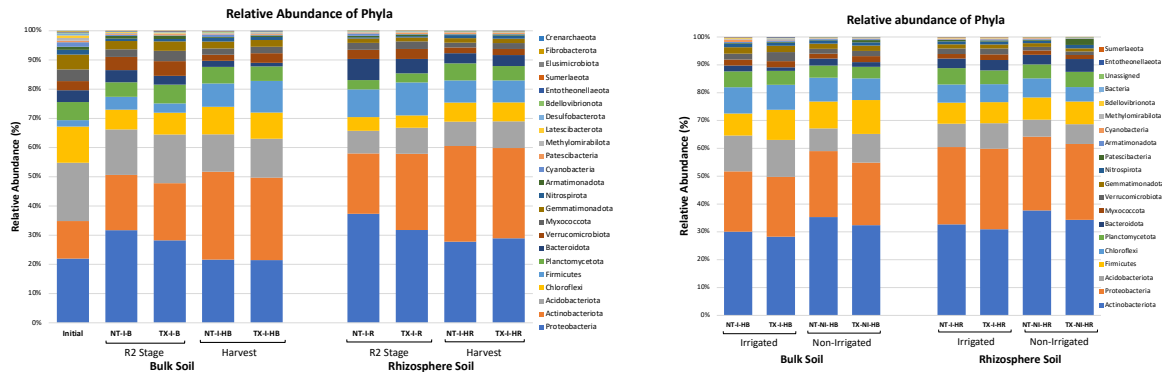


Figure 3-3 Relative abundances of phyla at initial, 7-week and harvest periods. Each stacked bar plot represents the average of 3 biological replicates.

All bulk and rhizosphere-associated sequences were classified into 39 phyla. Among them, top 20 phyla are shown in Figure 3-3. In the initial samples, the most abundant phyla included *Proteobacteria* (21.83%), *Acidobacteria* (19.8%), *Actinobacteria* (12.79%) and *Chloroflexi* (12.32%). We observed similar changes in the proportions of phyla in bulk and rhizosphere soils during the two growth stages. The relative abundances of *Proteobacteria* were increased at 7 weeks and slightly reduced during the harvest time, while the proportions of *Actinobacteria* was increased at harvest (Figure 3-3). Proportions of *Actinobacteria* surpassed during harvest in all conditions.

Similarly, we compared the effects of irrigation on the relative proportions of phyla during the harvest period (Figure 3-3). Although, overall proportions of *Actinobacteria* (28.18 - 37.64%) were higher during harvest, their abundance increased under the drought condition (i.e., non-irrigated condition).

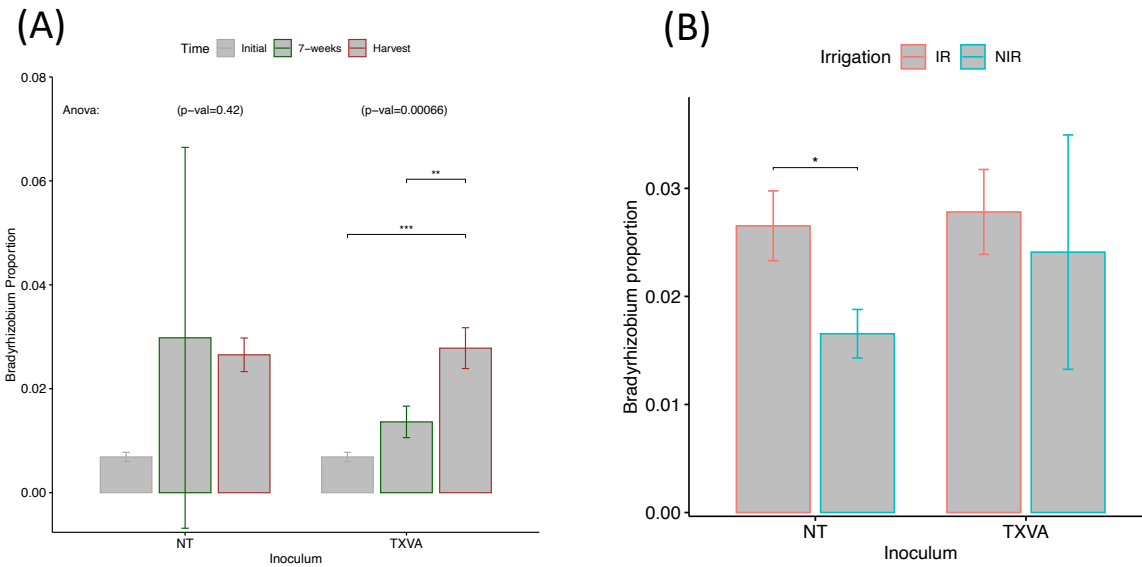


Figure 3-4 Proportions of the genus *Bradyrhizobium* in the rhizosphere soil between NT and TXVA treatments at 3 time points including initial, 7 weeks, and harvest (A) and during harvest (B). ANOVA was done for each group followed by tukey's hsd to quantify differences in proportions at 3 time points. Welch's t-test was done to compare means of proportions in sub figure B.

We compared the proportions of the genus *Bradyrhizobium* in TXVA and NT-treated rhizosphere soils to identify the effect of developmental stages and irrigation. In the NT samples, there was high variability in the *Bradyrhizobium* proportion at 7 weeks and no significant increase was observed at any time point. In contrast to the NT treatment, there was a significant increase of the *Bradyrhizobium* proportion in the TXVA-treated samples from initial to harvest samples (Figure 3-4 A). This indicates controlled abundance and persistence of *Bradyrhizobium* in the TXVA treated rhizosphere. Also, the proportion of *Bradyrhizobium* is significantly decreased in the NT rhizosphere in response to drought (Figure 3-4 B). There was no significant change in the proportion of *Bradyrhizobium* in the TXVA treated rhizosphere. This suggests increased drought tolerance of *Bradyrhizobium* in the rhizosphere soil.

Alpha and beta diversity analysis:

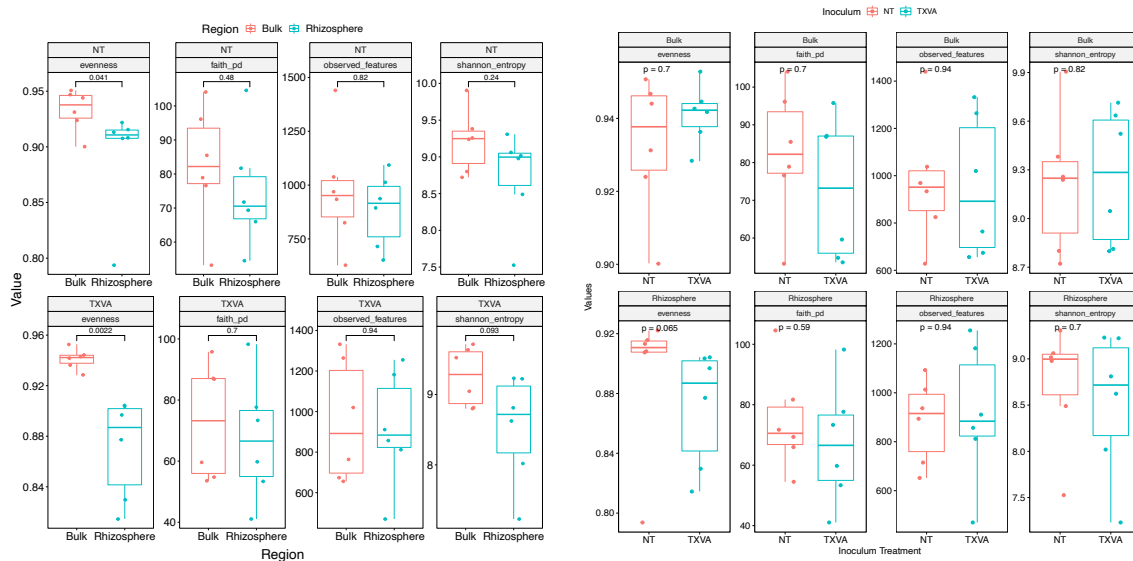


Figure 3-5 Differences in alpha diversity between bulk and rhizosphere soil among NT and TXVA samples. P-value was calculated by Wilcox's test.

We used four beta diversity metrics on the rarefied ASV table to investigate the differences in community structure. We observed a significant difference in the microbiome at three time points based on Bray-Curtis (PERMANOVA, $p = 0.0009$, $R^2 = 0.171$), Jaccard (PERMANOVA, $p = 0.0009$, $R^2 = 0.106$), Unweighted UniFrac (PERMANOVA, $p = 0.0009$, $R^2 = 0.147$), and Weighted UniFrac (PERMANOVA, $p = 0.0009$, $R^2 = 0.403$) distance matrices. Largest variation was observed among samples from different time points (PERMANOVA; 16.184, p -val=0.001). The difference in beta diversity was more significant between bulk and rhizosphere soil in 7-week samples ($R^2 = 0.33$, p -val=0.0009) than harvest samples ($R^2 = 0.22$, p -val=0.0009). Proteobacteria and the Bacteroidota are the most dominant phyla in the 7-weeks rhizosphere soil, whereas the bulk soil was dominated by Acidobacteriota (Figure 3-6). Similarly, the harvest soil was dominated by Actinobacteriota (Figure 3-6).

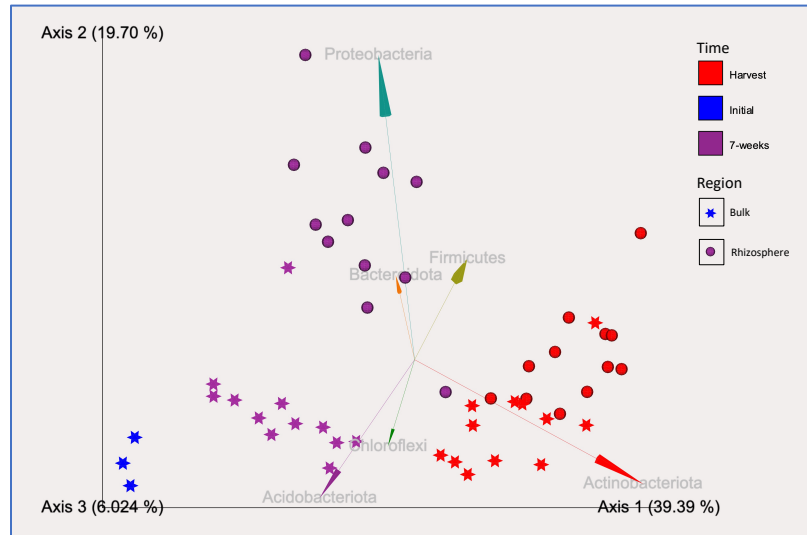


Figure 3-6 Principal coordinate analysis based on Weighted UniFrac distance.

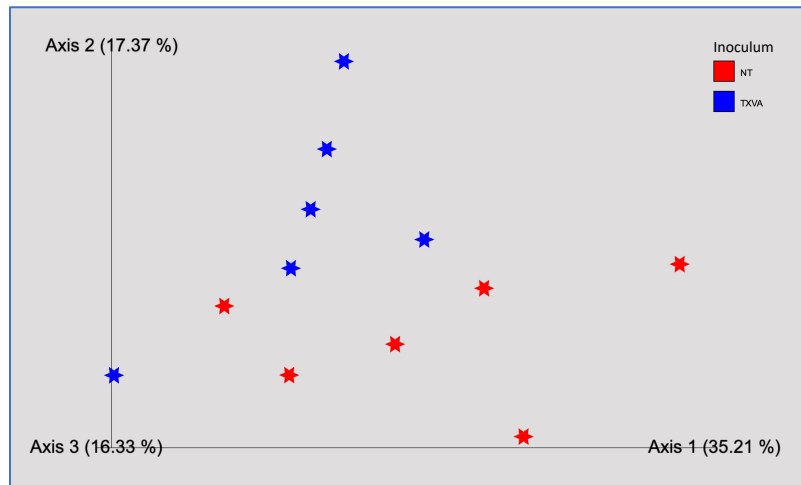


Figure 3-7 Principal coordinate analysis based on Weighted UniFrac distance among NT and TXVA samples in 7-weeks rhizosphere.

Adonis PERMANOVA test showed 15% ($R^2 = 0.157822$, $p = 0.038$) variation explained by NT and TXVA rhizosphere microbiomes based on Weighted UniFrac distance (Figure 3-7). However, the community difference was not observed using Bray-Curtis (PERMANOVA, $p = 0.171$, $R^2 =$

0.104), Jaccard (PERMANOVA, $p = 0.425$, $R^2 = 0.092$), and Unweighted UniFrac (PERMANOVA, $p = 0.448$, $R^2 = 0.09$) distance matrices. This suggests that the difference was due to the abundance of phylogenetically distantly related ASVs. The observed difference in beta diversity in response to inoculant treatments was not observed during harvest (PERMANOVA, $R^2 = 0.12$, $p = 0.232$), indicating a short-term effect of the inoculant application.

Differential abundance of taxa:

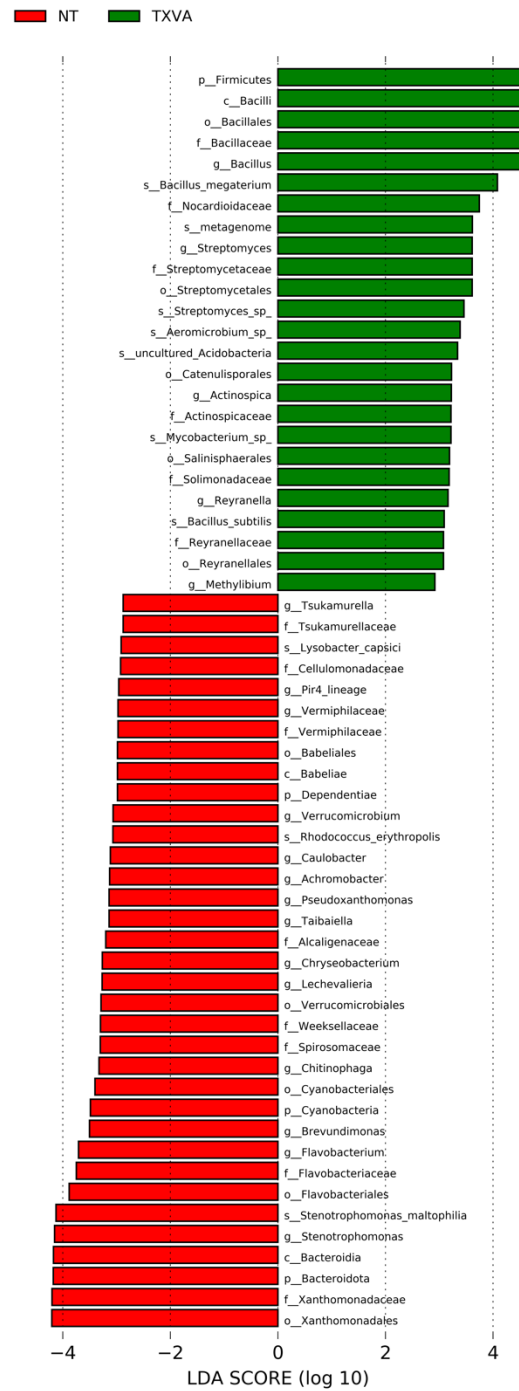


Figure 3-8 Differentially abundant taxa between NT and TXVA treated rhizosphere soil in 7-weeks samples.

Bacillus megaterium (LDA = 4.08, p-val = 0.0163), *Bacillus subtilis* (LDA = 3.09, p-val = 0.041), *Streptomyces* spp. (LDA = 3.45, p-val = 0.00388), *Mycobacterium* spp. (LDA = 3.22, p-val = 0.028), *Actinospica* (LDA = 3.225, p-val = 0.04) and *Methylibium* (LDA = 2.92, p-val = 0.041) are differentially abundant in the TXVA-treated rhizosphere soil (Figure 3-8). On the other hand, bacterial genera, such as *Stenotrophomonas maltophilia* (LDA = 4.12, p-val = 0.037), *Flavobacterium* (LDA = 3.71, p-val = 0.0039), *Pseudoxantomonas* (LDA = 3.14, p-val = 0.037), *Verrucomicrobium* (LDA = 3.07, p-val = 0.004), *Chitinophaga* (LDA = 3.33, p-val = 0.0039), *Brevundimonas* (LDA = 3.5, p-val = 0.042), *Lechevalieria* (LDA = 3.27, 0.01), *Chryseobacterium* (LDA = 3.27, p-val = 0.024), *Tsukamurella* (LDA = 2.88, p-val = 0.022), *Taibaiella* (LDA = 3.14, p-val = 0.0091), *Achromobacter* (LDA = 3.13, p-val = 0.037), *Caulobacter* (LDA = 3.12, p-val = 0.037), *Rhodococcus erythropolis* (LDA = 3.07, p-val = 0.046), *Vermiphilaceae* (LDA = 2.97, p-val = 0.036) and *Lysobacter capsica* (LDA = 2.91, p-val = 0.022), remained enriched in NT rhizosphere samples. At the phylum level, Firmicutes (LDA = 4.63, p-val = 0.037) were enriched in the TXVA-treated rhizosphere soil, whereas Bacteroidota (LDA = 4.93, p-val = 0.01), Cyanobacteria (LDA = 3.49, p-val = 0.04) and Deendentiae (LDA = 2.98, p-val = 0.06) were enriched in the NT rhizosphere soil (Figure 3-8).

Diversity in the root nodules:

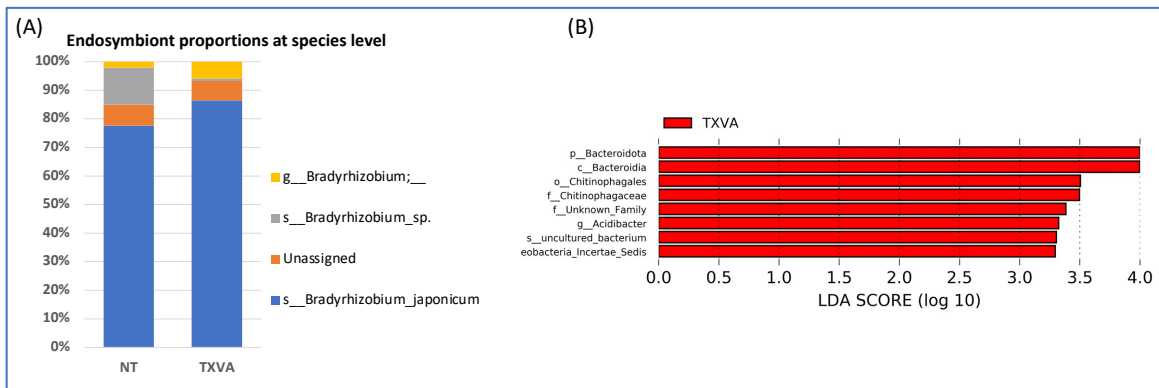


Figure 3-9 Relative abundances of the most abundant endosymbiont inside the root nodules (A) and the differential abundance of taxa in nodules between NT and TXVA treated samples (B). Relative abundance in NT and TXVA samples represents the average of 6 replicates.

We observed large diversity in the nodule samples; however, the proportion of unassigned taxa and those related to *Bradyrhizobium* are higher (Figure 3-9 A). The proportion of *Bradyrhizobium japonicum* is higher in TXVA nodules (86.24 ± 0.12) than NT nodules (77.51 ± 0.24). However, the proportion of unassigned species of *Bradyrhizobium* was higher in NT nodules (12.96 ± 0.26) than TXVA nodules (0.91 ± 0.02). LEFSe analysis showed the differential abundance of phylum Bacteroidota in TXVA nodules (Figure 3-9 B).

Comparison of network properties of rhizosphere microbiomes between NT and TXVA treatments:

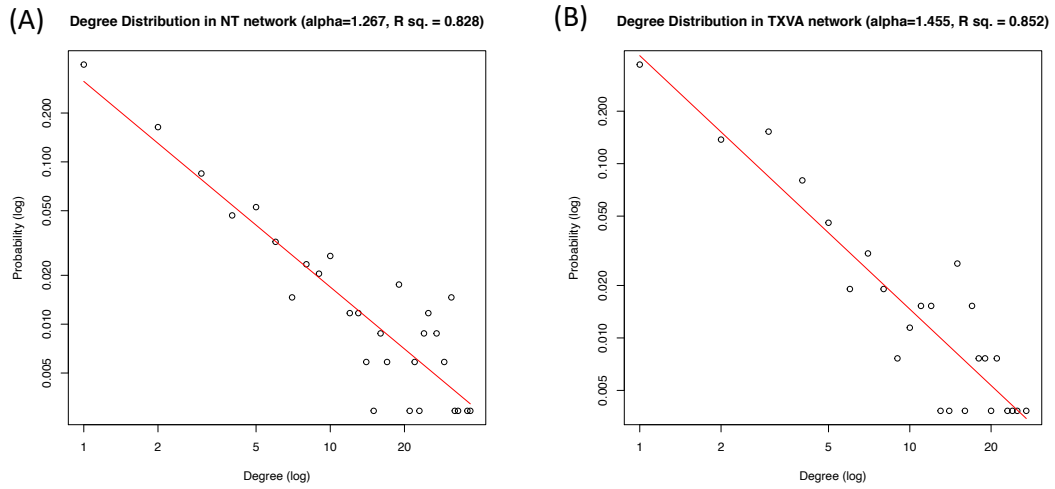


Figure 3-10 Scale-free topology of the NT (A) and TXVA (B) rhizosphere networks.

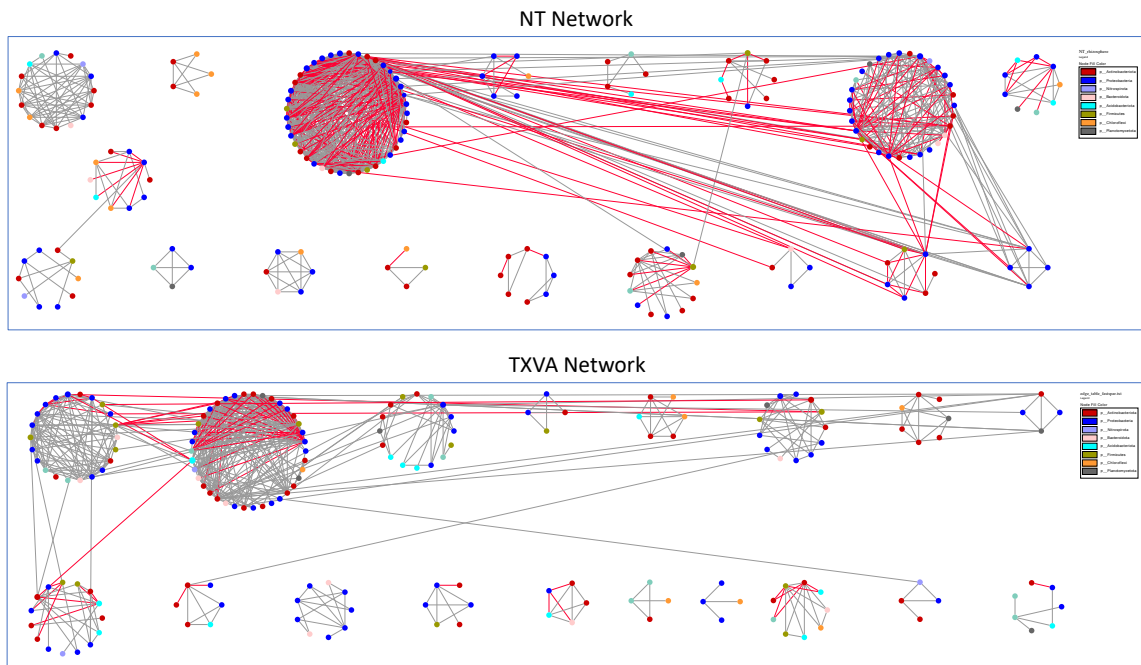


Figure 3-11 Cooccurrence network of NT and TXVA treated rhizosphere soils.

We compared the rhizosphere networks between NT and TXVA treatments. Rhizosphere networks constituted 342 nodes for NT and 266 for TXVA connected with 919 and 585 edges, respectively (Figure 3-11). Both networks followed scale-free topology (Figure 3-10) as indicated by the power-law distributions (Kolmogorov-Smirnov test, $p\text{-val} > 0.05$) of node degrees, suggesting non-random co-occurrence patterns of the network. Similarly, modularity, clustering coefficient, network diameter, and average path length were larger than the corresponding random networks, suggesting that the networks are non-random real-world networks. Comparatively, the TXVA network had higher modularity, network density, network diameter, and average path length than the NT network (Table 3-2). On the other hand, the clustering coefficient was smaller in the TXVA than NT network. A higher proportion of positive edges (85.47%) in the TXVA network was observed compared to that in the NT network (68.88%).

Table 3-2 Network topological properties of NT and TXVA network.

Network	Nodes	Edges	+ve edges	-ve edges	Modularity	Density	Clustering coefficient	Network diameter	Average path length
NT	342	919	68.88%	31.12%	0.65	0.01576	0.624834	7.395	3.3779
TXVA	266	585	85.47%	14.53%	0.71	0.0166	0.562364	9.945	4.187
Random NT	342	919	NA	NA	0.395±0.000	NA	0.0156±0.0000	7.211±0.0	3.645±0.000
Random TXVA	266	585	NA	NA	0.46±0.0003	NA	0.0165±0.0001	8.069±0.0	3.899±0.001

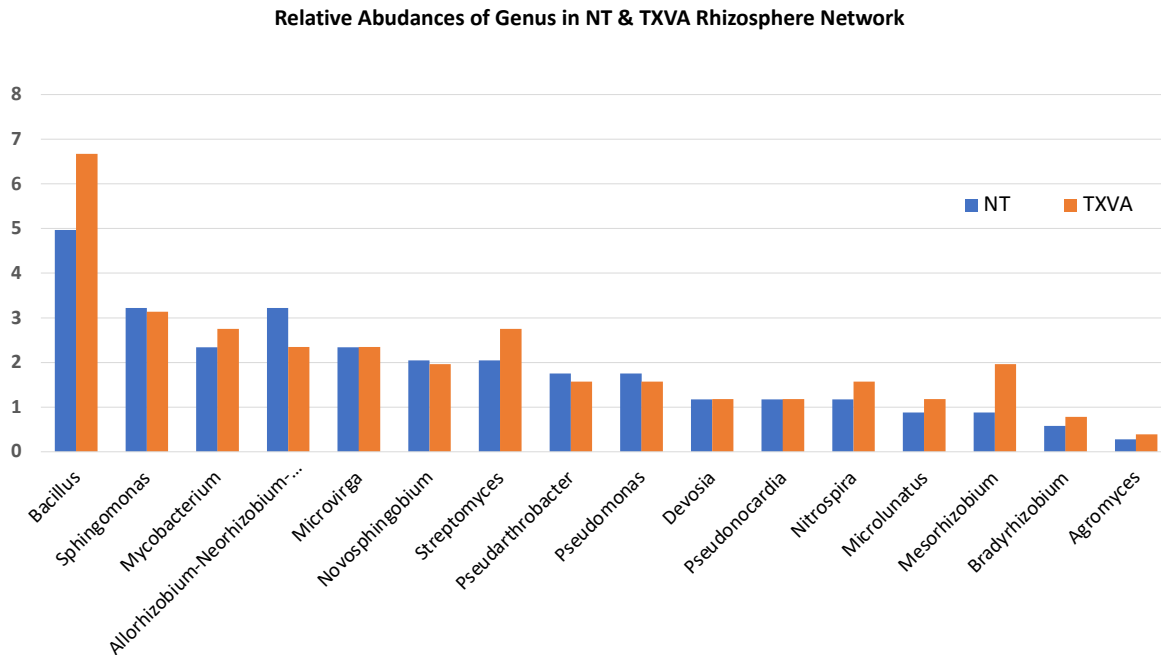


Figure 3-12 Relative abundances of genus in NT and TXVA rhizosphere network.

We compared the relative proportions of PGPR in the rhizosphere network. In the TXVA rhizosphere network, proportions of *Bacillus*, *Mycobacterium*, *Streptomyces*, *Nitrospira*, *Microtholunatus*, *Mesorhizobium*, *Bradyrhizobium* and *Agromyces* are higher than those in the NT rhizosphere network. On the other hand, proportions of *Sphingomonas*, *Allorhizobium*, *Novosphingobium*, *Pseudoarthrobacter* and *Pseudomonas* are higher in the NT network compared to the TXVA network.

Predicted functions:

We used PICRUS2 and FAPROTAX to compare the predicted functional potential of microbial communities. In the drought condition during harvest, we observed higher metabolic potentials for lipopolysaccharide biosynthesis ($p < 0.05$) and fatty acid biosynthesis ($P < 0.05$) in the TXVA

treated rhizosphere soil (Figure 3-13). Similarly, there was a significant reduction ($P < 0.05$) in N-fixation by the NT-associated rhizobacterial community in the drought condition than the irrigated control (Figure 3-14). However, the difference was not statistically significant in the TXVA samples. Also, the overall N-fixation was slightly higher in the TXVA samples under the drought condition, although the difference was not significant.

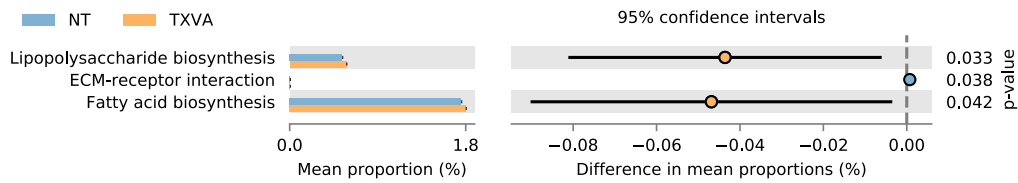


Figure 3-13 Differences in PICRUSt2 predicted functions between NT and TXVA during harvest in non-irrigated condition.

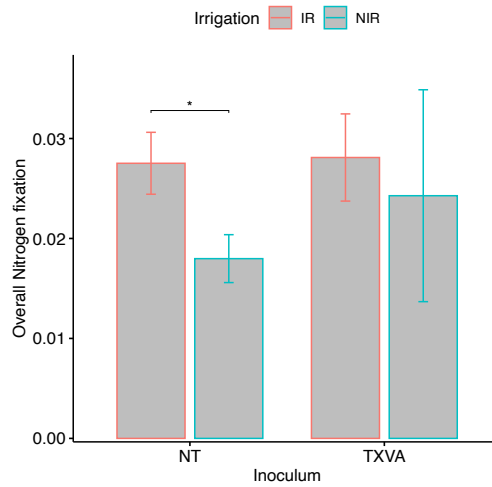


Figure 3-14 Differences in abundance of Overall Nitrogen fixation in rhizosphere soil between irrigated and non-irrigated conditions during harvest.

Discussion:

Inoculation increased nodulation and soybean yield:

Endosymbionts and the rhizosphere microbiota play a significant role on the overall growth and the productivity of leguminous crops such as soybeans. However, these endosymbionts including free living PGPR suffer from environmental stresses, thereby limiting the sustainability in the agricultural field. In this study, we investigated the effects of drought-tolerant *B. japonicum* strain (i.e., the TXVA strain) on the soybean growth and the rhizosphere/nodule microbial community. We used 16S rRNA gene-based analysis of the microbial community. Inoculation of the TXVA strain showed a significant increase in soybean yield under the non-irrigated condition compared to the irrigated control (Figure 3-1). Our result is in concurrence with several past studies where inoculation of *Bradyrhizobium* strains increased soybean yield and performance (Egamberdieva, Jabborova, et al., 2016; Głodowska et al., 2017; H. Zhang et al., 2003). The increased yield in the drought condition may be attributed to the N-fixing and nutrient-solubilizing abilities of the applied inoculant. As observed from predicted functions, TXVA treated rhizosphere samples did not show significant decrease in N-fixation under drought condition, which may have contributed to higher yield (Figure 3-14). Additionally, we observed a significant increase in the number of total root nodules as well as the nodules associated with the tap root (Figure 3-1) in TXVA-inoculated plants. Differentially abundant *Bacillus subtilis* (Figure 3-8, Figure 3-12) in TXVA samples may have contributed to higher nodule numbers. *B. subtilis* was found to work in synergism with *B. japonicum* to increase nodule count and N-fixation in soybean plants (Tsigie et al., 2011). It has been observed that more nodule numbers in the bio-inoculant treated samples correspond with higher N-fixation rates in the soybean plant (H. Zhang et al., 2003) because of

the increased overall leghemoglobin content in soybean nodules after the treatment (Halwani et al., 2021). In addition, nodules act as a shelter to many endosymbionts during environmental stresses. Although there were high nodule numbers in TXVA-inoculated soybeans under the irrigated condition, no yield difference was observed in the irrigated condition. This could possibly indicate that plants fulfill the remaining nutrient requirement from the environment as the available water facilitates absorption of nutrients under the irrigated condition. Increased nodule counts under the normal condition (Figure 3-1) and sustained N-fixation under drought condition indicates higher nodulation efficiency and functional constancy of drought-tolerant inoculant under the drought stress. Also, the persistence of the TXVA inoculant in the rhizosphere soil is higher during harvest under both irrigated and non-irrigated conditions (Figure 3-4).

Changed alpha and beta diversity:

We analyzed the alpha and beta diversity of the microbiome of the bulk soil, rhizosphere soil, and the nodules. An overall positive impact on the microbial community was observed. The bacterial community significantly changed across the growth stages, suggesting a preserved natural phenomena in the soil. The 7-week rhizosphere microbial community was mostly dominated by *Proteobacteria* and *Bacteroidetes*, whereas those at harvest were dominated by *Actinobacteria* (Figure 3-3, Figure 3-6). Multiple studies have confirmed the alteration in the microbial community in response to growth phases (JIN et al., 2009; Sugiyama et al., 2014). Similarly, spatial variability among bulk and rhizosphere microbiome was also observed at both 7-weeks and harvest. However, the difference was more prominent at 7-weeks, where evenness was significantly reduced in rhizosphere soil in both NT and TXVA samples (Figure 3-5), suggesting the strong influence of plant root exudates. Such colonization is a favorable trait for plant growth. Although the difference

was not statistically significant, the evenness appeared to be reduced by TXVA inoculation. Under the influence of plant root exudates, we observed a significant change in rhizosphere bacterial community structure in response to inoculum treatment at 7-weeks samples using the Weighted UniFrac distance matrix. However, the effect was transient because it was not observed during harvest. Weighted UniFrac considers the abundance (giving more weight to the abundant species) and the phylogenetic relatedness among (Lozupone et al., 2007). This observation suggests that the TXVA strain increased the abundance of the phylogenetically related bacterial population in the rhizosphere.

Inoculation increased PGPR abundance:

Increased abundance of *Firmicutes* and *Bacillus* in TXVA inoculated samples showed favorable conditions for plant growth, as both have N-fixing and phosphate solubilizing abilities. In addition, *Firmicutes* have been shown to increase the utilization of plant-derived carbon under soil amendments by biochar (Liao et al., 2019). Enrichment of *B. subtilis* in TXVA treated rhizosphere, and the higher abundance of *Bacillus* in TXVA suggests mutually beneficial relationships, potentially increasing soybean growth and yield. It has been established that *B. subtilis* works synergistically with *B. japonicum* to give maximum soybean yield (Atieno et al., 2012; Tsigie et al., 2011). In addition, *B. subtilis* strain 101 is known to work as a pest control agent (MPCA) (Felici et al., 2008). One of the mechanisms by which *B. subtilis* confer drought tolerance in plants is the production of 1-Aminocyclopropane-1-carboxylate (ACC) deaminase (H.G. et al., 2020). ACC deaminase reduces the level of ethylene, a plant hormone that retards normal root growth and triggers senescence under drought (Naylor & Coleman-Derr, 2018).

Inoculation altered co-occurrence patterns and network topology:

“Co-occurrence networks are robust to small differences in sample sites or near-steady-state community conditions, and that while some sensitivity is lost, the specificity of the resulting networks remains reliable” (Berry & Widder, 2014). Scale-free topology and random null model network comparison ensured that both NT and TXVA rhizosphere networks are real-world microbial co-occurrence networks. As indicated by the network topologies such as modularity, density, and diameter (Table 3-2), microbial communities in TXVA samples have a more complex network than NT samples, although the number of ASVs is less in TXVA. The complexity of the network in TXVA possibly suggests more information sharing and resource distribution in the rhizosphere, thereby favoring the soybean yield. Our result agrees with the finding of Tao and co-authors, where the network complexity was highly correlated with the maize phenotype (Tao et al., 2018). In addition, a smaller average path length in the NT network indicates a small-world network favoring quick response to perturbations and information/resource sharing (Faust & Raes, 2012). Similarly, the NT network has higher transitivity (Table 3-2) or average clustering coefficient, which has been interpreted as the presence of degradation pathways or niche filtering (Röttjers & Faust, 2018). On the other side, TXVA provides more shared niches. The proportion of negative edges in the NT network is higher.

Enhanced predicted functional potential:

Comparison of predicted functions of the microbiome during harvest showed increased lipopolysaccharide (LPS), and fatty acid biosynthesis processes in TXVA inoculated rhizosphere under drought conditions (Figure 3-13) LPS is an integral part of the outer membrane of gram-negative bacteria that is essential for survival and protection against environmental stress. The

absence of a thick peptidoglycan layer and the inability to form endospore make gram-negatives more prone to damage caused by abiotic stresses. It is essential for *B. japonicum* infection to soybean plants (Stacey et al., 1991). Similarly, some fatty acids such as homoserine lactone is associated with quorum sensing in *B. japonicum* (Lindemann et al., 2011).

References:

- Acosta-Martínez, V., Cotton, J., Gardner, T., Moore-Kucera, J., Zak, J., Wester, D., & Cox, S. (2014). Predominant bacterial and fungal assemblages in agricultural soils during a record drought/heat wave and linkages to enzyme activities of biogeochemical cycling. *Applied Soil Ecology*, 84, 69–82. <https://doi.org/10.1016/j.apsoil.2014.06.005>
- Alves, B. J. R., Boddey, R. M., & Urquiaga, S. (2003). The success of BNF in soybean in Brazil. *Plant and Soil*, 252(1), 1–9. <https://doi.org/10.1023/A:1024191913296>
- Atieno, M., Herrmann, L., Okalebo, R., & Lesueur, D. (2012). Efficiency of different formulations of Bradyrhizobium japonicum and effect of co-inoculation of Bacillus subtilis with two different strains of Bradyrhizobium japonicum. *World Journal of Microbiology and Biotechnology*, 28(7), 2541–2550. <https://doi.org/10.1007/s11274-012-1062-x>
- Barberán, A., Bates, S. T., Casamayor, E. O., & Fierer, N. (2012). Using network analysis to explore co-occurrence patterns in soil microbial communities. *ISME Journal*, 6(2), 343–351. <https://doi.org/10.1038/ismej.2011.119>
- Bastian, M., Heymann, S., & Jacomy, M. (2009). Gephi : An Open Source Software for Exploring and Manipulating Networks. *International AAAI Conference on Weblogs and Social Media.*, 13. <https://doi.org/10.1136/qshc.2004.010033>
- Berry, D., & Widder, S. (2014). Deciphering microbial interactions and detecting keystone species with co-occurrence networks. *Frontiers in Microbiology*, 5(MAY). <https://doi.org/10.3389/fmicb.2014.00219>

- Bolyen, E., Rideout, J. R., Dillon, M. R., Bokulich, N. A., Abnet, C. C., Gabriel, A., Ghalith, A., Alexander, H., Alm, E. J., Arumugam, M., Asnicar, F., Bai, Y., Bisanz, J. E., Bittinger, K., Brejnrod, A., Brislawn, C. J., Brown, C. T., Benjamin, J., Mauricio, A., ... Willis, A. D. (2018). QIIME 2 : Reproducible , interactive , scalable , and extensible microbiome data science. *PeerJ Preprints*, 6:e27295v2.
- Callahan, B. J., Mcmurdie, P. J., Rosen, M. J., Han, A. W., Johnson, A. J. A., & Holmes, S. P. (2016). DADA2 : High-resolution sample inference from Illumina amplicon data. *Nature Methods*, 13(7). <https://doi.org/10.1038/nmeth.3869>
- Dias, M. P., Bastos, M. S., Xavier, V. B., Cassel, E., Astarita, L. V., & Santarém, E. R. (2017). Plant growth and resistance promoted by *Streptomyces* spp. in tomato. *Plant Physiology and Biochemistry*, 118, 479–493. <https://doi.org/10.1016/j.plaphy.2017.07.017>
- Egamberdieva, D., Jabborova, D., & Berg, G. (2016). Synergistic interactions between *Bradyrhizobium japonicum* and the endophyte *Stenotrophomonas rhizophila* and their effects on growth, and nodulation of soybean under salt stress. *Plant and Soil*, 405(1–2), 35–45. <https://doi.org/10.1007/s11104-015-2661-8>
- Erdős, P., & Rényi, A. (2011). On the evolution of random graphs. In *The Structural and Dynamics of Networks* (pp. 38–82). Princeton:Princeton University Press. <https://doi.org/https://doi.org/10.1515/9781400841356.38>
- Faust, K., & Raes, J. (2012). Microbial interactions: From networks to models. *Nature Reviews Microbiology*, 10(8), 538–550. <https://doi.org/10.1038/nrmicro2832>
- Felici, C., Vettori, L., Giraldi, E., Forino, L. M. C., Toffanin, A., Tagliasacchi, A. M., & Nuti, M. (2008). Single and co-inoculation of *Bacillus subtilis* and *Azospirillum brasilense* on

- Lycopersicon esculentum: Effects on plant growth and rhizosphere microbial community. *Applied Soil Ecology*, 40(2), 260–270. <https://doi.org/10.1016/j.apsoil.2008.05.002>
- Friedman, J., & Alm, E. J. (2012). Inferring Correlation Networks from Genomic Survey Data. *PLoS Computational Biology*, 8(9), 1–11. <https://doi.org/10.1371/journal.pcbi.1002687>
- Głodowska, M., Schwinghamer, T., Husk, B., & Smith, D. (2017). Biochar Based Inoculants Improve Soybean Growth and Nodulation. *Agricultural Sciences*, 08(09), 1048–1064. <https://doi.org/10.4236/as.2017.89076>
- H.G., G., S., B. S., M., M., N., S., Prasad, M., Aiyaz, M., K.N., A., & S.R., N. (2020). Induction of drought tolerance in tomato upon the application of ACC deaminase producing plant growth promoting rhizobacterium *Bacillus subtilis* Rhizo SF 48. *Microbiological Research*, 234(January), 126422. <https://doi.org/10.1016/j.micres.2020.126422>
- Halwani, M., Reckling, M., Egamberdieva, D., Omari, R. A., Bellingrath-Kimura, S. D., Bachinger, J., & Bloch, R. (2021). Soybean Nodulation Response to Cropping Interval and Inoculation in European Cropping Systems. *Frontiers in Plant Science*, 12(June). <https://doi.org/10.3389/fpls.2021.638452>
- Hernández-Montiel, L. G., Chiquito-Contreras, C. J., Murillo-Amador, B., Vidal-Hernández, L., Quiñones-Aguilar, E. E., & Chiquito-Contreras, R. G. (2017). Efficiency of two inoculation methods of *Pseudomonas putida* on growth and yield of tomato plants. *Journal of Soil Science and Plant Nutrition*, 17(4), 1003–1012. <https://doi.org/10.4067/S0718-95162017000400012>
- Herridge, D. F., Peoples, M. B., & Boddey, R. M. (2008). Global inputs of biological nitrogen fixation in agricultural systems. In *Plant and Soil*. <https://doi.org/10.1007/s11104-008->

- JIN, J., WANG, G. H., LIU, X. B., LIU, J. D., CHEN, X. L., & HERBERT, S. J. (2009). Temporal and Spatial Dynamics of Bacterial Community in the Rhizosphere of Soybean Genotypes Grown in a Black Soil. *Pedosphere*, *19*(6), 808–816.
[https://doi.org/10.1016/S1002-0160\(09\)60176-4](https://doi.org/10.1016/S1002-0160(09)60176-4)
- Katoh, K., Misawa, K., Kuma, K., & Miyata, T. (2002). MAFFT : a novel method for rapid multiple sequence alignment based on fast Fourier transform. *Nucleic Acids Research*, *30*(14), 3059–3066.
- Kunert, K. J., Vorster, B. J., Fenta, B. A., Kibido, T., Dionisio, G., & Foyer, C. H. (2016). Drought stress responses in soybean roots and nodules. *Frontiers in Plant Science*, *7*(JULY2016), 1–7. <https://doi.org/10.3389/fpls.2016.01015>
- Langille, M. G. I., Zaneveld, J., Caporaso, J. G., McDonald, D., Knights, D., Reyes, J. A., Clemente, J. C., Burkepile, D. E., Vega Thurber, R. L., Knight, R., Beiko, R. G., & Huttenhower, C. (2013). Predictive functional profiling of microbial communities using 16S rRNA marker gene sequences. *Nature Biotechnology*, *31*(9), 814–821.
<https://doi.org/10.1038/nbt.2676>
- Liao, H., Li, Y., & Yao, H. (2019). Biochar Amendment Stimulates Utilization of Plant-Derived Carbon by Soil Bacteria in an Intercropping System. *Frontiers in Microbiology*, *10*(June), 1–13. <https://doi.org/10.3389/fmicb.2019.01361>
- Lindemann, A., Pessi, G., Schaefer, A. L., Mattmann, M. E., Christensen, Q. H., Kessler, A., Hennecke, H., Blackwell, H. E., Greenberg, E. P., & Harwood, C. S. (2011). Isovaleryl-homoserine lactone, an unusual branched-chain quorum-sensing signal from the soybean

symbiont *Bradyrhizobium japonicum*. *Proceedings of the National Academy of Sciences of the United States of America*, 108(40), 16765–16770.

<https://doi.org/10.1073/pnas.1114125108>

Louca, S., Parfrey, L. W., & Doebeili, M. (2016). Decoupling function and taxonomy in the global ocean microbiome. *Science (New York, N.Y.)*, 353(6305), 1272–1277.

<https://doi.org/10.1126/science.aaf4507>

Lozupone, C. A., Hamady, M., Kelley, S. T., & Knight, R. (2007). Quantitative and qualitative β diversity measures lead to different insights into factors that structure microbial communities. *Applied and Environmental Microbiology*, 73(5), 1576–1585.

<https://doi.org/10.1128/AEM.01996-06>

Mizrahi-Man, O., Davenport, E. R., & Gilad, Y. (2013). Taxonomic Classification of Bacterial 16S rRNA Genes Using Short Sequencing Reads: Evaluation of Effective Study Designs. *PLoS ONE*. <https://doi.org/10.1371/journal.pone.0053608>

Naumann, G., Alfieri, L., Wyser, K., Mentaschi, L., Betts, R. A., Carrao, H., Spinoni, J., Vogt, J., & Feyen, L. (2018). Global Changes in Drought Conditions Under Different Levels of Warming. *Geophysical Research Letters*, 45(7), 3285–3296.

<https://doi.org/10.1002/2017GL076521>

Naylor, D., & Coleman-Derr, D. (2018). Drought stress and root-associated bacterial communities. *Frontiers in Plant Science*, 8(January), 1–16.

<https://doi.org/10.3389/fpls.2017.02223>

Newman, M. E. J., & Girvan, M. (2004). Finding and evaluating community structure in networks. *Physical Review E - Statistical, Nonlinear, and Soft Matter Physics*, 69(2 2), 1–

16. <https://doi.org/10.1103/PhysRevE.69.026113>

Niraula, S., Choi, Y. K., Payne, K., Muir, J. P., Kan, E., & Chang, W. S. (2021). Dairy effluent-saturated biochar alters microbial communities and enhances bermudagrass growth and soil fertility. *Agronomy*, *11*(9). <https://doi.org/10.3390/agronomy11091794>

Okon, Y., & Labandera-Gonzalez, C. A. (1994). Agronomic applications of azospirillum: An evaluation of 20 years worldwide field inoculation. *Soil Biology and Biochemistry*, *26*(12), 1591–1601. [https://doi.org/10.1016/0038-0717\(94\)90311-5](https://doi.org/10.1016/0038-0717(94)90311-5)

Price, M. N., Dehal, P. S., & Arkin, A. P. (2010). FastTree 2 – Approximately Maximum-Likelihood Trees for Large Alignments. *PLoS ONE*, *5*(3). <https://doi.org/10.1371/journal.pone.0009490>

Rascovan, N., Carbonetto, B., Perrig, D., Díaz, M., Canciani, W., Abalo, M., Alloati, J., González-Anta, G., & Vazquez, M. P. (2016). Integrated analysis of root microbiomes of soybean and wheat from agricultural fields. *Scientific Reports*, *6*(1150), 1–12. <https://doi.org/10.1038/srep28084>

Reiter, S., Romelczyk, S., Broaddus, M., Clarke, T., Fimon, L., Flanagan, R., Gregg, C., Jones, B., Jones, T., Lawrence, W., Longest, R., Parrish, M., Siegle, L., Stafford, C., Holshouser, D., & County, M. (2018). *Virginia On-Farm Soybean Research*. <https://www.sites.ext.vt.edu/newsletter-archive/soybean-test-plots/2018.pdf>

Rodríguez, H., & Fraga, R. (1999). Phosphate solubilizing bacteria and their role in plant growth promotion. *Biotechnology Advances*, *17*(4–5), 319–339. [https://doi.org/10.1016/S0734-9750\(99\)00014-2](https://doi.org/10.1016/S0734-9750(99)00014-2)

Röttgers, L., & Faust, K. (2018). From hairballs to hypotheses—biological insights from microbial

networks. *FEMS Microbiology Reviews*, 42(6), 761–780.

<https://doi.org/10.1093/femsre/fuy030>

Sadowsky, M. J., Tully, R. E., Cregan, P. B., & Keyser, H. H. (1987). Genetic Diversity in Bradyrhizobium japonicum Serogroup 123 and Its Relation to Genotype-Specific Nodulation of Soybean . *Applied and Environmental Microbiology*, 53(11), 2624–2630.

<https://doi.org/10.1128/aem.53.11.2624-2630.1987>

Salvagiotti, F., Cassman, K. G., Specht, J. E., Walters, D. T., Weiss, A., & Dobermann, A.

(2008). Nitrogen uptake , fixation and response to fertilizer N in soybeans : A review. *Field Crops Research*, 133(April), 1–13. <https://doi.org/10.1016/j.fcr.2008.03.001>

Shannon, P., Markiel, A., Owen Ozier, 2 Nitin S. Baliga, 1 Jonathan T. Wang, 2 Daniel Ramage, 2, Nada Amin, 2, Benno Schwikowski, 1, 5 and Trey Ideker^{2, 3, 4, 5}, 山本隆久, 豊田直平, 深瀬吉邦, & 大森敏行. (2003). Cytoscape: A Software Environment for Integrated Models of Biomolecular Interaction Networks. *Genome Research*, 13(22), 6.

<https://doi.org/10.1101/gr.1239303.metabolite>

Stacey, G., So, J. S., Roth, L. E., Lakshmi SK, B., & Carlson, R. W. (1991). A

lipopolysaccharide mutant of Bradyrhizobium japonicum that uncouples plant from bacterial differentiation. In *Molecular plant-microbe interactions : MPMI* (Vol. 4, Issue 4, pp. 332–340). <https://doi.org/10.1094/MPMI-4-332>

Sugiyama, A., Ueda, Y., Zushi, T., Takase, H., & Yazaki, K. (2014). Changes in the bacterial community of soybean rhizospheres during growth in the field. *PLoS ONE*, 9(6), 1–9.

<https://doi.org/10.1371/journal.pone.0100709>

Tao, J., Meng, D., Qin, C., Liu, X., Liang, Y., Xiao, Y., Liu, Z., Gu, Y., Li, J., & Yin, H. (2018).

Integrated network analysis reveals the importance of microbial interactions for maize growth. *Applied Microbiology and Biotechnology*, 102(8), 3805–3818.

<https://doi.org/10.1007/s00253-018-8837-4>

Tauer, L. W. (1989). Economic impact of future biological nitrogen fixation technologies on United States agriculture. *Plant and Soil*. <https://doi.org/10.1007/BF02370418>

Trabelsi, D., & Mhamdi, R. (2013). Microbial inoculants and their impact on soil microbial communities: A review. *BioMed Research International*, 2013.

<https://doi.org/10.1155/2013/863240>

Tsigie, A., Tilak, K. V. B. R., & Saxena, A. K. (2011). Field response of legumes to inoculation with plant growth-promoting rhizobacteria. *Biology and Fertility of Soils*, 47(8), 971–974.

<https://doi.org/10.1007/s00374-011-0573-1>

USDA. (2021). *World agricultural supply and demand estimates (WASDE)*.

<http://www.usda.gov/oce/commodity/wasde/>

Woese, C. R. (1987). *Bacterial Evolution Background* 51(2), 221–271.

Zhang, H., Prithiviraj, B., Charles, T. C., Driscoll, B. T., & Smith, D. L. (2003). Low temperature tolerant *Bradyrhizobium japonicum* strains allowing improved nodulation and nitrogen fixation of soybean in a short season (cool spring) area. *European Journal of Agronomy*, 19(2), 205–213. [https://doi.org/10.1016/S1161-0301\(02\)00038-2](https://doi.org/10.1016/S1161-0301(02)00038-2)

Chapter 4

Construction and Analysis of Weighted Gene Co-expression Network of *Bradyrhizobium japonicum* Under Desiccation Stress

Abstract:

Bradyrhizobium japonicum, a nitrogen-fixing endosymbiont of soybeans, has a positive impact on sustainable agriculture by reducing the use of chemical nitrogen fertilizers. To establish a symbiotic association with soybeans, it has to sustain environmental stresses and retain its functional traits such as nodulation and biological nitrogen fixation. Desiccation is one of the most prevalent limiting abiotic factors that affect these traits. Therefore, identifying key genes and relevant mechanisms involved in desiccation stress responses is important to develop a better nitrogen-fixing bioinoculant. Traditionally, most studies have focused on the identification of differentially expressed genes; however, underlying molecular mechanisms involve much more complex interactions among genes. Here, we performed a weighted gene co-expression network analysis (WGCNA) to identify the modular structure of genes in response to desiccation stress. Modules showing a strong positive correlation with desiccation duration were enriched with fatty acid biosynthesis, chaperones, structural molecule activity, and cytoplasmic function. In addition, identified modules were largely preserved in a network of combined microarray data generated from various experiments. This network analysis provides an evidence of gene modules whose co-expression changes as a function of time under desiccation stress. Furthermore, hub genes within each module will serve as potential candidates for experimental verification.

Introduction:

Bradyrhizobium japonicum, a nitrogen-fixing endosymbiont of soybean, is of agricultural significance because it provides usable nitrogen compounds (e.g., ammonia) to the host plant. To establish a successful symbiotic association with soybeans, *B. japonicum* has to sustain environmental stresses for prolonged time and maintain its physiological traits such as nodulation and nitrogen-fixing capability in soils as well as in plants. Since they are soil dwelling bacteria, their persistence is greatly affected by environmental fluctuations in their habitat soil (Streeter, 2007). In addition, survival of *B. japonicum* as a bio-inoculant in the field is a major concern that can affect the nodulation efficiency and crop yield. The growing threat of abiotic stresses associated with climate changes and global warming necessitates the development of a bio-inoculant that can survive for longer duration with maintenance of their symbiotic characteristics. Therefore, it is important to identify the mechanism that is related with the stress tolerance. The most significant environmental stress that affects the growth and survival of *B. japonicum* in the agricultural field is drought.

Desiccation stress (e.g., drought) is one of the most prevalent limiting factors in *B. japonicum* growth and overall nitrogen fixing ability by other plant growth promoting rhizobium (PGPR) strains in the agricultural soil (Potts, 1994). Most of the *Rhizobium* strains, including *B. japonicum*, are sensitive to desiccation stress (Boumahdi et al., 1999) in soil or on seeds during seed inoculum treatment (Streeter, 2007). Genes involved in the trehalose biosynthesis have largely been studied as key players to enhance desiccation tolerance in bacteria (Cytryn et al., 2007; Streeter, 2003), which ultimately enhances drought tolerance in associated plants (Vílchez et al., 2016). However, how these genes are interacting with other related physiological traits such

as desiccation-involved stress tolerance remains elusive. Therefore, identifying key genes and underlying mechanisms in response to desiccation stress is important to develop a novel bio-inoculant. Although greater efficiency has been achieved for the storage of bioinoculants (Streeter, 2007), their survival rate on seed surface or in the soil remains a major challenge. Desiccation-tolerant microorganisms have also shown to enhance plant drought tolerance (Vílchez et al., 2016) and plant growth (Molina-Romero et al., 2017). Studies on the identification of key molecular markers were largely based on the differential gene expression analysis (Cytryn et al., 2007). However, a molecular mechanism by which rhizobia deals with the desiccation stress could involve much more complex interactions among an entire set of genes. Despite extensive studies on desiccation stress, the actual cause of desiccation-induced cells death is still unknown. Gene co-expression network analysis could allow us to decipher how gene are connected in response to desiccation stress and which genes are responsible for coping with the increase of the stress in a steady manner.

Gene co-expression network analysis allows us to systematically extract new information by capturing relationships among transcripts from differential gene expression data. Weighted gene co-expression network analysis (WGCNA) is the most widely used method for construction and analysis of gene co-expression networks (Bakhtiarizadeh et al., 2018; Hu et al., 2018; W. Li et al., 2020; Liu et al., 2018). It utilizes adjacency matrix ($a_{ij} = S_{ij}^{\beta}$), defined by the co-expression similarity ($S_{ij} = |cor(x_i, x_j)|$) of genes i and j raised to a soft power (β). It further transforms adjacency matrix to topological overlap matrix (TOM), which is highly robust towards noise in the dataset, and separates functionally correlated genes into modules (Langfelder & Horvath, 2007). Although, there are several studies on *B. japonicum* in relation to drought and desiccation stresses (Cytryn et al., 2007; Sugawara et al., 2010) no report has been made for deciphering gene

co-expression network of this model organism. Therefore, to fulfil this knowledge gap, we performed WGCNA (Langfelder & Horvath, 2008) of *B. japonicum* USDA110 grown under desiccation stress and correlated functional modules to different desiccation periods. We discovered functionally related gene clusters whose expression changes with the progression of desiccation stress. In addition, we compared the network under desiccation stress with a network of combined gene expression data of *B. japonicum* from various experimental conditions, which is considered as the global network.

Materials & Methods:

Microarray data retrieval and preprocessing:

Table 4-1 GenePix Microarray datasets downloaded from NCBI GEO database.

S.N.	Accession no.	Arrays
1	GSE8036	4
3	GSE9125	18
4	GSE10295	6
5	GSE10296	4
6	GSE10298	6
7	GSE19039	12
8	GSE23296	16
9	GSE23870	6
10	GSE26380	6

11	GSE26531	12
12	GSE26960	6
13	GSE26961	6
14	GSE36913	6
15	GSE66091	24
16	GSE69999	6
	Total	138

Raw GenePix files of GSE9125 (Cytryn et al., 2007) and other *B. japonicum* USDA110 microarray data from 17 different experiments (Table 4-1) were obtained from the Gene Expression Omnibus (GEO) database at the National Center for Biotechnology Information (NCBI) (<https://www.ncbi.nlm.nih.gov/geo/query/acc.cgi?acc=GPL5341>). The experimental condition for the microarray data is as follow: i) Cells were harvested in a 0.4 μ m (47mm diameter) membrane filter, ii) cells were transferred to desiccators with hydrated (100% RH) and desiccated (27% RH) condition for 4, 24 and 72 hours, iii) cells were resuspended in ice-cold BMM for RNA extraction (Cytryn et al., 2007). All raw data were reanalyzed using ‘limma’ package in R. Background correction was done using ‘mle’ in ‘normexp’ method with offset value 50. Within-array, normalization was performed using ‘printtiploess’ followed by ‘Aquantile’. For simplicity and reproducibility of the data analysis, only GenePix Array data were included, and microarray datasets were preprocessed individually with same parameters.

Signed weighted gene co-expression network construction:

The WGCNA R software (R4.0.2) package was used to construct a signed co-expression network. The signed network takes into consideration of the sign of measured correlation coefficients between genes. Such networks can facilitate identification of modules with more significantly enriched functional groups (Horvath, 2011). At first, gene adjacency matrix was formulated by raising biweight midcorrelation (Bicor) coefficients to the soft-power 19. Bicor was used unless otherwise specified, because of its robustness to outliers (Langfelder & Horvath, 2008). The soft-power was selected based on the value at which the network approximately followed the scale-free topology with fitting index ($R^2 \geq 0.9$) (Figure 4-1). Subsequently, the weighted adjacency matrix was transformed into TOM and the corresponding dissimilarity matrix was calculated to minimize effects of noise and spurious associations. TOM was then used to cluster highly co-expressed genes by hierarchical clustering, followed by identification of modules using dynamic tree cut algorithm. Highly correlated modules were merged at 0.25 height of the dendrogram. Merged modules were further refined by rearranging genes among modules using additional k-means clustering step (1000 permutation), where eigengenes of each merged module are considered as the centroids (Botía et al., 2017).

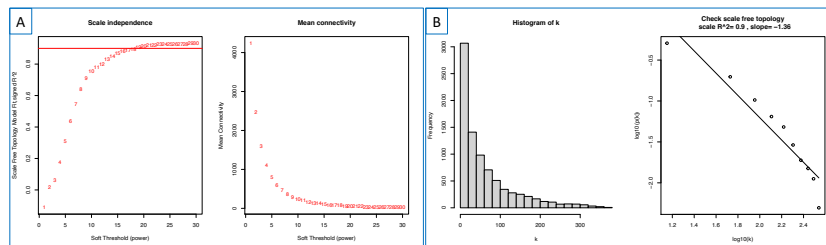


Figure 4-1: Selection of soft thresholding power to obtain scale independence and mean connectivity pattern (A) and connectivity pattern and scale free topology at selected soft threshold R-square value of 0.9 (B).

To study the relationship among modules, module eigengenes of modules were correlated (Spearman) with each other along with desiccation time as an additional branch. Highly correlated modules form meta-modules. Also, we calculated the number of genes that share significantly positive module memberships ($P < 0.05$) in modules.

Functional enrichment analysis of network modules:

Functional enrichment analysis was performed using DAVID (Database for Annotation, Visualization, and Integrated Discovery) (Dennis et al., 2003). Ensembl gene IDs of probes corresponding to each module were uploaded in the DAVID database and the *B. japonicum* USDA110 whole genome was selected as background. Annotation was performed with default settings. All P -values > 0.01 were considered as significantly enriched gene ontology (GO) terms.

Module preservation analysis:

To further validate the preservation of identified modules, we performed the module preservation analysis (Langfelder et al., 2011) with the test network from combined microarrays (120 arrays) generated from different experiments of *B. japonicum* (Table 4-1). To avoid possible bias, we did not include expression values from the desiccation network in the test network in addition to the outlier array, resulting in a total of 119 arrays. First, we compared the ranked connectivity to check if the datasets were comparable (Figure 4-2). After ensuring comparability, we applied *modulePreservation* function in the WGCNA package with the desiccation network as a reference and others as a test network, where we specified bicor and 1000 permutations to identify Z_{summary} preservation and medianRank preservation, respectively.

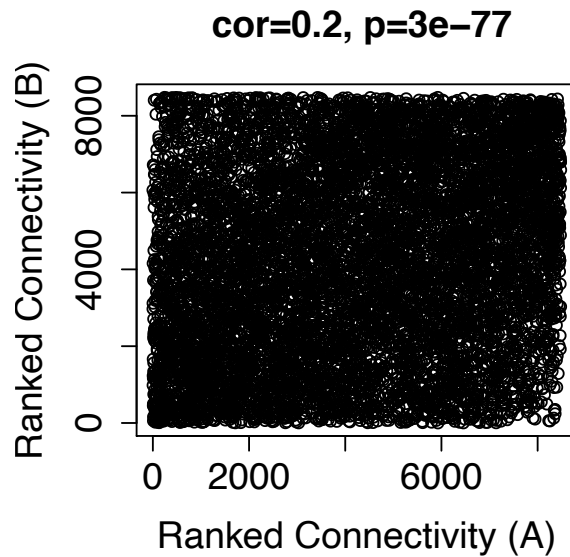


Figure 4-2: Correlation of connectivity pattern between probes under Desiccation stress (A) and random experimental condition (B).

Module trait relationships and detection of hub genes:

Module eigengenes (MEs) were Spearman-correlated with the time of desiccation. Positively correlated modules were selected for the visualization in Cytoscapes. Hub genes were selected based on high intramodular connectivity and high module membership values.

Results:

Network construction and identification of modules:

Similar to other biological networks, our network satisfies the scale free topology at soft thresholding power (β) of 19 as indicated by the straight line (Figure 4-1). This indicates that our network follows power law, which suggests that fewer nodes in the network have large numbers of connectivity (B. Zhang & Horvath, 2005). Initially, 38 modules were identified by WGCNA

hierarchical clustering, but they were merged into 16 modules based on high correlation (>0.75) among module eigengenes (Figure 4-3). After merging with k-means clustering, different color codes were used for 16 modules as follows: Black, Lightgreen, Darkolivegreen, Green, Brown, Grey60, Orange, Royalblue, Blue, Darkmagenta, Darkturquoise, Cyan, Yellowgreen, Pink, Darkgreen, and Darkred modules contain 324, 519, 418, 587, 853, 585, 560, 600, 985, 576, 388, 663, 430, 369, 286 and 337 genes, respectively (Figure 4-5).

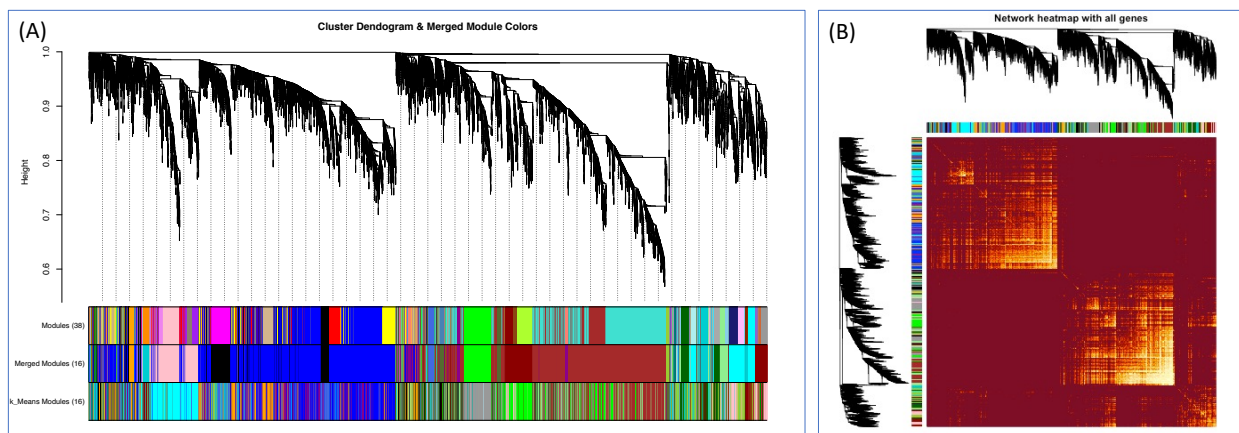


Figure 4-3 : Gene co-expression network construction and module detection in *B. japonicum* USDA110 under desiccation stress.

(A) Gene cluster dendrogram. Three colored horizontal bars represent modules obtained by hierarchical clustering, merging and k-means clustering, respectively, from top to bottom. (B) TOM plot of the network. Yellow region along the diagonal represents modules.

Relationship among modules:

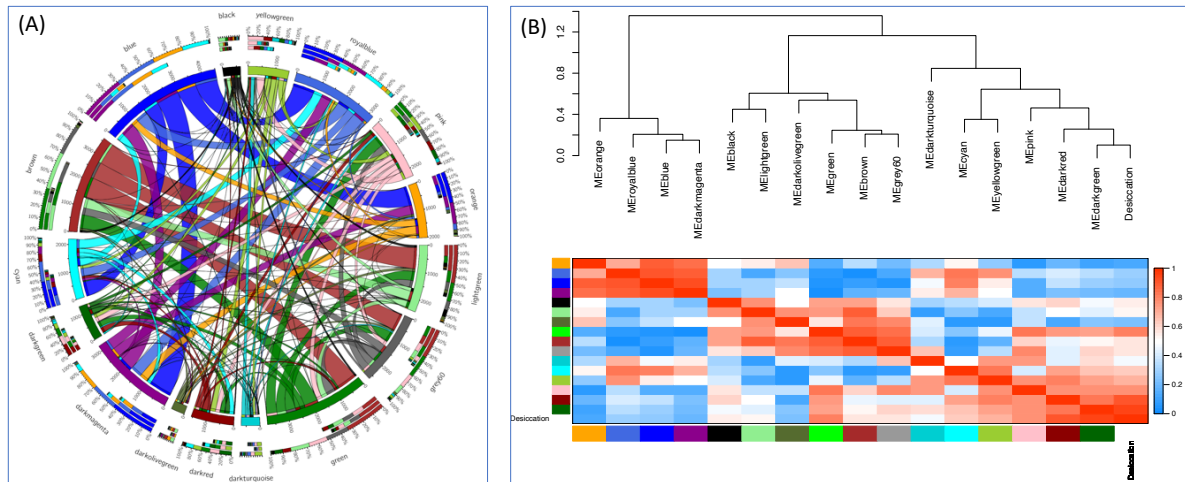


Figure 4-4 A relationship among modules. (A) Circos plot showing shared module membership among modules. (B) Cluster dendrogram of module eigengenes along with the desiccation branch node (top panel) and adjacency heatmap (bottom panel).

Module membership (MM) of genes is largely shared among modules, suggesting that modules are inter-connected. Specifically, a large proportion of genes in the Darkred module share MM with Darkgreen, Pink and Green modules (Figure 4-4A). On the other hand, the network modules are grouped into 3 meta-modules as indicated by the correlation of module eigengenes. We incorporated desiccation time periods of 24, 48, and 72 h as an additional node in the dendrogram, which is associated with darkred, darkgreen, and pink meta-modules. Modules within each meta-module have high adjacency (Figure 4-4B).

Module and desiccation stress relationship:

Module eigengene of each module was Spearman rank correlated with desiccation time. Among 16 modules, 5 modules (Darkgreen, Darkred, Pink, Green, and Yellowgreen) were positively

correlated, whereas 3 modules (Orange, Darkmagenta, and Darkolivegreen) were negatively correlated with the desiccation time (Figure 4-5 A). Thus, high expression values of the genes within those positively correlated modules indicates strong connections among each other. In comparison of module significance (MS) across all modules, higher significance was observed in Darkgreen and Darkred modules (Figure 4-5 B). This indicates that these gene clusters are strongly associated with the desiccation stress response. MS quantifies the average gene significance (GS) measure for all genes in each module (Langfelder & Horvath, 2008). Furthermore, GS and intramodular connectivity (kME) of all genes within the 5 modules, which had positive correlation with desiccation time, showed strong positive correlation with their MM to the respective module (Figure 4-6). This suggests that genes with high MM tend to have high GS towards the desiccation stress. It also indicates the robustness of the identified modules and their property.

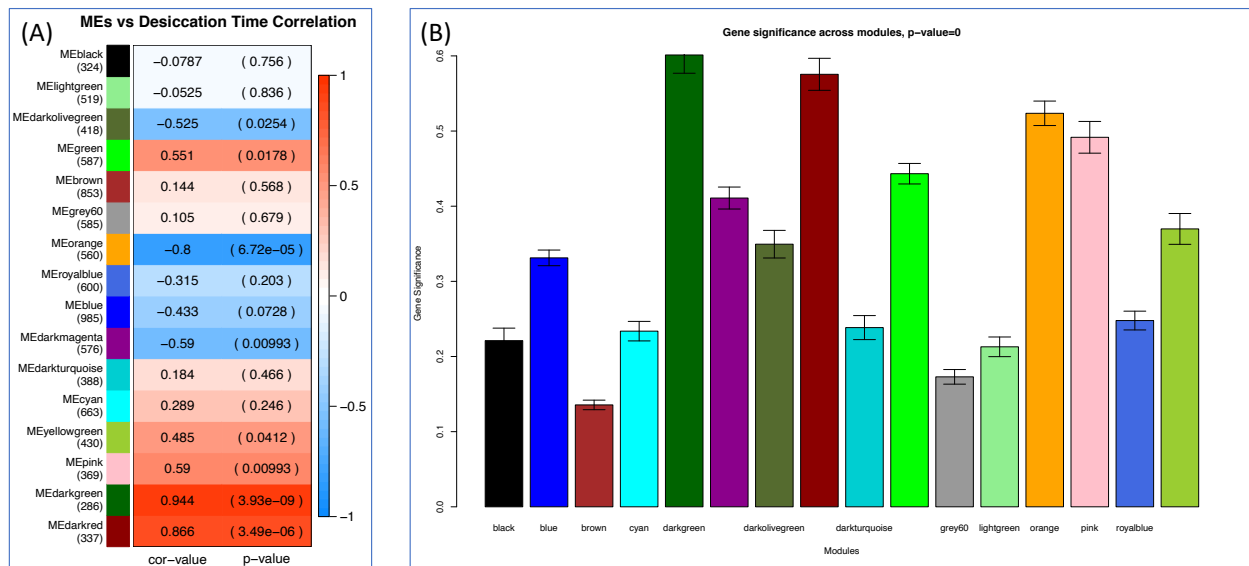


Figure 4-5 : A relationship between module eigengenes and desiccation time. (A) Correlation shows Spearman correlation and values in parentheses shows the number of genes in the respective modules. (B) Gene significance of identified modules.

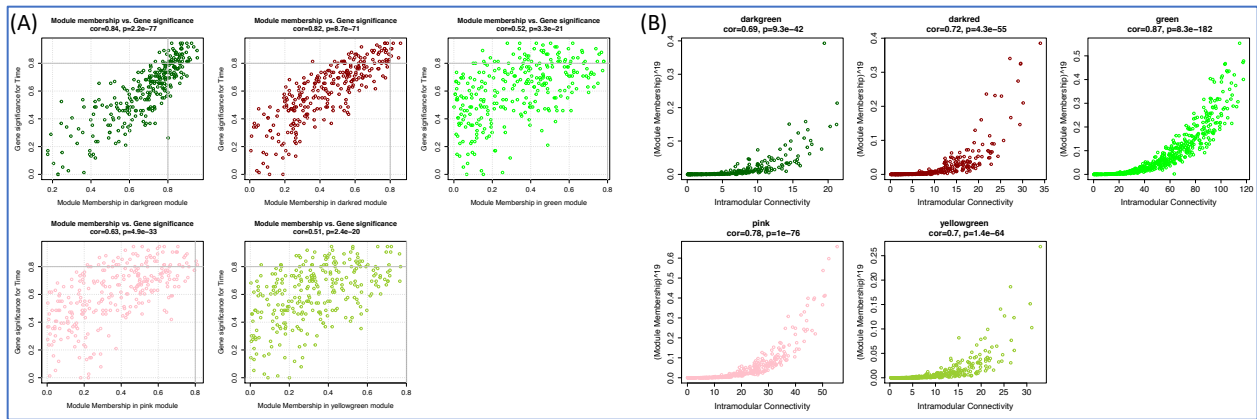


Figure 4-6 Scatterplot of (A) Module membership vs Gene significance for desiccation time in the five significant and (B) Scatterplot of module membership vs intramodular connectivity in the five significant modules in desiccation stress response.

Functional enrichment analysis:

A co-expression module may represent a noise due to lack of optimal parameters for clustering genes. Therefore, we performed functional enrichment analysis of modules that are positively correlated with the desiccation time. All 5 modules were significantly enriched with genes in different GO terms and KEGG pathways (Table 4-2). This provides evidence of the biological meaningfulness and functional roles of the network modules. Two modules (Darkgreen and Darkred) which are highly correlated with desiccation time were enriched with cytoplasm, fatty acid biosynthesis, and chaperon binding proteins. Similarly, the Pink module is enriched with functions associated with cell motility and extracellular regions, while the Yellowgreen module is associated with ribosomes.

Table 4-2 Functional enrichment analysis of modules that are positively correlated with the time of desiccation. The enrichment analysis was performed using a DAVID functional enrichment tool.

Modules	Category	Term	%	pValue	BH
Darkgreen	GOTERM_CC_DIRECT	GO:0005737~cytoplasm	10.53	3.39E-04	0.00745401
	GOTERM_BP_DIRECT	GO:0006633~fatty acid biosynthetic process	2.10	8.82E-04	0.09698671
darkred	GOTERM_CC_DIRECT	GO:1990220~GroEL-GroES complex	1.19	2.16E-04	0.00560767
	GOTERM_MF_DIRECT	GO:0051087~chaperone binding	1.19	2.39E-04	0.03320928
	GOTERM_BP_DIRECT	GO:0006986~response to unfolded protein	1.19	2.57E-04	0.01489122
	GOTERM_BP_DIRECT	GO:0051085~chaperone mediated protein folding requiring cofactor	1.19	2.57E-04	0.01489122
	GOTERM_MF_DIRECT	GO:0051082~unfolded protein binding	1.19	5.80E-04	0.04029768
pink	GOTERM_CC_DIRECT	GO:0005576~extracellular region	2.45	8.36E-05	0.00238288
	GOTERM_BP_DIRECT	GO:0071973~bacterial-type flagellum-dependent cell motility	2.45	1.52E-04	0.01661433
	GOTERM_CC_DIRECT	GO:0009288~bacterial-type flagellum	1.63	1.59E-04	0.00238288
	GOTERM_MF_DIRECT	GO:0005198~structural molecule activity	1.90	1.60E-04	0.02550509
	KEGG_PATHWAY	bja02020:Two-component system	4.89	1.38E-03	0.10199092
	GOTERM_MF_DIRECT	GO:0003735~structural constituent of ribosome	2.45	2.91E-03	0.23136308
	KEGG_PATHWAY	bja03010:Ribosome	2.45	5.46E-03	0.20186178
	GOTERM_BP_DIRECT	GO:0006412~translation	2.45	7.68E-03	0.41875697
yellowgreen	GOTERM_MF_DIRECT	GO:0003735~structural constituent of ribosome	3.76	1.61E-08	2.95E-06
	UP_KEYWORDS	Ribosomal protein	3.76	6.02E-08	4.47E-06
	KEGG_PATHWAY	bja03010:Ribosome	3.76	6.03E-08	3.98E-06
	UP_KEYWORDS	Ribonucleoprotein	3.76	7.84E-08	4.47E-06
	GOTERM_BP_DIRECT	GO:0006412~translation	3.76	1.94E-07	2.67E-05
	UP_KEYWORDS	RNA-binding	3.52	2.05E-06	7.79E-05
	UP_KEYWORDS	rRNA-binding	2.58	1.43E-05	4.06E-04
	GOTERM_MF_DIRECT	GO:0019843~rRNA binding	2.11	1.13E-04	0.01031713
	GOTERM_CC_DIRECT	GO:0022625~cytosolic large ribosomal subunit	1.88	2.62E-04	0.00734261
	GOTERM_CC_DIRECT	GO:0022627~cytosolic small ribosomal subunit	1.17	2.98E-03	0.04172204
green	UP_KEYWORDS	Signal	13.40	2.80E-05	0.00392217
	UP_KEYWORDS	Cytoplasm	7.04	9.90E-05	0.00692823
	GOTERM_CC_DIRECT	GO:0005737~cytoplasm	8.76	1.83E-03	0.07137151

Module preservation:

We performed module preservation analysis to evaluate the preservation of connectivity patterns of modules observed in the desiccation network (reference network) as well as in the random network (test network). We hypothesized that the network properties should not vary largely in terms of connectivity because genes related to a particular pathway tend to have a similar connectivity pattern, irrespective of the environmental perturbation (Langfelder et al., 2011). Most of the modules were weakly to moderately preserved ($2 < Z_{\text{summary}} > 10$) and 4 modules were highly preserved ($Z_{\text{summary}} > 10$) as observed by the Z_{summary} statistics (Figure 4-7). On the other hand, *medianRank* summarizes the observed preservation statistics to compare relative preservation among multiple modules, irrespective of the module size. Lower median rank shows stronger preservation than a module with a higher median rank (Langfelder et al., 2011). After further exploration, we observed that density-based preservation was stronger than connectivity-based preservation in Pink, Green, Yellowgreen, and Darkgreen nodules in descending order. In contrast, the Darkred module showed higher preservation in the connectivity pattern than the density. All these modules showed preservation in both density and connectivity, except for the Yellowgreen module.

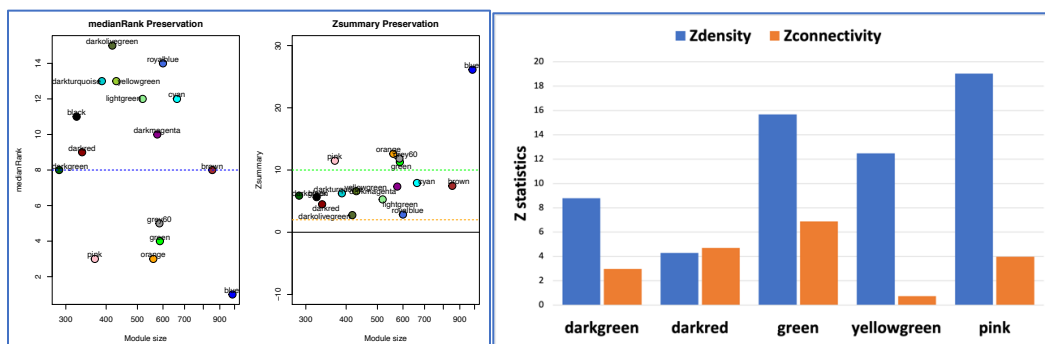


Figure 4-7 Module preservation analysis of Desiccation network modules.

Discussion:

In the previous study, Cytryn and colleagues reported differentially expressed genes at different levels of desiccation stress and concluded that several other protective mechanisms are also required for its survival under the stress (Cytryn et al., 2007). Here, we employed a co-expression network approach to identify functional groups and associated key genes that are responsible for the cell survival as a function of desiccation time.

Microarray technology mainly suffers from noises in the dataset (Hong et al., 2013), which can result in the lack of power to identify true biomarkers. As network analysis is based on the correlation measure, it is robust to handle noises in the dataset and identify a system-level relationship among genes that are even expressed in low abundance (van Dam et al., 2018). We created adjacency matrix using bicor measure, which is better than Spearman and Pearson correlation in handling outliers (Langfelder & Horvath, 2012; Song et al., 2012). Furthermore, TOM, implemented in WGCNA, not only minimizes the effects of noises and spurious associations in correlation matrix, but also leads to biologically meaningful results by considering the neighborhood similarity (Yip & Horvath, 2007). Bicor, in conjunction with TOM, often leads to refined module clustering in terms of functional enrichments (Song et al., 2012). In addition, log fold-change values represent true relative expressions of genes under desiccation stress at each time point, thereby minimizing the effects of variation caused by signal intensities among replicates (Hong et al., 2013). After careful consideration of noises and outliers, and after data transformation, the *B. japonicum* network constructed by the fold change values under desiccation stress followed scale free degree distribution (Figure 4-1). As opposed to random networks, scale free networks have fewer nodes (genes) with the large number of connections, considered as

network hubs, irrespective of the size of the network. This property is testified as a hallmark to define a true biological network (Albert, 2005). Scale free topology of our network further suggests that it is less affected by random node removal (Jeong et al., 2001), and hence unlikely to be affected by noises.

Biological genome or transcriptome networks can be complex and difficult to interpret. Module based network clustering helps us identify functional groups and associate these modules to physiological traits. Modules are densely connected groups of genes or transcripts that may perform similar functional roles and have relatively sparse intermodular connections (Albert, 2005; van Dam et al., 2018). We identified that the network under desiccation stress is modular in structure. However, there is a high level of crosstalk across modules. In fact, the fraction of genes having confined MM is miniscule in comparison to those with shared MM (Figure 4-4.A). Similarly, the module eigengene (ME) clustering indicates that the whole network is divided into 3 meta-modules, where desiccation stress is associated with the Darkred, Darkgreen, Pink, Yellowgreen, Cyan, and Darkturquoise modules (Figure 4-4.B). Furthermore, we identified modules associated with the desiccation stress. Darkred, Darkgreen, Pink, Green and Yellowgreen modules have high average GS and are positively correlated with desiccation time (Figure 4-5A/B). Significance of these 5 modules towards desiccation stress is further supported by ME clustering and their adjacency heatmap (Figure 4-4). Although the Green module is in a separate meta-module, it has high adjacency with desiccation as shown in Figure 4-4B. This could be due to the high number of genes in the module containing shared MM with other modules in the associated meta-module (Figure 4-4.A). Our result suggests that ME clustering is influenced by the shared MM. These modules are biologically meaningful and are associated with certain functional groups (Table 4-2).

We performed a module preservation analysis to evaluate the robustness and reproducibility across independent datasets. Since modules may represent certain biological pathways (Langfelder & Horvath, 2008), preservation of connectivity of genes in these modules with respect to independent test networks provides strong evidence of pathway-related genes. We observed a weak to strong connection of genes as indicated by the moduleRank Preservation and Zsummary Preservation statistics (Figure 4-7A). Zsummary represents composite preservation statistic as a mean of Z_{density} and $Z_{\text{connectivity}}$ (Langfelder et al., 2011). Comparatively, module nodes remain densely connected in the test network; however, the connectivity pattern may change based on the physiological condition (Figure 4-7B). Pink ($Z_{\text{summary}}=11.497$) and Green ($Z_{\text{summary}}=11.278$) modules show strong evidence of preservation, followed by Yellowgreen ($Z_{\text{summary}}=6.60$), Darkgreen ($Z_{\text{summary}}=5.88$), and Darkred ($Z_{\text{summary}}=4.49$) modules (Figure 4-7). More specifically, the highest preservation of the Blue module ($Z_{\text{summary}}=26.122$), that is enriched with integral components of cell membranes and nitrogen fixation, suggests that this cluster of genes tend to remain intact at all conditions. This also suggests that once the survival of bacteria is attained under stressful conditions, the inherent nitrogen-fixation ability is unlikely to be affected. The module preservation statistics further justifies the biological relevance of modules identified in the desiccation network and their reproducible transcriptome assembly, which is a common property of a given biological system (Oldham et al., 2008) .

WGCNA measures connectivity of a gene with all other genes within the entire network, known as intermodular connectivity or within a particular module, known as intra-modular connectivity (kME) (Horvath, 2011). Among these two measures, intra-modular connectivity has been found to be more reliable for the selection of hub genes that are biologically important. Networks are extremely sensitive to hub gene removal, leading to significant loss of topological

properties (Jeong et al., 2001). Gene with high kME tend to have high MM and act as module hubs (Figure 4-6B). On the other hand, we observed high correlations between MM and GS (Figure 4-6A), suggesting that hub genes in desiccation related modules also tend to express more with the severity of desiccation. Our approach for hub gene selection has been previously supported and verified in similar studies (Hu et al., 2018; Jeong et al., 2001; W. Li et al., 2020).

Rhizobia mainly suffer damages of cytoplasmic membrane layer and furthers the leakage of intracellular materials under desiccation stress (Bushby & Marshall, 1977), particularly affecting the fatty acid composition of lipopolysaccharide layer (Boumahdi et al., 1999). Therefore, maintenance of cytoplasmic membrane integrity is of prime importance in desiccation resistance. In our analysis, we observed a positive correlation of Darkgreen ($\rho=0.944$, $P\text{-val}=3.93e^{-09}$) and Pink ($\rho=0.59$, $P\text{-val}=0.009$) modules associated with fatty acid biosynthesis and extracellular region proteins, respectively, with desiccation time (Figure 4-5.A). Similarly, the Darkred module is also highly correlated ($\rho=0.866$, $P\text{-val}=3.49e^{-06}$) with desiccation time (Figure 4-5A), which is enriched with chaperone proteins (Table 4-2). Molecular chaperones are a group of proteins that are involved in a wide array of stress responses. Particularly, included are heat shock proteins (hsp) and GroEL/ES-complex that protect proteins from degradation under environmental stresses (Fourie & Wilson, 2020). Enrichment of functions related to stress responses puts on the right direction towards the identification of individual stress response genes. In the Darkred module, a gene encoding LD transpeptidase (LDT) (blr5047) has been found as one of the key hub genes, which shows strong topological overlap with another hub gene encoding ABC transporter substrate binding protein (blr6648) (Figure 4-8).

We identified several hypothetical proteins, such as bsr1472, bli2567, bli4620, and bli6167, as key hub genes in Darkred and Darkgreen modules (Figure 4-8;Figure 4-9). These proteins with unknown function could play an essential role in desiccation stress response and are candidate genes for further verification. Functional properties of about 30% of genes in *B. japonicum* USDA110 remain elusive (Kaneko et al., 2002), and a large proportion of those genes could be responsible for cell survival under desiccation stress. However, these unassigned genes could have important functions for survival and growth. For example, in *Saccharomyces cerevisiae*, one of the most widely studied fungi, 13% of genes of unassigned function were discovered to be essential for optimal growth in minimal medium (Guri et al., 2002). Taken together, our results suggest that *B. japonicum* responds to desiccation as a highly connected group or module of transcripts which share a common biological function. Therefore, the identified hub genes can be further validated using molecular and physiological approaches.

References:

- Albert, R. (2005). Scale-free networks in cell biology. *Journal of Cell Science*, *118*(21), 4947–4957. <https://doi.org/10.1242/jcs.02714>
- Bakhtiarizadeh, M. R., Hosseinpour, B., Shahhoseini, M., Korte, A., & Gifani, P. (2018). Weighted gene co-expression network analysis of endometriosis and identification of functional modules associated with its main hallmarks. *Frontiers in Genetics*, *9*(OCT), 1–15. <https://doi.org/10.3389/fgene.2018.00453>
- Botía, J. A., Vandrovцова, J., Forabosco, P., Guelfi, S., D'Sa, K., Hardy, J., Lewis, C. M., Ryten, M., Weale, M. E., Ramasamy, A., Trabzuni, D., Smith, C., & Walker, R. (2017). An additional k-means clustering step improves the biological features of WGCNA gene co-expression networks. *BMC Systems Biology*, *11*(1), 1–16. <https://doi.org/10.1186/s12918-017-0420-6>
- Boumahdi, M., Mary, P., & Hornez, J. P. (1999). Influence of growth phases and desiccation on the degrees of unsaturation of fatty acids and the survival rates of rhizobia. *Journal of Applied Microbiology*, *87*(4), 611–619. <https://doi.org/10.1046/j.1365-2672.1999.00860.x>
- Bushby, H. V. A., & Marshall, K. C. (1977). Desiccation-induced damage to the cell envelope of root-nodule bacteria. *Soil Biology and Biochemistry*, *9*(3), 149–152. [https://doi.org/10.1016/0038-0717\(77\)90066-9](https://doi.org/10.1016/0038-0717(77)90066-9)
- Cytryn, E. J., Sangurdekar, D. P., Streeter, J. G., Franck, W. L., Chang, W. S., Stacey, G., Emerich, D. W., Joshi, T., Xu, D., & Sadowsky, M. J. (2007). Transcriptional and physiological responses of *Bradyrhizobium japonicum* to desiccation-induced stress. *Journal of Bacteriology*, *189*(19), 6751–6762. <https://doi.org/10.1128/JB.00533-07>

Dennis, G., Sherman, B. T., Hosack, D. A., Yang, J., Gao, W., Lane, H. C., & Lempicki, R. A. (2003). DAVID: Database for Annotation, Visualization, and Integrated Discovery.

Genome Biology, 4(5). <https://doi.org/10.1186/gb-2003-4-9-r60>

Fourie, K. R., & Wilson, H. L. (2020). Understanding groel and dnaK stress response proteins as antigens for bacterial diseases. *Vaccines*, 8(4), 1–13.

<https://doi.org/10.3390/vaccines8040773>

Guri, G., Angela M., C., Dow, S., Lucau-danila, A., Anderson, K., Arkin, A. P., Astromoff, A., Bakkoury, M. El, Bangham, R., Benito, R., Brachat, S., Andre, B., Jaramillo, D. F., Kelly, D. E., Kelly, S. L., & Ko, P. (2002). Functional profiling of the *Saccharomyces cerevisiae* genome. *Nature*, 418, 387–391.

Hong, H., Hong, Q., Liu, J., Tong, W., & Shi, L. (2013). Estimating relative noise to signal in DNA microarray data. *International Journal of Bioinformatics Research and Applications*, 9(5), 433–448. <https://doi.org/10.1504/IJBRA.2013.056085>

Horvath, S. (2011). Weighted Network Analysis: Applications in Genomics and Systems Biology. In *Vasa*.

<http://medcontent.metapress.com/index/A65RM03P4874243N.pdf>
<http://books.google.com/books?hl=en&lr=&id=ZCh06NgMFesC&oi=fnd&pg=PR7&dq=Weighted+Network+Analysis+Applications+in+Genomics+and+Systems+Biology&ots=UftEQkglGt&sig=0OCeKtqOe6658Na0o5SwbYK6MzM%5C>

Hu, Y., Pan, J., Xin, Y., Mi, X., Wang, J., Gao, Q., & Luo, H. (2018). Gene expression analysis reveals novel gene signatures between young and old adults in human prefrontal cortex.

Frontiers in Aging Neuroscience, 10(AUG), 1–15. <https://doi.org/10.3389/fnagi.2018.00259>

- Jeong, H., Mason, S. P., Barabási, A. L., & Oltvai, Z. N. (2001). Lethality and centrality in protein networks. *Nature*, *411*(6833), 41–42. <https://doi.org/10.1038/35075138>
- Kaneko, T., Nakamura, Y., Sato, S., Minamisawa, K., Uchiumi, T., Sasamoto, S., Watanabe, A., Idesawa, K., Iriguchi, M., Kawashima, K., Kohara, M., Matsumoto, M., Shimpo, S., Tsuruoka, H., Wada, T., Yamada, M., & Tabata, S. (2002). Complete genomic sequence of nitrogen-fixing symbiotic bacterium *Bradyrhizobium japonicum* USDA110. *DNA Research*, *9*(6), 189–197. <https://doi.org/10.1093/dnares/9.6.189>
- Langfelder, P., & Horvath, S. (2007). Eigengene networks for studying the relationships between co-expression modules. *BMC Systems Biology*, *1*, 54. <https://doi.org/10.1186/1752-0509-1-54>
- Langfelder, P., & Horvath, S. (2008). WGCNA: an R package for weighted correlation network analysis. *BMC Bioinformatics*, *9*, 559. <https://doi.org/10.1186/1471-2105-9-559>
- Langfelder, P., & Horvath, S. (2012). Fast R Functions for Robust Correlations and Hierarchical Clustering. *Journal of Stat Software*, *46*(11), i11. <https://www.ncbi.nlm.nih.gov/pmc/articles/PMC3624763/pdf/nihms412728.pdf>
- Langfelder, P., Luo, R., Oldham, M. C., & Horvath, S. (2011). Is my network module preserved and reproducible? *PLoS Computational Biology*, *7*(1). <https://doi.org/10.1371/journal.pcbi.1001057>
- Li, W., Wang, L., Wu, Y., Yuan, Z., & Zhou, J. (2020). Weighted gene co-expression network analysis to identify key modules and hub genes associated with atrial fibrillation. *International Journal of Molecular Medicine*, *45*(2), 401–416. <https://doi.org/10.3892/ijmm.2019.4416>

- Liu, W., Li, L., Long, X., You, W., Zhong, Y., Wang, M., Tao, H., Lin, S., & He, H. (2018). Construction and Analysis of Gene Co-Expression Networks in *Escherichia coli*. *Cells*, 7(3), 19. <https://doi.org/10.3390/cells7030019>
- Molina-Romero, D., Baez, A., Quintero-Hernández, V., Castañeda-Lucio, M., Fuentes-Ramírez, L. E., Bustillos-Cristales, M. del R., Rodríguez-Andrade, O., Morales-García, Y. E., Munive, A., & Muñoz-Rojas, J. (2017). Compatible bacterial mixture, tolerant to desiccation, improves maize plant growth. *PLoS ONE*, 12(11), 1–21. <https://doi.org/10.1371/journal.pone.0187913>
- Oldham, M. C., Konopka, G., Iwamoto, K., Langfelder, P., Kato, T., Horvath, S., & Geschwind, D. H. (2008). Functional organization of the transcriptome in human brain. *Nature Neuroscience*, 11(11), 1271–1282. <https://doi.org/10.1038/nn.2207>
- Potts, M. (1994). Desiccation tolerance of prokaryotes. *Microbiological Reviews*, 58(4), 755–805. <https://doi.org/10.1128/membr.58.4.755-805.1994>
- Song, L., Langfelder, P., & Horvath, S. (2012). Comparison of co-expression measures: Mutual information, correlation, and model based indices. *BMC Bioinformatics*, 13(1). <https://doi.org/10.1186/1471-2105-13-328>
- Streeter, J. G. (2003). Effect of trehalose on survival of *Bradyrhizobium japonicum* during desiccation. *Journal of Applied Microbiology*, 95(3), 484–491. <https://doi.org/10.1046/j.1365-2672.2003.02017.x>
- Streeter, J. G. (2007). Factors affecting the survival of *Bradyrhizobium* applied in liquid cultures to soya bean [*Glycine max* (L.) Merr.] seeds. *Journal of Applied Microbiology*, 103(4), 1282–1290. <https://doi.org/10.1111/j.1365-2672.2007.03352.x>

- Sugawara, M., Cytryn, E. J., & Sadowsky, M. J. (2010). Functional role of *Bradyrhizobium japonicum* trehalose biosynthesis and metabolism genes during physiological stress and nodulation. *Applied and Environmental Microbiology*, *76*(4), 1071–1081.
<https://doi.org/10.1128/AEM.02483-09>
- van Dam, S., Vösa, U., van der Graaf, A., Franke, L., & de Magalhães, J. P. (2018). Gene co-expression analysis for functional classification and gene-disease predictions. *Briefings in Bioinformatics*, *19*(4), 575–592. <https://doi.org/10.1093/bib/bbw139>
- Vílchez, J. I., García-Fontana, C., Román-Naranjo, D., González-López, J., & Manzanera, M. (2016). Plant drought tolerance enhancement by trehalose production of desiccation-tolerant microorganisms. *Frontiers in Microbiology*, *7*(SEP), 1–11.
<https://doi.org/10.3389/fmicb.2016.01577>
- Yip, A. M., & Horvath, S. (2007). Gene network interconnectedness and the generalized topological overlap measure. *BMC Bioinformatics*, *8*, 1–14. <https://doi.org/10.1186/1471-2105-8-22>
- Zhang, B., & Horvath, S. (2005). A general framework for weighted gene co-expression network analysis. *Statistical Applications in Genetics and Molecular Biology*, *4*(1).
<https://doi.org/10.2202/1544-6115.1128>

Chapter 5

Conclusion

Increased anthropogenic activities and global warming at an alarming rate necessitate the adoption of alternative strategies in agriculture such as biofertilizer application, soil amendment with biochar, and development of transgenic crops. Our research addresses some of the key measures to mitigate abiotic stresses, increase crop productivity, and enhance overall soil fertility. In this research, there are three foci: i) the sensible use of the drought-tolerant biofertilizer, ii) finding a way to improve biofertilizers by identifying novel biomarkers, and iii) the concurrent use of mechanical measures that can improve its performance and add benefits to cope with environmental stresses. Although biofertilizers can compensate for the required nutrient input in place of chemical fertilizers, their use alone may not be sufficient to fulfill the growing food demand. This is due to the fact that their vitality and persistence may differ depending on different field conditions and locally adopted agricultural practices (Schmidt & Gaudin, 2018). Therefore, in addition to developing a novel bio-inoculant exploring a new way to increase the agronomic potential of biofertilizers and their impact on native microbial communities is an equally important aspect.

The novel drought-tolerant *Bradyrhizobium* sp. TXVA strain showed promising results under the rainfed condition by increasing soybean yield and root nodule numbers. In addition, it altered the bacterial community in the rhizosphere at 7 weeks and enriched the proportion of plant growth-promoting rhizobia (PGPR). A previous study suggests that a bio-inoculant induces

synergistic effects with native microbiota (Molina-Romero et al., 2017) on maize growth, which is further supported by our current study where the co-presence of other microbial species has increased by the inoculant treatment in comparison to the control (i.e., no treatment). Our research identified several possible mechanisms by which the TXVA strain enhances plant growth. The first potential mechanism would be increasing the persistence of the host endosymbiont under the drought condition. Secondly, it would increase the abundance of PGPR that show higher tolerance towards environmental stresses. Third, it would change the co-occurrence pattern of microbial communities in the rhizosphere where mutual exclusion is proportionately decreased. Increased abundance of *Bacillus subtilis* and *Bacillus megaterium* in the TXVA-treated rhizosphere soil suggests the possibility of combining the TXVA strain and *Bacillus* spp. to increase their synergetic performance. Other studies indicated that biofertilizers showed better performance when the inoculant *Bradyrhizobium japonicum* was used in combination with other bio-inoculants such as *B. subtilis* and *Stenotrophomonas rhizophila* (Atieno et al., 2012; Egamberdieva, Wirth, et al., 2016).

Additionally, a molecular approach to identify marker genes governing stress tolerance would provide an additional benefit to identification and development of a novel bio-inoculant. Weighted gene co-expression network analysis (WGCNA) of *B. japonicum* under desiccation stress allowed us to find a unique perspective to observe the interaction among genes under desiccation stress rather than only focusing on the differential gene expression. Hence, we were able to identify modules or clusters of strongly connected genes that function as a group in response to desiccation stress. The module-based analysis provides a direct advantage by minimizing the complexity of large genomic interactions and thus allows separation of functionally related genes (Langfelder & Horvath, 2007). The current study offers a first comprehensive evaluation of the

gene co-expression network in *B. japonicum* USDA110. We identified several modules in association with the severity of desiccation stress. Since desiccation is a severe form of drought, this research can also be directly related to drought stress tolerance. Evidence suggests that desiccation-tolerant microbes increase drought tolerance in plants (Vílchez et al., 2016). Therefore, this study could help to identify potential hub genes responsible for the persistence of the bio-inoculant under drought and desiccation stress.

We examined the effects of dairy effluent saturated wood biochar on Bermudagrass growth, soil nutrient composition and microbial communities in a greenhouse study. Saturation with dairy effluents ameliorated the nutrient composition of pristine biochar and increased its efficiency. Due to its physicochemical properties such as nutrient sequestration, increased water holding capacity, and large surface area, biochar provides an excellent micro-habitat to native soil microbes (Lehmann et al., 2011) as well as bio-inoculants (Khan et al., 2021). Although this study has been performed on Bermudagrass (non-food crop species in the U.S.), the result suggests that biochar amendment with nutrients and biofertilizers could also be applied to major cash crops such as corn and soybeans. Several studies report beneficial impact of pristine biochar on the growth and productivity of these cash crops under field condition (Egamberdieva, Wirth, et al., 2016; Ma et al., 2019; Pandit et al., 2018). Additionally, enrichment of nitrogen-fixing rhizobia after the biochar treatment indicates that it could play a vital role in leguminous plants, because biological nitrogen fixation (BNF) is in high demand of the legume-rhizobium symbiosis. Biochar based *B. japonicum* strain 532C inoculant improved soybean growth and nodulation (Głodowska et al., 2017). Similarly, co-amendment of biochar with nutrient and biofertilizer has shown to increase wheat growth and grain yield (Khan et al., 2021).

In the future, this research will be extended by examining the effects of the drought-tolerant bio-inoculant across a sequence of growing seasons with crop rotation. Our research has been limited to one Soybean growing season, which may not reflect an actual impact on the rhizosphere microbiome in response to prolonged use of the bio-inoculant in the same field. Simultaneously, investigating the persistence of the biofertilizer in the same field for a longer duration could be another interesting avenue for research projects. In fact, there are only a handful of studies that focus on the dynamics of the microbial community at multiple growing seasons (Mendes et al., 2014; Q. Yao et al., 2017). Although we measured the relative abundance of bacterial communities in the current study, we were not able to evaluate changes in the absolute abundance of the TXVA strain. The whole-genome sequencing of the TXVA strain is underway in the Chang lab, which could help us develop unique primer sets for a molecular marker to identify the TXVA strain from the bacterial population in soil. In addition to the development of the molecular marker, identification of genome variants among the TXVA strain and other known *Bradyrhizobium* spp. strains using a comparative genomics approach would be a great way to infer any evolutionary changes to adaptation.

We also plan to examine the effects of biochar on soybean growth and fertility under drought stress. Although several studies have reported the beneficial effects of biochar on soybean growth (Ma et al., 2019; Suppadit et al., 2012; Y. Zhang et al., 2020), we have not found any research to date on investigating the effects of biochar on the microbiome in the soybean rhizosphere under drought conditions. Biochar amendment to soil has been suggested to increase microbial activities and protect them against environmental stresses (Palansooriya et al., 2019; Y. Zhang et al., 2020). Therefore, soil amended with the drought-tolerant strain-embedded biochar could be an excellent way to improve efficiency and persistence of the applied bio-inoculant under

severe environmental stresses. This could also be a cost-effective alternative to expensive chemical fertilizers and mitigate drought stress in arid regions of the world.

Furthermore, validation of the hub genes identified by network analysis is a great way to test the hypothesis and identify a novel molecular marker for desiccation stress tolerance. Quantification of expression levels of the hub genes under desiccation stress using qRT-PCR and construction of a series of knock-out mutants for specific hub genes can be done to validate the hypothesis that these hub genes are essential for survival under desiccation stress. For example, a *B. japonicum* USDA110 mutant (Δ blr2567), was constructed by the site-directed mutagenesis; however, its validation is underway. Blr2567 is a hypothetical protein, which was identified as one of the intramodular hub genes in the module that showed strong positive correlation with the desiccation time. The network was constructed using microarray data, which may not present low level gene expression due to hybridization limitations on the microarray chip. It would be better if the network analysis were conducted with RNA-seq expression data, which could provide higher resolutions for low expressed genes.

Overall, our research provides scientific evidence and comprehensive evaluation of biofertilizer applications to attain sustainable agriculture. It further suggests possible measures to improve agronomic efficiency of biofertilizers in the field and synergistically improve crop yield, thereby minimizing the use of chemical fertilizers. This would also help to alleviate negative effects of other abiotic stresses due to global warming.

References:

- Atieno, M., Herrmann, L., Okalebo, R., & Lesueur, D. (2012). Efficiency of different formulations of *Bradyrhizobium japonicum* and effect of co-inoculation of *Bacillus subtilis* with two different strains of *Bradyrhizobium japonicum*. *World Journal of Microbiology and Biotechnology*, 28(7), 2541–2550. <https://doi.org/10.1007/s11274-012-1062-x>
- Egamberdieva, D., Wirth, S., Behrendt, U., Abd-Allah, E. F., & Berg, G. (2016). Biochar treatment resulted in a combined effect on soybean growth promotion and a shift in plant growth promoting rhizobacteria. *Frontiers in Microbiology*, 7(FEB), 1–11. <https://doi.org/10.3389/fmicb.2016.00209>
- Głodowska, M., Schwingamer, T., Husk, B., & Smith, D. (2017). Biochar Based Inoculants Improve Soybean Growth and Nodulation. *Agricultural Sciences*, 08(09), 1048–1064. <https://doi.org/10.4236/as.2017.89076>
- Khan, Z., Rahman, M. H. U., Haider, G., Amir, R., Ikram, R. M., Ahmad, S., Schofield, H. K., Riaz, B., Iqbal, R., Fahad, S., Datta, R., Baaz-Eem, A., Sabagh, A. E. L., & Danish, S. (2021). Chemical and biological enhancement effects of biochar on wheat growth and yield under arid field conditions. *Sustainability (Switzerland)*, 13(11), 1–18. <https://doi.org/10.3390/su13115890>
- Langfelder, P., & Horvath, S. (2007). Eigengene networks for studying the relationships between co-expression modules. *BMC Systems Biology*, 1, 54. <https://doi.org/10.1186/1752-0509-1-54>
- Lehmann, J., Rillig, M. C., Thies, J., Masiello, C. A., Hockaday, W. C., & Crowley, D. (2011). Biochar effects on soil biota - A review. *Soil Biology and Biochemistry*, 43(9), 1812–1836.

<https://doi.org/10.1016/j.soilbio.2011.04.022>

Ma, H., Egamberdieva, D., Wirth, S., & Bellingrath-Kimura, S. D. (2019). Effect of Biochar and Irrigation on Soybean- Rhizobium Symbiotic Performance and Soil. *Agronomy*, 9(626).

Mendes, L. W., Kuramae, E. E., Navarrete, A. A., Van Veen, J. A., & Tsai, S. M. (2014). Taxonomical and functional microbial community selection in soybean rhizosphere. *ISME Journal*, 8(8), 1577–1587. <https://doi.org/10.1038/ismej.2014.17>

Molina-Romero, D., Baez, A., Quintero-Hernández, V., Castañeda-Lucio, M., Fuentes-Ramírez, L. E., Bustillos-Cristales, M. del R., Rodríguez-Andrade, O., Morales-García, Y. E., Munive, A., & Muñoz-Rojas, J. (2017). Compatible bacterial mixture, tolerant to desiccation, improves maize plant growth. *PLoS ONE*, 12(11), 1–21. <https://doi.org/10.1371/journal.pone.0187913>

Palansooriya, K. N., Wong, J. T. F., Hashimoto, Y., Huang, L., Rinklebe, J., Chang, S. X., Bolan, N., Wang, H., & Ok, Y. S. (2019). Response of microbial communities to biochar-amended soils: a critical review. *Biochar*, 1(1), 3–22. <https://doi.org/10.1007/s42773-019-00009-2>

Pandit, N. R., Mulder, J., Hale, S. E., Zimmerman, A. R., Pandit, B. H., & Cornelissen, G. (2018). Multi-year double cropping biochar field trials in Nepal: Finding the optimal biochar dose through agronomic trials and cost-benefit analysis. *Science of the Total Environment*, 637–638, 1333–1341. <https://doi.org/10.1016/j.scitotenv.2018.05.107>

Schmidt, J. E., & Gaudin, A. C. M. (2018). What is the agronomic potential of biofertilizers for maize? A meta-analysis. *FEMS Microbiology Ecology*, 94(7), 1–10. <https://doi.org/10.1093/femsec/fiy094>

Suppadit, T., Phumkokrak, N., & Pounsuk, P. (2012). The Effect of using Quail Litter Biochar on Soybean (*Glycine max* L. Merr.) Production. *Chilean Journal of Agricultural Research*, 72(2), 244–251. <https://doi.org/10.4067/s0718-58392012000200013>

Vílchez, J. I., García-Fontana, C., Román-Naranjo, D., González-López, J., & Manzanera, M. (2016). Plant drought tolerance enhancement by trehalose production of desiccation-tolerant microorganisms. *Frontiers in Microbiology*, 7(SEP), 1–11. <https://doi.org/10.3389/fmicb.2016.01577>

Yao, Q., Liu, J., Yu, Z., Li, Y., Jin, J., Liu, X., & Wang, G. (2017). Changes of bacterial community compositions after three years of biochar application in a black soil of northeast China. *Applied Soil Ecology*, 113, 11–21. <https://doi.org/10.1016/j.apsoil.2017.01.007>

Zhang, Y., Ding, J., Wang, H., Su, L., & Zhao, C. (2020). Biochar addition alleviate the negative effects of drought and salinity stress on soybean productivity and water use efficiency. *BMC Plant Biology*, 20(1), 1–11. <https://doi.org/10.1186/s12870-020-02493-2>